University of Cyprus

DEPARTMENT OF PHYSICS

SUPERSYMMETRIC QCD ON A SPACETIME LATTICE

DOCTOR OF PHILOSOPHY DISSERTATION

HERODOTOS HERODOTOU

2024

University of Cyprus

Department of Physics

Supersymmetric QCD on a Spacetime Lattice

Herodotos Herodotou

A dissertation submitted to the University of Cyprus in partial fulfillment of the requirements for the degree of Doctor of Philosophy.

May 2024

Validation page

Doctoral Candidate: Herodotos Herodotou

Doctoral Thesis Title: Supersymmetric QCD on a Spacetime Lattice

The present Doctoral Dissertation was submitted in partial fulfillment of the requirements for the Degree of Doctor of Philosophy at the ***Department of Physics*** *and was approved on May 20, 2024 by the members of the* ***Examination Committee****.*

Examination Committee:

Research Supervisor: Prof. Haralambos Panagopoulos _____

Committee Chairman: Prof. Fotios Ptochos _____

Committee Member: Prof. Constantia Alexandrou_____

Committee Member: Prof. Giannis Koutsou_____

Committee Member: Prof. Ettore Vicari _____

Declaration of doctoral candidate

The present doctoral dissertation was submitted in partial fulfillment of the requirements for the degree of Doctor of Philosophy of the University of Cyprus. It is a product of original work of my own, unless otherwise mentioned through references, notes, or any other statements.

Herodotos Herodotou

_____

Περίληψη

Σε αυτή τη διατριβή, παρουσιάζουμε δύο διαφορετικές μελέτες: Λεπτομερής Βαθμονόμηση (fine-tuning) των Σταθερών Σύζευξης Yukawa και Quartic στην Υπερσυμμετρική Θεωρία QCD και Επανακανονικοποίηση Τελεστών Τεσσάρων Κουάρκ στη Θεωρία QCD.

Τα υπερσυμμετρικά μοντέλα που εφαρμόζονται σε ισχυρά αλληλεπιδρώντα συστήματα προσφέρουν συναρπαστικές προοπτικές για την αποκάλυψη νέας φυσικής πέρα από το Καθιερωμένο Πρότυπο. Τα τελευταία χρόνια, οι αριθμητικές μελέτες υπερσυμμετρικών επεκτάσεων της QCD στο πλέγμα καθίστανται πιο εφικτές. Σε αυτή τη διατριβή, περιγράφουμε πολλά κίνητρα για να εμβαθύνουμε στη μελέτη υπερσυμμετρικών θεωριών χρησιμοποιώντας τεχνικές πλέγματος. Ωστόσο, διάφορα εμπόδια προκύπτουν από την παραβίαση της Υπερσυμμετρίας στο πλέγμα, όπως η απαίτηση λεπτομερής βαθμονόμησης (fine-tuning) στην απογυμνωμένη (bare) Λαγκρανζιανή της θεωρίας. Η προσέγγισή μας για την αντιμετώπιση αυτών των ζητημάτων περιλαμβάνει την πλήρη αποκατάσταση όλων των συμμετρίων της δράσης, οι οποίες παραβιάζονται στο πλέγμα, καθώς πλησιάζουμε στο όριο του συνεχούς. Προτείνουμε επίσης μερικούς τρόπους για να μειωθεί ο αριθμός των παραμέτρων που χρειάζονται λεπτομερή βαθμονόμηση (fine-tuning), προκειμένου να καταστούν ευκολότεροι οι αριθμητικοί υπολογισμοί στο πλέγμα.

Για την πρώτη μελέτη, διερευνούμε τη λεπτομερή βαθμονόμηση (fine-tuning) της σταθεράς σύζευξης Yukawa (αλληλεπιδράσεις gluino-quark-squark) και της σταθεράς σύζευξης quartic (αλληλεπιδράσεις τεσσάρων squark) στην $\mathcal{N} = 1$ υπερσυμμετρική θεωρία QCD, διακριτοποιημένη στον Ευκλείδειο χωρόχρονο. Χρησιμοποιούμε τη θεωρία διαταραχών σε επίπεδο ενός βρόχου και στη χαμηλότερη τάξη της πλεγματικής σταθεράς. Χρησιμοποιείται, επίσης, το Modified Minimal Subtraction Scheme ($\overline{\text{MS}}$), το οποίο εξ ορισμού, απαιτεί διαταρακτικούς υπολογισμούς, στο συνεχές και/ή στο πλέγμα. Στο πλέγμα, χρησιμοποιούμε τη διακριτοποίηση Wilson για πεδία γλουονίου, κουάρκ και γλουίνο. Για πεδία squark χρησιμοποιούμε naïve διακριτοποίηση. Όλες οι συναρτήσεις Green και οι παράγοντες επανακανονικοποίησης είναι αναλυτικές εκφράσεις ανάλογες απροσδιόριστων παραμέτρων: του αριθμού των χρωμάτων, N_c, του αριθμού των γεύσεων, N_f και της παραμέτρου βαθμίδος α. Η γνώση αυτών των παραγόντων επανακανονικοποίησης είναι απαραίτητη προκειμένου να συσχετιστούν αριθμητικά αποτελέσματα, που προέρχονται από μη διαταρακτικές μελέτες, με τις επανακανονικοποιημένες, «φυσικές» συναρτήσεις Green της θεωρίας.

Οι δυσκολίες αυτής της μελέτης έγκεινται στο γεγονός ότι διαφορετικά συστατικά των πεδίων squark αναμειγνύονται μεταξύ τους σε κβαντικό επίπεδο και οι συμμετρίες της δράσης, όπως η ομοτιμία (parity) και η σύζευξη των συμμετριών φορτίου (charge conjugation), επιτρέπουν μια πρόσθετη σταθερά σύζευξης Yukawa. Συνεπώς, για την κατάλληλη προσαρμογή των όρων Yukawa, αυτές οι μείξεις πρέπει να λαμβάνονται υπόψη στις συνθήκες επανακανονικοποίησης. Σημειώστε ότι ενώ παρέχουμε τα αποτελέσματα των παραγόντων επανακανονικοποίησης για τις σταθερές σύζευξης Yukawa τόσο σε διαστατική οσο και σε πλεγματική ομαλοποίηση, παρουσιάζουμε τα αποτελέσματα των παραγόντων επανακανονικοποίησης για τις σταθερές σύζευξης quartic μόνο σε διαστατική ομαλοποίηση. Οι υπολογισμοί που αφορούν την επανακανονικοποίηση των σταθερών σύζευξης quartic στο πλέγμα βρίσκονται σε εξέλιξη.

Για τη δεύτερη μελέτη, εκτελούμε υπολογισμούς για να μελετήσουμε την επανακανονικοποίηση των τελεστών τεσσάρων κουάρκ στο πλαίσιο της QCD. Χρησιμοποιούμε δύο σχήματα επανακανονικοποίησης: το Gauge Invariant Renormalization Scheme (GIRS), το οποίο έχει κάποια πελονεκτήματα σε σύγκριση με άλλα σχήματα, ειδικά σε μη διαταρακτικές έρευνες στο πλέγμα, και το Modified Minimal Subtraction Scheme ($\overline{\text{MS}}$). Από τους διαταρακτικούς υπολογισμούς μας εξάγουμε τα πινακοστοιχεία των πινάκων μετατροπής μεταξύ αυτών των δύο σχημάτων επανακανονικοποίησης. Μία δυσκολία στη μελέτη των τελεστών τεσσάρων κουάρκ είναι το γεγονός ότι τελεστές με διαφορετικούς πίνακες Dirac αναμειγνύονται μεταξύ τους κατά την επανακανονικοποίηση. Επιπλέον, οι υπολογισμοί στο GIRS, σε μια δεδομένη τάξη στη θεωρία διαταραχών, περιλαμβάνουν διαγράμματα με περισσότερο από ένα βρόχο. Σημειώνουμε ότι εστιάζουμε τόσο σε τελεστές τεσσάρων κουάρκ με $\Delta F = 2$ που διατηρούν την ομοτιμία όσο και σε τελεστές που την παραβιάζουν.

Η εξαγωγή των πινακοστοιχείων των πινάκων μετατροπής απαιτεί τον υπολογισμό των συναρτήσεων Green δύο σημείων, οι οποίες περιλαμβάνουν δύο τελεστές τεσσάρων κουάρκ ή ένα τελεστή τεσσάρων κουάρκ και ένα τελεστή με δύο καυάρκ, καθώς και των συναρτήσεων Green τριών σημείων που περιλαμβάνουν ένα τελεστή τεσσάρων κουάρκ και δύο τελεστές με δύο κουάρκ. Όλοι οι τελεστές στις συναρτήσεις Green βρίσκονται σε διακριτά χωροχρονικά σημεία. Επιπλέον, επικεντρωνόμαστε τόσο σε τελεστές τεσσάρων κουάρκ που διατηρούν την ομοτιμία όσο και σε τελεστές που την παραβιάζουν. Η σημασία των αποτελεσμάτων μας έγκειται στη δυνατότητά τους να βελτιώσουν την κατανόησή μας για τα φαινόμενα της QCD, προσφέροντας πολύτιμες γνώσεις για τα πινακοστοιχεία του πίνακα Cabibbo–Kobayashi–Maskawa (CKM) και ρίχνοντας φως στη μη διαταρακτική επανακανονικοποίηση και μίξη των τελεστών τεσσάρων κουάρκ.

Abstract

In this thesis, we present two projects: Fine-Tuning of the Yukawa and Quartic Couplings in Supersymmetric QCD and Gauge-invariant Renormalization of Four-quark Operators in Lattice QCD.

Supersymmetric models applied to strongly interacting systems offer exciting prospects for uncovering new physics beyond the Standard Model. In recent years, numerical lattice studies of supersymmetric extensions of QCD have become more attainable. In this thesis, we outline numerous motivations to delve into the study of supersymmetric theories using lattice techniques. Nevertheless, various well-known obstacles emerge from the breaking of supersymmetry in a lattice-regulated theory, such as the requirement for fine-tuning of the theory's bare Lagrangian. Our approach to address these issues involves mandating that all symmetries of the action, which are broken on the lattice, must be fully restored as the continuum limit is approached. We also propose some ways to reduce the amount of the parameters that need fine-tuning in order to render the numerical lattice calculations easier.

For the first project, we investigate the fine-tuning of the Yukawa (gluino-quark-squark interactions) and quartic (four-squark interactions) couplings of $\mathcal{N} = 1$ supersymmetric QCD, discretized on a Euclidean lattice. We use perturbation theory at one-loop level and to the lowest order in the lattice spacing. The Modified Minimal Subtraction Scheme ($\overline{\text{MS}}$) is employed; by its definition, this scheme requires perturbative calculations, in the continuum and/or on the lattice. On the lattice, we utilize the Wilson formulation for gluon, quark and gluino fields; for squark fields we use naïve discretization. All Green's functions and renormalization factors are analytic expressions depending on the number of colors, N_c, the number of flavors, N_f, and the gauge parameter, α, which are left unspecified. Knowledge of these renormalization factors is necessary in order to relate numerical results, coming from nonperturbative studies, to the renormalized, "physical" Green's functions of the theory.

The sheer difficulties of this study lie in the fact that different components of squark fields mix among themselves at the quantum level and the action's symmetries, such as parity and charge conjugation, allow an additional Yukawa coupling. Consequently, for an appropriate fine-tuning of the Yukawa terms, these mixings must be taken into account in the renormalization conditions. Note that while we provide the results of

the renormalization factors for the Yukawa couplings in both dimensional and lattice regularization, we present the outcomes of the renormalization factors for the quartic couplings only in dimensional regularization. The computations regarding the renormalization of the quartic couplings on the lattice are underway.

For the second project, we perform calculations to determine the renormalization of the four-quark operators in the framework of QCD. We employ a Gauge Invariant Renormalization Scheme (GIRS), which can be advantageous compared to other schemes, especially in nonperturbative lattice investigations, and the Modified Minimal Subtraction Scheme ($\overline{\text{MS}}$). From our perturbative computations we extract the elements of the conversion matrices between these two renormalization schemes at the next leading order. A formidable issue in the study of the four-quark operators is the fact that operators with different Dirac matrices mix among themselves upon renormalization. Furthermore, computations in GIRS, at a given order in perturbation theory, involve diagrams with more than one loop. Note that we focus on both Parity Conserving and Parity Violating four-quark operators with $\Delta F = 2$.

The extraction of the elements of the conversion matrices entails the calculation of two-point Green's functions, which involve products of two four-quark operators or one four-quark operator and one bilinear operator, as well as three-point Green's functions which involve one four-quark and two bilinear operators; all operators are situated at distinct spacetime points. Moreover, we concentrate on both Parity Conserving and Parity Violating four-quark operators. The significance of our results lies in their potential to refine our understanding of QCD phenomena, offering valuable insights into the precision of Cabibbo–Kobayashi–Maskawa (CKM) matrix elements and shedding light on the nonperturbative treatment of complex mixing patterns associated with four-quark operators.

Acknowledgements

I would like to express my sincere gratitude to my supervisor, Prof. Haralambos Panagopoulos, for his invaluable guidance, support, and advice throughout the course of my research. His expertise and encouragement have been instrumental in shaping this thesis.

I am also deeply thankful to Dr. Marios Costa and Dr. Gregoris Spanoudes for their essential support, constructive feedback, and valuable discussions. Their contributions have significantly enriched the quality of this work.

Furthermore, I am grateful to the University of Cyprus for providing financial support through a scholarship, which has enabled me to pursue my academic endeavors and carry out this research.

Last but certainly not least, I extend my heartfelt thanks to my family, my parents and my brother, and to my friends for their unconditional love, encouragement, and understanding. Their constant support and belief in me have been a source of strength and motivation throughout this journey.

Contents

List of Figures

List of Tables

Chapter 1

Introduction

1.1 Quantum Chromodynamics

Quantum Chromodynamics (QCD) is the fundamental theory that describes the interactions of quarks, which are fermions, through the exchange of gluons, which are gauge bosons. Quarks are the elementary constituents of nucleons and interact through the strong nuclear force. There are six different flavors of quarks with different masses: up, down, charm, strange, top, and bottom, and three different types of color charges conventionally named: red, green, and blue. The QCD action consists of two parts: the action of gluons and the action of quarks, and each action remains invariant under local gauge transformations of the non-abelian SU(3) group. The number three of this group refers to the three color charges of quarks and the eight generators correspond to the eight types of gluons, each carrying a color charge. This characteristic indicates that gluons can interact with themselves, distinguishing them from photons, which do not exhibit self-interactions.

The dynamics of QCD involve complex phenomena such as the asymptotic freedom which sets it apart from other theories. This phenomenon describes the behavior of quarks and gluons at short distances where the strong force between them weakens significantly. This makes the strong force different from the forces in everyday experiences, where they typically become stronger at shorter distances.

An other complex feature of QCD is confinement; despite the freedom of quarks and gluons to move independently, they are never observed as isolated particles. Instead,

these elementary particles are confined within larger, color-neutral entities called hadrons, which are separated to baryons and mesons. The exact mechanisms behind confinement remain an active area of research, representing one of the outstanding challenges in understanding the behavior of the strong force. Confinement is observed in low-energy regions and thus, we cannot study it smoothly as the perturbation theory breaks down in these regions. Therefore, it is important to introduce a nonperturbative approach to the theory. Currently, the most effective method is the discretization of the spacetime in the framework of QCD. This theory is called Lattice QCD and it is the only way to study QCD nonperturbatively through numerical simulations.

1.2 Quantum Chromodynamics on the Lattice

The first that established the lattice formulation of QCD was Kenneth Wilson, back in 1974, who introduced lattice gauge theory as a way to regulate non-abelian gauge theories [1]. Some years latter, a group of physicists, including Michael Creutz, collaborated to apply lattice techniques specifically to QCD [2]. Over the years, the lattice QCD methodology matured through the contributions of many researchers while the computational techniques and algorithms have been improving. Therefore, this theory paved the way for a comprehensive understanding of the non-perturbative aspects of the strong force, providing valuable insights into the behavior of quarks and gluons at both high and low energy scales.

The lattice formulation of QCD introduces a discretized spacetime lattice with lattice spacing a to represent the continuous Euclidean spacetime of quantum field theory. Lattice QCD, as a powerful numerical technique, can be applied so as to make QCD finite in high-energy regimes with the finite lattice spacing a acting as an ultraviolet regulator. The presence of the lattice spacing a induces a momentum cutoff, constraining the integration domain to the finite interval of $-\pi/a < p_\mu < \pi/a$ (first Brillouin zone) in cases where lattice calculations are conducted in momentum space. At high energies, where quarks and gluons behave almost as free particles, perturbative methods, such as Feynman diagram calculations, can also be applied. However, at low energies, where phenomena such as confinement and the formation of hadrons arise, the strong force becomes non-perturbative and only lattice QCD

provides a framework for investigating QCD. At low-energy regimes, the finite lattice size L acts as an infrared regulator.

The continuum quantum field theory can be recovered by extrapolating lattice results towards an infinitely large lattice size ($L \to \infty$) and approaching the limit of an infinitesimally small lattice spacing ($a \to 0$). As we fine-tune the Lagrangian bare parameters and take the regulator to the continuum limit, the lattice calculations converge to the predictions of the continuum quantum field theory. This extrapolation process is fundamental for bridging the gap between the discretized lattice world and the continuous behavior expected in the underlying quantum field theory.

To derive nonperturbative physical results from numerical simulations on the lattice, establishing an appropriate nonperturbative renormalization framework is essential. Numerous non-perturbative techniques are available for computing renormalization constants of composite operators in lattice field theory. These methods aim to reduce systematic errors that arise when extracting physical predictions from lattice operator matrix elements. A main non-perturbative renormalization scheme used in lattice field theory to determine renormalization constants is the RI-MOM scheme. This scheme relies on numerically evaluating correlation functions of operators between external quark and/or gluon states in momentum space. Specifically, this involves computing the amputated Green's function, in the Landau gauge and at a specified large Euclidean scale, $p^2 = \mu^2$, with the condition that it matches its tree-level value in the chiral limit. Several studies have successfully utilized RI-MOM scheme and highlight the efficacy and applicability of this scheme in practical renormalization calculations within lattice field theory [3–5].

Another nonperturbative renormalization approach, known as the Schrödinger functional scheme [6–8], utilizes the finite size of lattices used in simulations to set the renormalization scale. This method employs continuum perturbation theory to convert results from the Schrödinger functional scheme to the $\overline{\text{MS}}$ scheme. While theoretically elegant, its practical application demands substantial effort and must be repeated for each new operator. In contrast, the RI-MOM method stands out for its relatively straightforward implementation, allowing for the treatment of all desired operators within a single simulation. However, the Schrödinger functional method is explicitly gauge invariant, whereas the RI-MOM method necessitates gauge fixing.

Gauge-invariant Renormalization Scheme (GIRS) is also an efficient non-perturbative renormalization scheme, which was introduced in Ref. [9] and was inspired by the coordinate space (X-space) renormalization approach [10]. GIRS represents a method for renormalizing composite operators on the lattice, preserving gauge invariance and independence from mass. In GIRS, one has to calculate correlation functions of gauge-invariant composite operators at different spacetime points. In numerous scenarios, the renormalization factors of operators within GIRS can be determined by analyzing only two-point Green's functions. However, when mixing is present, in many cases, the investigation of three-point Green's functions becomes necessary as well.

Lattice techniques are not limited to QCD alone. We can extend lattice QCD to supersymmetric (SUSY) theories, where there is a symmetry between fermions and bosons. SUSY is a theoretical framework which provides potential solutions to some of the unresolved questions in particle physics, such as the hierarchy problem. The use of lattice techniques in the context of SUSY have their origins in several studies conducted in the late 1970s and in the 1980s [11, 12]. Extending lattice QCD techniques to supersymmetric theories involves adapting numerical simulations to accommodate the unique features of supersymmetry, such as the presence of superpartners for each particle. However, supersymmetric lattice field theories present additional challenges, but they offer a unique opportunity to explore the non-perturbative aspects of supersymmetry and the interplay between supersymmetry and the strong force.

1.3 Perturbative Lattice QCD Calculations

Perturbative lattice QCD calculations constitute a powerful approach in theoretical particle physics, particularly for providing a starting point to explore the nonperturbative aspects of the strong force and for connecting lattice QCD with physical values. Perturbative calculations are accurate when the coupling constant is small. However, QCD is known for its strong coupling at low energies, making perturbative methods challenging in such regimes.

To combine lattice results and experimental data, we have to renormalize lattice fields and bare parameters of the Lagrangian, such as bare couplings and masses. We also have to renormalize lattice operators. The easier way to perform the aforementioned

renormalization is by using perturbation theory as a nonperturbative determination through numerical simulations may be proven challenging or even impossible since a possible mixing with other operators may arise. When nonperturbative calculation of renormalization factors is possible, it allows comparisons with corresponding perturbative outcomes at a specific renormalization scale. Hence, we can check the reliability of both perturbative and nonperturbative methods. In addition, by applying lattice techniques to perturbative QCD, we can explore the behavior of quarks and gluons at intermediate energies, bridging the gap between the perturbative and non-perturbative regimes.

Moreover, perturbative lattice calculations are much more accurate than nonperturbative one except the calculations of mixing coefficients of operators of lower dimensionality which contain inverse powers of the lattice spacing and thus they diverge in the limit where the lattice spacing goes to zero. Furthermore, lattice perturbation theory helps us to reduce lattice artifacts, which appear when we extrapolate the lattice theory to the continuum limit, from measured quantities and get accurate predictions from lattice results. Lattice perturbation theory is also essential since by using it, we can recover the continuum symmetries, which are broken by the lattice regularization (such as chiral symmetry), in the continuum limit and investigate which of these symmetries are anomalous.

An other important implementation of perturbative lattice calculations is the computation of the conversion factors between different renormalization schemes. For instance, we can evaluate the conversion factor between a nonperturbative scheme on the lattice (like the modified regularization-independent (RI′) scheme) and a continuum scheme (like the $\overline{\text{MS}}$ scheme). Note that as continuum schemes are defined perturbatively, the evaluation of these conversion factors can be determined only perturbatively.

Lattice perturbation theory can also be extended to supersymmetric QCD (SQCD) since supersymmetric models of strongly coupled theories are a very promising models for new physics Beyond the Standard Model (SM). However, there are several well-known obstacles arising from the breaking of SUSY in a regularized theory on the lattice [13], including the necessity for fine-tuning of the theory's bare Lagrangian [14–16]. This extension is crucial because there is a lack of research on the nonperturbative aspects of SQCD due to the extensive fine-tuning required for the numerous operators involved in lattice simulations. However, nonperturbative calculations in the framework

of the supersymmetric Yang-Mills (SYM) theory have been conducted, such as the study of the mass spectrum and chiral properties by employing Wilson fermions for gauge groups SU(2) [17] and SU(3) [18, 19]. A potential strategy to address this challenge and guide the fine-tuning process involves employing lattice perturbation theory. This method has shown success in studying two-dimensional supersymmetric gauge theories [20, 21]. In the coming years, it is expected that simulations of SQCD will become feasible.

In perturbative QCD, calculations are typically performed using Feynman diagrams, which represent different orders of perturbation theory, and help us to systematically organize and compute various contributions to physical observables. Comparing lattice perturbation theory with continuum perturbation theory, we note that the properties of the path integral, Wick's theorem and the combinatorial rules on the lattice are similar to the continuum. Nevertheless, the Feynman diagrams become much more complicated on the lattice since the expressions of interaction vertices and of the propagators are more complex. We also have an infinite number of interaction vertices on the lattice (unlike the continuum) but we are restricted to use a finite number of them at any given order in the coupling constant. However, there are still more interaction vertices on the lattice and thus, there are more Feynman diagrams. Therefore, most of the researchers are restricted to one-loop and to the lowest order in lattice spacing calculations. Although, higher-loop calculations contain a huge number of terms and they are time and labour consuming, a few studies perform them in recent years, such as the studies of the $\mathcal{O}(a^2)$ corrections to various fermionic matrix elements [22–24].

While perturbative lattice QCD has made significant progress in understanding the strong force in certain regimes, challenges persist, especially when dealing with phenomena such as confinement and the formation of hadronic bound states. Researchers continue to refine techniques; particularly, they try to reduce the dependence of the results on the lattice spacing by improving the lattice actions. Improved lattice actions contain discretized versions of the continuum Dirac operator that respect key symmetries and desired properties. Some examples are: (1) Standard Wilson fermions which introduce a term to the lattice Dirac operator to deal with the fermion doubling problem, (2) Clover fermions that incorporate a clover term into the lattice Dirac operator, which helps in reducing the lattice artifacts associated with Wilson fermions, (3) Domain Wall fermions which introduce an extra dimension (the fifth dimension) and localize fermionic fields on a four-dimensional boundary, (4)

Overlap fermions that combine aspects of domain wall fermions and Ginsparg-Wilson fermions, ensuring exact chiral symmetry on the lattice.

1.4 Current Trends of Lattice Field Theory

Recent advancements in lattice field theory have brought about significant progress in various areas of particle physics research. One major focus lies in the investigation of hadron structure, where lattice QCD calculations are utilized to study form factors and gravitational form factors [25]. These studies have seen improvements in controlling lattice artifacts and enhancing theoretical accuracy, paving the way for a deeper understanding of the internal structure of hadrons. Moreover, there is a growing interest in understanding the partonic structure of hadrons, particularly through lattice calculations of x-dependent parton distributions [25]. Another recent trend of the lattice field theory is the use of generative machine learning models in order to overcome challenges in Monte Carlo sampling of lattice field theories, such as critical slowing down and topological freezing [26].

Additionally, lattice QCD simulations contribute significantly to our understanding of the phase diagram of strongly interacting matter, particularly focusing on the chiral/deconfinement transition and its relation to heavy ion collision experiments [27]. Furthermore, lattice QCD studies are extending to explore rare processes, such as the invisible decay $J/\psi \rightarrow \gamma\nu\bar{\nu}$, providing theoretical predictions to aid experimental searches for phenomena beyond the Standard Model [28].

Quantum computing also plays a role in advancing lattice QCD simulations [29]. However, challenges remain in developing fault-tolerant quantum computers and overcoming theoretical and algorithmic obstacles for simulating gauge theories on quantum architectures. Precision calculations of nucleon form factors are also being conducted using lattice QCD, contributing to our understanding of nucleon structure [30]. Additionally, efforts in understanding hadron physics and quark flavor physics through lattice QCD methods have been conducted [31–35].

Another essential current application of lattice field theory is the non-perturbative lattice studies of strongly coupled gauge theories other than QCD for testing composite models and providing theoretical inputs for experimental searches for new physics, offering a window into physics beyond the standard model [36]. Lastly, lattice QCD

calculations aim to provide precise predictions for the hadronic vacuum polarization contribution to improve the precision of the Standard Model and enhance sensitivity to physics beyond the Standard Model [37].

1.5 Thesis Overview

In this dissertation we present two projects: Fine-Tuning of the Yukawa and Quartic Couplings in Supersymmetric QCD and Gauge-invariant Renormalization of Four-quark Operators in Lattice QCD. Note that in these projects the bare amputated Green's functions are computed by using a symbolic package in Mathematica that the lattice group of University of Cyprus has developed.

In Chapter 2, especially in subsections 2.1 - 2.5, we provide a well-established background of supersymmetry. We include this for completeness and in order to lead to our presentation of SQCD in the continuum in subsection 2.6. These topics are closely related to the first project: Fine-Tuning of the Yukawa and Quartic Couplings in Supersymmetric QCD.

In Chapter 3, we discuss the reasons behind exploring SUSY on the lattice, as well as we outline the obstacles encountered in such investigations. A main obstacle arising from the breaking of supersymmetry in a regularized theory on the lattice, including the necessity for fine-tuning of the theory's bare Lagrangian. Moreover, we delve into $\mathcal{N} = 1$ supersymmetric theory on the lattice in the Wess-Zumino gauge and its associated symmetries. Understanding this chapter is crucial for comprehending the content covered in Chapter 4.

In Chapter 4, we address the problem of fine-tuning of the $\mathcal{N} = 1$ SQCD bare Lagrangian via perturbative calculations so as to restore supersymmetry in the continuum limit. Specifically, we study the renormalization of the Yukawa (gluino-squark-quark interactions) and the quartic (four-squark interactions) couplings. To deduce the renormalization factors and the coefficients of the counterterms we compute, perturbatively to one-loop and to the lowest order in the lattice spacing, the relevant three-point and four-point Green's functions using both dimensional and lattice regularizations. All Green's functions and renormalization factors are analytic expressions depending on the number of colors, N_c, the number of flavors, N_f, and the gauge parameter, α, which are left unspecified. The quantities,

which we calculate in this chapter, are important ingredients in extracting nonperturbative information for supersymmetric theories through lattice simulations. Furthermore, the renormalization factors are necessary ingredients in relating lattice matrix elements to physical amplitudes. Noting that on the lattice, we utilize the Wilson formulation for gluon, quark and gluino fields; for squark fields we use naïve discretization.

In Chapter 5 we discuss the second project: Gauge-invariant Renormalization of Four-quark Operators in Lattice QCD. We concentrate only in four-quark operators which involved in flavor-changing $\Delta F = 2$ processes. The primary goal outlined in this research is to examine the renormalization of four-quark operators using both GIRS and $\overline{\text{MS}}$ schemes. Specifically, we aim to obtain the elements of the conversion matrices between GIRS and $\overline{\text{MS}}$. While these matrices depend on both scales, they remain regularization-independent, allowing us to compute them using dimensional regularization. This approach facilitates perturbative computations to higher-loop orders. To determine the aforementioned elements of the conversion matrices, we calculate the first quantum corrections for the two-point and three-point Green's functions using coordinate space within dimensional regularization, where we regulate the theory in $D \equiv 4 - 2\epsilon$ dimensions. By imposing renormalization conditions on these bare one-loop Green's functions, we derive perturbative renormalization constants for a complete set of $\Delta F = 2$ four-quark operators and also provide their gauge-invariant mixing patterns. Furthermore, in this Chapter, we offer a comprehensive analysis of the GIRS scheme, highlighting its benefits and its drawbacks.

Lastly, in Chapter 6 we provide a summary and present the conclusions drawn from our study.

In this thesis, there are also two appendices:

In Appendix A, we explore the path integral over the gluino field in order to clarify its Majorana nature within the functional integral framework, and the way to properly address it in the calculation of Feynman diagrams.

In Appendix B, for the sake of completeness, we depict diagrams that do not exist for $\Delta F = 2$ four-quark operators and they contribute to the Green's functions involving products of four-quark operators with $\Delta F < 2$. Moreover, we present additional Feynman diagrams that emerge specifically on the lattice.

Chapter 2

Supersymmetry

2.1 Introduction

In physics, a symmetry of a system is a physical or mathematical feature that is preserved or remains unchanged under a transformation. The understanding of a physical system relies heavily on knowledge of its symmetry structure. The most important symmetry result is Noether's theorem which states that when a system is unchanged under a continuous symmetry, we can derive a conserved quantity. Examples of it are the conservation of energy, momentum and angular momentum due to time and space translations and rotation symmetry, respectively. Therefore, we aim firstly to understand the symmetries of a system, and then we can investigate the laws that are compatible with them. Note that subsections 2.1 - 2.5 are well-established background; we include it for completeness, and in order to lead to our presentation of SQCD in subsection 2.6.

The local SU(3)×SU(2)×U(1) gauge symmetry is an internal symmetry that essentially defines the Standard Model (SM). The strong forces are based on the non-abelian SU(3) group whilst the electroweak forces are based on the non-abelian SU(2)×U(1) gauge group which is broken down spontaneously to the U(1) symmetry of the electromagnetic interactions. Besides internal symmetries, we have also the global spacetime (Poincaré) symmetry, as it is postulated for all relativistic quantum field theories [38].

The only symmetries that can exist, except spacetime and internal symmetries, are "Supersymmetries". It is commonly known that the formalism of symmetries is

expressed by commutation relations. For instance, in the case of continuous symmetries, the formalism consists of groups that are called Lie groups with generators that obey only commutation relations. Now, in order to construct a supersymmetry, we need to take into account not only commutation relations but also anticommutation relations. Supersymmetry is an extension of the Poincaré Lie algebra; it is a graded Lie algebra.

A supersymmetric theory can be formulated using not only spacetime variables in the Minkowski spacetime, but also anticommuting parameters, θ and $\bar{\theta}$. This space is called superspace where we can create superfields. Superfields are fields that can be expressed as Taylor series in the powers of θ and $\bar{\theta}$ and phenomenologically, their components are used to describe particles. They are also used to construct supersymmetric gauge theories.

In Quantum Field Theory there are two basic classes of particles: bosons, which have an integer-valued spin and follow Bose–Einstein statistics, and fermions, which have a half-integer-valued spin and follow Fermi–Dirac statistics. In supersymmetry, each particle from one class has an associated particle in the other, known as its superpartner, the spin of which differs by a half-integer. Particles and their supersymmetric partners have the same mass and the same quantum numbers under internal global symmetries. Note that each fermion has two bosonic superpartners since the fermion has two degrees of freedom due to its spin.

As supersymmetry is not supported by any experimental evidence, it breaks down spontaneously. Thus, particles and their superpartners do not have the same mass. However, there are important reasons that supersymmetry plays prominent roles in modern theoretical physics and that the Minimal Supersymmetric Standard Model is one of the best possible extensions of the SM. Over the past decades, supersymmetry has been considered a prime candidate for resolving a number of open problems related to the SM, such as the candidates to explain the nature of dark matter [39], which arise from the lightest supersymmetric particles [40], and the unification of the electromagnetic, weak and strong forces at the Planck scale ($M_P = 10^{19}\,GeV$) suggested by Grand Unified Theory (GUT) [41, 42]. Furthermore, supersymmetry would resolve the hierarchy problem [41]; a problem that concerns the large discrepancy between aspects of the weak force and gravity. Supersymmetry is also a part of string theory [43], a theory of quantum gravity. Lastly, it can be used as a tool to improve our understanding of quantum field theory.

Introduction to the Supersymmetric Algebra

Firstly, before we introduce the algebra of supersymmetry, we should introduce the Scattering Matrix S, a matrix that acts on the initial state of a system and gives a final state. That is, S-matrix has elements which express the probability amplitude of a physical system going from an initial state to a final state. The dimensions of this matrix are infinite since the number of possible states of a system is also infinite. But the matrix elements are not independent due to the fact that a physical theory could obey some symmetries.

The Coleman-Mandula theorem enables us to find the symmetries of the S-matrix and it starts with the following assumptions [44]:

- The S-matrix is based on a local, relativistic theory of quantum fields in four-dimensional spacetime
- There are only a finite number of different particles associated with single-particle states of a given mass
- There is an energy gap between the vacuum and the single-particle states

The corollary of this theorem is that the S-matrix has symmetries of space-time translations, Lorentz transformations and a limited number of internal symmetries. That is, the most general Lie algebra of the symmetries of the S-matrix contains:

- the space-time translation operators, P_m, which transform the four-vector position of a state
- the operators of Lorentz transformations, M_{mn}
- finite number of Hermitian operators, B_l, which are Lorentz scalar (internal symmetries).

The latter operators, besides being invariant under Lorentz transformations, also belong to the algebra of a compact Lie group.

We observed, based on the Coleman-Mandula theorem, that only those three kinds of continuous symmetries of the S-matrix are allowed. However, this theorem takes into account only generators that satisfy commutation relations, i.e. "even" objects. We can generalize this algebra if, in addition to B_l, P_m and M_{mn}, some other generators are added, which we will call "odd". Consequently, there will be both commutation and anticommutation relations between the generators in our algebra. These relations

take the following form:

$$\begin{aligned} \{Q, Q'\} &= X \\ [X, X'] &= X'' \\ [Q, X] &= Q'' \,, \end{aligned} \tag{2.1}$$

where Q, Q' and Q'' stand for the odd (anticommuting) elements of the algebra and X, X′ and X″ for the even (commuting) elements.

The most general supersymmetric algebra is the following:

$$\begin{aligned} [P_m, P_n] &= 0 \\ [P_m, Q_a^L] &= [P_m, \bar{Q}_{\dot{a}L}] = 0 \\ [P_m, B_l] &= [P_m, X^{\widehat{LM}}] = 0 \\ \{Q_a^L, \bar{Q}_{\dot{a}M}\} &= 2\sigma_{a\dot{a}}^{\ m} P_m \delta^L{}_M \\ \{Q_a^L, Q_b^M\} &= \epsilon_{ab} X^{\widehat{LM}} \\ \{\bar{Q}_{\dot{a}L}, \bar{Q}_{\dot{b}M}\} &= \epsilon_{\dot{a}\dot{b}} X^{\dagger}_{\widehat{LM}} \\ [X^{\widehat{LM}}, \bar{Q}_{\dot{a}K}] &= [X^{\widehat{LM}}, Q_a^K] = 0 \\ [X^{\widehat{LM}}, X^{\widehat{KN}}] &= [X^{\widehat{LM}}, B_l] = 0 \\ [B_l, B_m] &= i c_{lm}^{\ \ k} B_k \\ [Q_a^L, B_l] &= S^L_{l\ M} Q_a^M \\ [\bar{Q}_{\dot{a}L}, B^l] &= -S^{*l}_{\ \ L\ \ M} \bar{Q}_{\dot{a}M} \\ X^{\widehat{LM}} &= \alpha^{l,\widehat{LM}} B_l \,, \end{aligned} \tag{2.2}$$

where S is a hermitian matrix. Operators Q have a spinor index a and act to the left-handed spinors, which are spinors that transform based on the $\mathrm{M}(\frac{1}{2}, 0)$ representation of the Lorentz group. Operators $\bar{Q}$ have a spinor index $\dot{a}$ and act to the right-handed spinors, which are spinors that transform based on the $\mathrm{M}(0, \frac{1}{2})$ representation of the Lorentz group. Operator $\bar{Q}$ is the hermitian conjugate of the operator Q.

We can prove that the more Q and $\bar{Q}$ operators we have, the more supersymmetric particles we have. The number of operators Q and $\bar{Q}$ is shown by the indices $L, M, K = 1, .., \mathcal{N}$. Furthermore, the indices $a, b, \dot{a}, \dot{b} = 1, 2$ of the above operators refer to the Weyl spinors. The latin indices $m, n, l = 1, ..., 4$ denote the components of the Lorentz vector. The objects X are called central charges because they commute with all the

other generators. Also, all generators except Q are commuted objects. Lastly, the notation $X^{\widehat{LM}}$ denotes that the objects X are antisymmetric with respect to L and M.

Note that in order to prove the equations (2.2), the Coleman-Mandula theorem and the Jacobi identities are needed. The algebra of supersymmetry is called Graded Lie Algebra and it is the only compatible with the symmetries of the S-matrix and with the relativistic quantum field theory. Graded Lie Algebra also contains the operators of Lorentz transformations M_{mn} but for brevity the commutation relations related with them have not been included in equation (2.2).

Representations of the Supersymmetric Algebra

In this subsection, we will study irreducible supersymmetric representations of the $\mathcal{N}$=1 supersymmetric algebra. To achieve this, we will start from a single-particle state that we call vacuum state, denoted by Ω_{spin}, and we will act with the supersymmetric operators on this state. Therefore, states that belong to the same representation will be created and the superpartners of the vacuum state Ω_{spin} will arise.

Below, we will prove that in every supersymmetric representation there is an equal number of bosonic and fermionic states. Firstly, we introduce an operator $(-)^{N_F}$ which acts on fermionic and bosonic states as follows:

$$\begin{aligned}(-)^{N_F}(boson) &= (boson)\\ (-)^{N_F}(fermion) &= -(fermion)\,.\end{aligned} \tag{2.3}$$

Suppose we have a state $|\psi\rangle$ and a new state $|\psi_{new}\rangle = Q_a|\psi\rangle$. The state $|\psi_{new}\rangle$ will be a fermion if the state $|\psi\rangle$ is a boson and vice versa due to the spin index of the operator Q. Therefore, it follows:

$$\begin{aligned}(-)^{N_F}|\psi\rangle &= \pm|\psi\rangle\\ (-)^{N_F}Q_a|\psi\rangle &= \mp Q_a|\psi\rangle\,.\end{aligned} \tag{2.4}$$

We can multiply the first relation by the operator Q_a from the left and equate the two relations. Hence, we have:

$$\begin{aligned}(-)^{N_F}Q_a|\psi\rangle &= -Q_a(-)^{N_F}|\psi\rangle \\ \Rightarrow \{Q_a,(-)^{N_F}\} &= 0\,.\end{aligned} \tag{2.5}$$

Now, we have:

$$tr[(-)^{N_F}\{Q_a^A,\bar{Q}_{\dot{b}B}\}] = tr[(-)^{N_F}(Q_a^A\bar{Q}_{\dot{b}B}+\bar{Q}_{\dot{b}B}Q_a^A)]\,. \tag{2.6}$$

If we use the cyclic property of the trace and the anticommutation relation in the equation (2.5) we get the following result:

$$tr[(-)^{N_F}\{Q_a^A,\bar{Q}_{\dot{b}B}\}] = tr[-Q_a^A(-)^{N_F}\bar{Q}_{\dot{b}B}+Q_a^A(-)^{N_F}\bar{Q}_{\dot{b}B}] = 0\,. \tag{2.7}$$

Also, considering the above relation and the anticommutation relation presented earlier:

$$\{Q_a^A,\bar{Q}_{\dot{b}B}\} = 2\sigma_{a\dot{b}}^m P_m\delta^A{}_B\,, \tag{2.8}$$

we conclude:

$$\begin{aligned}0 = tr[(-)^{N_F}\{Q_a^A,\bar{Q}_{\dot{b}B}\}] &= 2\sigma_{a\dot{b}}{}^m\delta^A{}_B tr[(-)^{N_F}P_m] \\ \Rightarrow tr[(-)^{N_F}] &= 0\,.\end{aligned} \tag{2.9}$$

Given that $[P_m,Q_a^L] = [P_m,\bar{Q}_{\dot{a}L}] = 0$, the states appearing from the action of the operator Q on the vacuum (which is an eigenstate of P_m, with eigenvalue p_m), have the same eigenvalue as the vacuum. Therefore, in the space of these states, the operator P_m acts as a multiple of the unit operator. We know that we can define the trace as shown below:

$$tr[(-)^{N_F}] = \sum\langle\psi|(-)^{N_F}|\psi\rangle\,. \tag{2.10}$$

with the above sum spanning all states of a representation. Since the left hand side of the above equation is zero, the states in the right hand side must be half bosonic

and half fermionic so that the equality is satisfied. In this way we proved that in a representation we have the same number of bosonic and fermionic states.

Let us focus on representations of the supersymmetric algebra corresponding to states of a particle with mass $\tilde{m} \neq 0$. Therefore, the momentum operator will take the form $P^2 = -\tilde{m}^2$. Suppose we choose a frame of reference in which the particle we are studying is at rest and thus, $P_m = (-\tilde{m}, 0, 0, 0)$. We know that acting in this state with operators Q, the supersymmetric partners of the vacuum state will arise. Consequently, the new states will have the same rest mass as the vacuum states. In this frame of reference the following anticommutation relations apply (compare with Eq. (2.2)):

$$\begin{aligned} \{Q_a^A, \bar{Q}_{\dot{b}B}\} &= 2\tilde{m}\delta_{a\dot{b}}\delta^A{}_B \\ \{Q_a^A, Q_b^B\} &= \{\bar{Q}_{\dot{a}A}, \bar{Q}_{\dot{b}B}\} = 0\,, \end{aligned} \tag{2.11}$$

where the indices A and B run from 1 to $\mathcal{N}$ depending on which supersymmetric algebra we study.

At this time, we can define the creation operators $(\alpha_a{}^A)^\dagger$:

$$(\alpha_a{}^A)^\dagger = \frac{1}{\sqrt{2\tilde{m}}}\bar{Q}_{\dot{a}A}\,, \tag{2.12}$$

and the annihilation operators $\alpha_a{}^A$:

$$\alpha_a{}^A = \frac{1}{\sqrt{2\tilde{m}}}Q_a^A\,. \tag{2.13}$$

By using the definitions of the creation and annihilation operators, the relations (2.11) take the following form:

$$\begin{aligned} \{\alpha_a{}^A, (\alpha_b{}^B)^\dagger\} &= \delta_a{}^b\delta^A{}_B \\ \{\alpha_a{}^A, \alpha_b{}^B\} &= \{(\alpha_a{}^A)^\dagger, (\alpha_b{}^B)^\dagger\} = 0\,. \end{aligned} \tag{2.14}$$

By definition, when the creation operators act on a vacuum state (Ω), the states of a representation are created as follows:

$$\Omega^{(n)a_1}{}_{A_1}{}^{\ldots a_n}{}_{A_n} = \frac{1}{\sqrt{n!}}(\alpha_{a_1}{}^{A_1})^\dagger \cdots (\alpha_{a_n}{}^{A_n})^\dagger\Omega\,, \tag{2.15}$$

where the indices a_i run from 1 to 2 and the indices A_i run from 1 to $\mathcal{N}$. The vacuum state (Ω) is defined as follows:

$$\alpha_a{}^A\Omega = 0\,. \tag{2.16}$$

Since the creation operators $(\alpha_a^A)^\dagger$ anticommutes, the state $\Omega^{(n)}$ is antisymmetric under permutations of the indices a_i or A_i. So, in the above product of operators we cannot have two operators with the same indices a_i or A_i because we would get zero.

Considering that each creation operator has $2\mathcal{N}$ components, it follows that, for any value of n, there are $\begin{pmatrix} 2\mathcal{N} \\ n \end{pmatrix}$ different states. Summing up all the values that n takes, we get the dimensionality of our representation:

$$d = \sum_{n=0}^{2\mathcal{N}} \begin{pmatrix} 2\mathcal{N} \\ n \end{pmatrix} = 2^{2\mathcal{N}}\,. \tag{2.17}$$

Therefore, this representation contains $2^{2\mathcal{N}}$ states, of which $2^{2\mathcal{N}-1}$ are bosonic and $2^{2\mathcal{N}-1}$ are fermionic.

Now, for $\mathcal{N}$=1 the fundamental representation (i.e. the representation obtained starting from a vacuum state with spin 0) consists of the following states:

$$\begin{aligned} \Omega \\ (\alpha_a)^\dagger\Omega \\ \frac{1}{\sqrt{2}}(\alpha_a)^\dagger(\alpha_b)^\dagger\Omega = -\frac{1}{2\sqrt{2}}\epsilon^{ab}(\alpha^c)^\dagger(\alpha_c)^\dagger\Omega\,. \end{aligned} \tag{2.18}$$

The state Ω has zero spin, the state $(\alpha_a)^\dagger\Omega$ has spin $\frac{1}{2}$ and the state $\frac{1}{\sqrt{2}}(\alpha_a)^\dagger(\alpha_b)^\dagger\Omega$ has spin 0.

However, there are cases where the vacuum state Ω_j has spin j greater than zero. The table 2.1 shows the particles that exist in such cases as well as the particles that exist in the fundamental representation.

Representations, for which the vacuum state has spin j greater than 3/2, contain particles with spin greater than 2, and consequently do not find application in nature, since quantization of particles with spin greater than 2 leads to violation of unitarity. We can also find the supersymmetric representations for the cases $\mathcal{N} > 1$. Certainly,

Spin	Ω_0	$\Omega_{\frac{1}{2}}$	Ω_1	$\Omega_{\frac{3}{2}}$
0	2	1	0	0
$\frac{1}{2}$	1	2	1	0
1	0	1	2	1
$\frac{3}{2}$	0	0	1	2
2	0	0	0	1

TABLE 2.1: Supersymmetric representations for $\mathcal{N}$=1 [44].

the $\mathcal{N} = 1$ case is the one that has more application in the phenomenology of Physics beyond the Standard Model (BSM), and can be studied in a more controlled way in numerical simulations. The cases for $\mathcal{N} > 4$ are rejected as the fundamental representation contains states with spin eigenvalue greater than 2.

2.2 Scalar Multiplet

In this section, we study the simplest theory of supersymmetry. This theory includes a scalar field A, a spinor field ψ and a scalar, auxiliary field F. The field F is called auxiliary as it can be expressed in terms of the other fields of the theory, i.e. in terms of the fields A and ψ. Of course, this theory cannot describe nature completely since in this theory there are only fields with spin $\frac{1}{2}$, such as the spinor field, and spin 0, such as the fields A and F, whilst in nature there are particles with spin 1.

Firstly, we represent how the scalar field A transforms under a supersymmetric transformation [44]:

$$A' = e^{\xi Q + \bar{\xi}\bar{Q}} A \,, \tag{2.19}$$

where ξ and $\bar{\xi}$ are anticommuting, independent parameters with a spinor index and thus, with two degrees of freedom. Note that the product ξQ has no spinor indices since operators Q have spinor indices, too. Below, we present commutation and anticommutation relations with the parameters ξ and $\bar{\xi}$ and the operators Q, $\bar{Q}$ and P_m:

$$\{\xi^a, \xi^b\} = \{\xi^a, Q_b\} = \{\xi^a, \bar{\xi}^b\} = \{\xi^a, \bar{Q}_b\} = [P_m, \xi^a] = 0. \tag{2.20}$$

Similar relations are valid for $\bar{\xi}$.

Parameters ξ and $\bar{\xi}$ allow us to express the supersymmetric algebra in terms of commutators:

$$[\xi Q, \bar{\xi}\bar{Q}] = 2\xi\sigma^m\bar{\xi}P_m \tag{2.21}$$
$$[\xi Q, \xi Q] = [\bar{\xi}\bar{Q}, \bar{\xi}\bar{Q}] = 0 \tag{2.22}$$
$$[P^m, \xi Q] = [P^m, \bar{\xi}\bar{Q}] = 0\,, \tag{2.23}$$

where we follow the convention:

$$\xi Q = \xi^a Q_a \tag{2.24}$$
$$\bar{\xi}\bar{Q} = \bar{\xi}_{\dot{a}}\bar{Q}^{\dot{a}}. \tag{2.25}$$

Now, we will find the dimensions of the operator Q and the parameter ξ. Having in mind that:

$$\{Q_a, \bar{Q}_{\dot{b}}\} = 2\sigma^m_{a\dot{b}}P_m\,, \tag{2.26}$$

and the operator P_m has dimensions of energy, operator Q has dimensions $[\text{Energy}]^{\frac{1}{2}}$. Then, observing the Eq. (2.19), we conclude that the parameter ξ has dimensions $[\text{Energy}]^{-\frac{1}{2}}$.

We can Taylor expand the exponential in the Eq. (2.19):

$$A' = \sum_{N=0}^{\infty} \frac{(\xi Q + \bar{\xi}\bar{Q})^N}{N!} A. \tag{2.27}$$

The infinitesimal supersymmetric transformation of the field A, which is the first, non-trivial order of the above Taylor expansion, is:

$$\delta_\xi A = (\xi Q + \bar{\xi}\bar{Q}) \times A. \tag{2.28}$$

Similarly,

$$\delta_\xi \psi = (\xi Q + \bar{\xi}\bar{Q}) \times \psi. \tag{2.29}$$

The transformation δ_ξ satisfies:

$$\begin{aligned}(\delta_\eta\delta_\xi - \delta_\xi\delta_\eta)A &= 2(\eta\sigma^m\bar{\xi} - \xi\sigma^m\bar{\eta})P_m A \\ &= -2i(\eta\sigma^m\bar{\xi} - \xi\sigma^m\bar{\eta})\partial_m A\,,\end{aligned} \tag{2.30}$$

and

$$(\delta_\eta\delta_\xi - \delta_\xi\delta_\eta)\psi = -2i(\eta\sigma^m\bar{\xi} - \xi\sigma^m\bar{\eta})\partial_m\psi\,, \tag{2.31}$$

according to Eq. (2.21).

Starting with a scalar field A, we define the spinor field ψ as the field into which A transforms:

$$\delta_\xi A = \sqrt{2}\xi\psi. \tag{2.32}$$

Note that, if the field A has dimensions $[\text{Energy}]^l$, then the field ψ has dimensions $[\text{Energy}]^{l+\frac{1}{2}}$. The field ψ has spinor indices, and thus two degrees of freedom.

Now, under a supersymmetric transformation, the new field ψ transforms into a tensor field F and into the derivative of A:

$$\delta_\xi\psi = i\sqrt{2}\sigma^m\bar{\xi}\partial_m A + \sqrt{2}\xi F. \tag{2.33}$$

Obviously, the new field F is scalar and has dimensions $[\text{Energy}]^{l+1}$. The term with the parameter $\bar{\xi}$ in the above equation satisfies the Eq. (2.30).

By using the Eq. (2.31):

$$\begin{aligned}(\delta_\eta\delta_\xi - \delta_\xi\delta_\eta)\psi = &- 2i(\eta\sigma^n\bar{\xi} - \xi\sigma^n\bar{\eta})\partial_n\psi - i\sigma^n\bar{\sigma}^m\partial_m\psi[\eta\sigma^n\bar{\xi} - \xi\sigma^n\bar{\eta}] \\ &+ \sqrt{2}(\xi\delta_\eta F - \eta\delta_\xi F).\end{aligned} \tag{2.34}$$

We conclude that the only way for both equations, (2.31) and (2.34), to be valid simultaneously is if the field F undergoes the following transformation:

$$\delta_\xi F = i\sqrt{2}\bar{\xi}\bar{\sigma}^m\partial_m\psi. \tag{2.35}$$

It is noticeable that no other field appears in this theory; the field F is the last field that is introduced and has the higher dimensions. Furthermore, we notice that the

transformations of the three fields are linear. The aforementioned fields and their transformations are chosen in this way in order to construct a multiplet that consists component fields that are transformed according to Eqs.(2.30) and (2.31). Multiplets are the irreducible representations of an algebra and the multiplet in this section is called chiral or scalar multiplet.

At this moment, in order to create an action which is invariant under the infinitesimal supersymmetric transformations, we introduce a Lagrangian density that transforms as a total derivative. Below, we represent this Lagrangian density:

$$L = L_0 + mL_m \,, \tag{2.36}$$

where m is an arbitrary parameter. The kinetic term is equal to:

$$L_0 = i(\partial_m \bar{\psi})\bar{\sigma}^m \psi + A^* \Box A + F^* F \,, \tag{2.37}$$

and the mass term:

$$L_m = AF + A^* F^* - \frac{1}{2}\psi\psi - \frac{1}{2}\bar{\psi}\bar{\psi}. \tag{2.38}$$

The equations of motion from this Lagrangian density are:

$$i\bar{\sigma}^n \partial_n \psi + m\bar{\psi} = 0 \tag{2.39}$$

$$F + mA^* = 0 \tag{2.40}$$

$$\Box A + mF^* = 0 \,, \tag{2.41}$$

where $\Box$ is the d'Alembert operator. As we mentioned before, we notice that the field F (and F^*) is expressed in terms of the field A^* (and A). Thus, the field F is called auxiliary field and this theory contains two instead of three independent fields. Furthermore, when we substitute the Eq. (2.40) in the Eq. (2.41), it gives:

$$\Box A - m^2 A = 0. \tag{2.42}$$

Therefore, we construct a Lagrangian density that describes two free fields with the same mass. It is worth mentioning that the number of bosonic degrees of freedom is the same as the number of fermionic degrees of freedom as the field A is complex and the field ψ is a spinor.

2.3 Superfields and Superspace

Superspace is an extension of Minkowski space and consists not only the spacetime variables x_m but it also consists anticommuting parameters θ and $\bar{\theta}$. Superfields, which are a useful extension of fields, are functions of superspace and they consist component fields. Superfields also describe representations of the supersymmetric algebra with an elegant way and construct interacting Lagrangians.

Firstly, we introduce the group element:

$$G(x,\theta,\bar{\theta}) = e^{i(-x^m P_m + \theta Q + \bar{\theta}\bar{Q})}\,, \tag{2.43}$$

and then, by using Baker-Campbell-Hausdorff's formula and the commutation relations of the Eqs.(2.21)-(2.23), we can prove the following:

$$\begin{aligned} G(0,\xi,\bar{\xi})G(x^m,\theta,\bar{\theta}) &= e^{i(\xi Q+\bar{\xi}\bar{Q})}e^{i(-x^m P_m+\theta Q+\bar{\theta}\bar{Q})} \\ &= e^{i(\xi Q+\bar{\xi}\bar{Q}-x^m P_m+\theta Q+\bar{\theta}\bar{Q})-\frac{1}{2}[\xi Q+\bar{\xi}\bar{Q},-x^m P_m+\theta Q+\bar{\theta}\bar{Q}]} \\ &= G(x^m - i\xi\sigma^m\bar{\theta} + i\theta\sigma^m\bar{\xi}, \xi+\theta, \bar{\xi}+\bar{\theta}). \end{aligned} \tag{2.44}$$

Note that, when the operator $G(0,\xi,\bar{\xi})$ acts on a function of superspace, it changes the variables of the function in the following way:

$$\begin{aligned} x^m &\to x^m + i\theta\sigma^m\bar{\xi} - i\xi\sigma^m\bar{\theta} \\ \theta &\to \theta + \xi \\ \bar{\theta} &\to \bar{\theta} + \bar{\xi}. \end{aligned} \tag{2.45}$$

Considering an infinitesimal transformation of $G(0,\xi,\bar{\xi})$, we can understand that the aforementioned change of variables can only be generated if the following expression is valid:

$$\xi Q + \bar{\xi}\bar{Q} = \xi^a\left(\frac{\partial}{\partial\theta^a} - i\sigma_{a\dot{a}}{}^m\bar{\theta}^{\dot{a}}\partial_m\right) + \bar{\xi}_{\dot{a}}\left(\frac{\partial}{\partial\bar{\theta}_{\dot{a}}} - i\theta^a\sigma_{a\dot{b}}{}^m\epsilon^{\dot{b}\dot{a}}\partial_m\right). \tag{2.46}$$

Therefore, we obtain differential expressions that correspond to the operators Q and $\bar{Q}$:

$$\begin{aligned} Q_a &= \frac{\partial}{\partial\theta^a} - i\sigma_{a\dot{a}}{}^m\bar{\theta}^{\dot{a}}\partial_m \\ \bar{Q}_{\dot{a}} &= -\frac{\partial}{\partial\bar{\theta}^{\dot{a}}} + i\theta^a\sigma_{a\dot{a}}{}^m\partial_m. \end{aligned} \tag{2.47}$$

We could have studied right multiplication instead of left multiplication in the product of group elements. Then, we would have the following operators:

$$\begin{aligned} D_a &= \frac{\partial}{\partial\theta^a} + i\sigma_{a\dot{a}}{}^m\bar{\theta}^{\dot{a}}\partial_m \\ \bar{D}_{\dot{a}} &= -\frac{\partial}{\partial\bar{\theta}^{\dot{a}}} - i\theta^a\sigma_{a\dot{a}}{}^m\partial_m\,, \end{aligned} \tag{2.48}$$

which anticommute with the operators Q and $\bar{Q}$. We can also prove the following anticommutation relations:

$$\{D_a, \bar{D}_{\dot{a}}\} = -2i\sigma_{a\dot{a}}{}^m\partial_m \tag{2.49}$$

$$\{D_a, D_b\} = 0 \tag{2.50}$$

$$\{\bar{D}_{\dot{a}}, \bar{D}_{\dot{b}}\} = 0. \tag{2.51}$$

Now, the most general superfield can be expressed in terms of its power series expansion in θ and $\bar{\theta}$:

$$\begin{aligned} F(x,\theta,\bar{\theta}) = f(x) &+ \theta\phi(x) + \bar{\theta}\bar{\chi}(x) \\ &+ \theta\theta m(x) + \bar{\theta}\bar{\theta}n(x) + \theta\sigma^m\bar{\theta}\upsilon_m(x) \\ &+ \theta\theta\bar{\theta}\bar{\lambda}(x) + \bar{\theta}\bar{\theta}\theta\psi(x) + \theta\theta\bar{\theta}\bar{\theta}d(x). \end{aligned} \tag{2.52}$$

Products with higher powers of θ and $\bar{\theta}$ are zero due to the fact that θ and $\bar{\theta}$ are anticommuting parameters with spinor indices that run from 1 to 2.

Having in mind that the linear infinitesimal supersymmetric transformation of a field is defined in Eq. (2.28), the transformation law for a superfield can be defined as follows:

$$\begin{aligned}\delta_\xi F(x,\theta,\bar{\theta}) &\equiv (\xi Q + \bar{\xi}\bar{Q}) \times F = (\xi Q + \bar{\xi}\bar{Q})F \\ &= (\delta_\xi f(x)) + \theta(\delta_\xi \phi(x)) + \bar{\theta}(\delta_\xi \bar{\chi}(x)) \\ &\quad + \theta\theta(\delta_\xi m(x)) + \bar{\theta}\bar{\theta}(\delta_\xi n(x)) + \theta\sigma^m\bar{\theta}(\delta_\xi \upsilon_m(x)) \\ &\quad + \theta\theta\bar{\theta}(\delta_\xi \bar{\lambda}(x)) + \bar{\theta}\bar{\theta}\theta(\delta_\xi \psi(x)) + \theta\theta\bar{\theta}\bar{\theta}(\delta_\xi d(x)).\end{aligned} \tag{2.53}$$

When the operator $(\xi Q + \bar{\xi}\bar{Q})$ of the Eq. (2.46) acts on the superfield $F(x,\theta,\bar{\theta})$ of the Eq. (2.52), we take a result with different powers of θ and $\bar{\theta}$. By matching the appropriate powers of θ and $\bar{\theta}$ of this result with the powers of θ and $\bar{\theta}$ of the transformation $\delta_\xi F(x,\theta,\bar{\theta})$ of Eq. (2.53), we can generate the transformation laws for each component field. It is worth noticing that products or linear combination of superfields are also superfields due to the linearity of the operators Q and $\bar{Q}$.

In general, superfields form reducible representations of the supersymmetric algebra. The number of the component fields of a general superfield is high. However, we can reduce this number by imposing covariant constraints on superfields. In other words, superfields can satisfy an equation which can relate some component fields and thus, the number of independent component fields decreases. Examples of these constraints are $\bar{D}F = 0$ or $F = F^\dagger$. The former constraint characterize chiral or scalar superfields whilst the latter characterize vector superfields. There are some rules for the constraints of superfields. For instance, the supersymmetric transformed superfields must satisfy the constraints, as well. Furthermore, constraints, which yield the trivial value for superfield $\Phi = a =$ constant, are not accepted. Note that we can construct all renormalizable supersymmetric Lagrangians by using only scalar and vector superfields.

Imposing constraints on superfields is very useful especially for supersymmetric theories with $\mathcal{N} > 1$ as in these theories, there are $\mathcal{N}$ parameters of θ and the number of component fields increases significantly. Therefore, we impose constraints on superfields so as to simplify these theories.

2.4 Chiral Superfields

In the previous section, we presented superfields. In this section, we study a special case of them, the chiral superfields that are characterized by the condition:

$$\bar{D}_{\dot{a}}\Phi = 0. \tag{2.54}$$

Matter fields can be described by chiral superfields, which consist a spinor field and a scalar field like the scalar multiplet.

Note that, in this section, it is convenient to use the variables $y^m = x^m + i\theta\sigma^m\bar{\theta}$, θ and $\bar{\theta}$ instead of x^m, θ and $\bar{\theta}$. By using chain rule, we can express the partial derivative $\frac{\partial}{\partial\theta}$ as:

$$\frac{\partial}{\partial\theta} = i\sigma^m\bar{\theta}\frac{\partial}{\partial y^m} + \frac{\partial}{\partial\theta}. \tag{2.55}$$

Likewise, we can express the partial derivatives $\partial/\partial\bar{\theta}$ and $\partial/\partial x^m$ in terms of the new variables. Therefore, operators D_a and $\bar{D}_{\dot{a}}$ take the following expressions:

$$D_a = \frac{\partial}{\partial\theta^a} + 2i\sigma^m_{a\dot{a}}\bar{\theta}^{\dot{a}}\frac{\partial}{\partial y^m} \tag{2.56}$$

$$\bar{D}_{\dot{a}} = -\frac{\partial}{\partial\bar{\theta}^{\dot{a}}}. \tag{2.57}$$

Now, the most general superfield that satisfy the constraint of Eq. (2.54) is:

$$\begin{aligned}\Phi &= A(y) + \sqrt{2}\theta\psi(y) + \theta\theta F(y) \\ &= A(x) + i\theta\sigma^m\bar{\theta}\partial_m A(x) + \frac{1}{4}\theta\theta\bar{\theta}\bar{\theta}\Box A(x) \\ &\quad + \sqrt{2}\theta\psi(x) - \frac{i}{\sqrt{2}}\theta\theta\partial_m\psi(x)\sigma^m\bar{\theta} + \theta\theta F(x)\,,\end{aligned} \tag{2.58}$$

where we substitute $y^m = x^m + i\theta\sigma^m\bar{\theta}$ and we use Taylor expansion. It is apparent that the field Φ contains two scalar fields A and F and a spinor field ψ (Weyl spinor). We choose the names of these fields to coincide with the names of the fields of the scalar multiplet since they transform by the same way under an infinitesimal supersymmetric transformation.

Now, the hermitian conjugate of a chiral superfield $\Phi^\dagger$, which is a function of $y^{\dagger m} = x^m - i\theta\sigma^m\bar{\theta}$ and $\bar{\theta}$, can be expressed as:

$$\begin{aligned}\Phi^\dagger &= A^*(y^\dagger) + \sqrt{2}\bar{\theta}\bar{\psi}(y^\dagger) + \bar{\theta}\bar{\theta}F^*(y^\dagger) \\ &= A^*(x) - i\theta\sigma^m\bar{\theta}\partial_m A^*(x) + \frac{1}{4}\theta\theta\bar{\theta}\bar{\theta}\Box A^*(x) + \sqrt{2}\bar{\theta}\bar{\psi}(x) \\ &\quad + \frac{i}{\sqrt{2}}\bar{\theta}\bar{\theta}\theta\sigma^m\partial_m\bar{\psi}(x) + \bar{\theta}\bar{\theta}F^*(x).\end{aligned} \tag{2.59}$$

We can also express the operators D_a and $\bar{D}_{\dot{a}}$ in terms of the parameters $y^{\dagger m}, \theta$ and $\bar{\theta}$:

$$D_a = \frac{\partial}{\partial\theta^a} \tag{2.60}$$

$$\bar{D}_{\dot{a}} = -\frac{\partial}{\partial\theta^{\dot{a}}} - 2i\theta^a\sigma^m_{a\dot{a}}\frac{\partial}{\partial y^{\dagger m}}\,, \tag{2.61}$$

and we notice that $D_a\Phi^\dagger = 0$, which is the constraint that an antichiral superfield ($\Phi^\dagger$) satisfies. The product of chiral superfields $\Phi_1\Phi_2\cdots\Phi_n$ also satisfies the constraint of Eq. (2.54) and thus, is a chiral superfield and likewise for the product of antichiral superfields $\Phi_1^\dagger\Phi_2^\dagger\cdots\Phi_n^\dagger$.

We can prove that the $\theta\theta$ component of the products $\Phi_i\Phi_j$ and $\Phi_i\Phi_j\Phi_k$ and the $\theta\theta\bar{\theta}\bar{\theta}$ component of the product $\Phi_i^\dagger\Phi_j$ transform into a spacetime derivative under an infinitesimal supersymmetric transformation. Consequently, we can use the aforementioned components in order to construct a Lagrangian density as the corresponding action would be invariant under these transformations.

The most general supersymmetric renormalizable Lagrangian density that consists only chiral fields is:

$$L = \Phi_i^\dagger\Phi_i\,|_{\theta\theta\bar{\theta}\bar{\theta}} + [(\frac{1}{2}m_{ij}\Phi_i\Phi_j + \frac{1}{3}g_{ijk}\Phi_i\Phi_j\Phi_k + \lambda_i\Phi_i)\,|_{\theta\theta} + h.c.]\,, \tag{2.62}$$

where h.c. refers to the hermitian conjugate. Note that, the expression of the Lagrangian density is the same for the two sets of variables $x^m, \theta, \bar{\theta}$ and $y^m, \theta, \bar{\theta}$. The second term of the above Lagrangian density is a mass term and the third one is an interacting term. The parameters g_{ijk} and m_{ij} are symmetric under the change of their indices.

At this point, we represent the Lagrangian density in terms of the component fields:

$$\begin{aligned} L = i\partial_m \bar{\psi}_i \bar{\sigma}^m \psi_i + A_i^* \Box A_i + F_i^* F_i + [m_{ij}(A_i F_j - \frac{1}{2}\psi_i \psi_j) \\ + g_{ijk}(A_i A_j F_k - \psi_i \psi_j A_k) + \lambda_i F_i + h.c.] \,, \end{aligned} \tag{2.63}$$

where we have dropped all the total derivatives. By computing the equations of motion, we observe that the field F_i is auxiliary:

$$\begin{aligned} \frac{\partial L}{\partial F_k^*} &= F_k + \lambda_k^* + m_{ik}^* A_i^* + g_{ijk}^* A_i^* A_j^* = 0 \\ &\Rightarrow F_k = -(\lambda_k^* + m_{ik}^* A_i^* + g_{ijk}^* A_i^* A_j^*) \qquad (2.64) \\ \frac{\partial L}{\partial F_k} &= F_k^* + \lambda_k + m_{ik} A_i + g_{ijk} A_i A_j = 0 \\ &\Rightarrow F_k^* = -(\lambda_k + m_{ik} A_i + g_{ijk} A_i A_j). \qquad (2.65) \end{aligned}$$

The expression of the Lagrangian density only in terms of the two independent fields A_i and ψ_i is:

$$\begin{aligned} L = i\partial_m \bar{\psi}_i \bar{\sigma}^m \psi_i + A_i^* \Box A_i - \frac{1}{2} m_{ik} \psi_i \psi_k - \frac{1}{2} m_{ik}^* \psi_i \bar{\psi}_k \\ - g_{ijk} \psi_i \psi_j A_k - g_{ijk}^* \bar{\psi}_i \bar{\psi}_j A_k^* - \mathcal{V}(A_i, A_j^*) \,, \end{aligned} \tag{2.66}$$

where the potential takes the form $\mathcal{V} = F_k^* F_k$. Due to supersymmetry, this potential is greater or equal to zero. Absolute minima of the potential are the points where $F_k = 0$. In order to find the mass of the component fields, we firstly have to eliminate the linear terms of the fields by making a shift $\Phi_i \to \Phi_i + a_i$. Masses of the fermionic field and of the bosonic field have to be the same.

2.5 Vector Superfields

Vector superfields are superfields which satisfy the following condition:

$$V = V^\dagger. \tag{2.67}$$

They describe gauge fields and they consist spinor fields, scalar fields and a vector field. We can achieve a more comprehensive understanding of them by analyzing their power

series expansions in θ and $\bar{\theta}$.

$$\begin{aligned} V(x,\theta,\bar{\theta}) = C(x) + i\theta\chi(x) - i\bar{\theta}\bar{\chi}(x) + \frac{i}{2}\theta\theta[M(x)+iN(x)] - \frac{i}{2}\bar{\theta}\bar{\theta}[M(x)-iN(x)] \\ - \theta\sigma^m\bar{\theta}\upsilon_m(x) + i\theta\theta\bar{\theta}[\bar{\lambda}(x) + \frac{i}{2}\bar{\sigma}^m\partial_m\chi(x)] - i\bar{\theta}\bar{\theta}\theta[\lambda(x) + \frac{i}{2}\sigma^m\partial_m\bar{\chi}(x)] \\ + \frac{1}{2}\theta\theta\bar{\theta}\bar{\theta}[D(x) + \frac{1}{2}\Box C(x)]. \end{aligned} \tag{2.68}$$

The fields C, D, M, N and υ_m have to be real so as $V(x,\theta,\bar{\theta})$ satisfy the constraint of Eq. (2.67). The component fields C, D, M and N are scalar fields, the fields χ and λ are Weyl spinors and the field υ_m is a vector field.

Note that, without loss of generality, the coefficients of the powers of θ and $\bar{\theta}$ have been chosen in this way so as to transform in a simple way under the following transformation:

$$V \to V + \Phi + \Phi^\dagger\,, \tag{2.69}$$

where Φ and $\Phi^\dagger$ are chiral and antichiral superfields, respectively. From the definitions of the previous section:

$$\begin{aligned} \Phi + \Phi^\dagger = A + A^* + \sqrt{2}(\theta\psi + \bar{\theta}\bar{\psi}) + \theta\theta F + \bar{\theta}\bar{\theta}F^* \\ + i\theta\sigma^m\bar{\theta}\partial_m(A - A^*) + \frac{i}{\sqrt{2}}\theta\theta\bar{\theta}\bar{\sigma}^m\partial_m\psi \\ + \frac{i}{\sqrt{2}}\bar{\theta}\bar{\theta}\theta\sigma^m\partial_m\bar{\psi} + \frac{1}{4}\theta\theta\bar{\theta}\bar{\theta}\Box(A + A^*). \end{aligned} \tag{2.70}$$

Therefore, under the transformation of Eq. (2.69) component fields transform as:

$$\begin{aligned} &C \to C + A + A^* \\ &\chi \to \chi - i\sqrt{2}\psi \\ &M + iN \to M + iN - 2iF \\ &\upsilon_m \to \upsilon_m - i\partial_m(A - A^*) \\ &\lambda \to \lambda \\ &D \to D. \end{aligned} \tag{2.71}$$

We observe that the transformation of the vector field υ_m reminds a gauge transformation as the quantity $A - A^*$ is imaginary. Thus, we call the transformation

of Eq. (2.69) gauge transformation.

Now, we can choose a special gauge which is called Wess-Zumino gauge. In this gauge the fields C, χ, M and N are all zero whilst the vector field υ_m transforms in the usual gauge transformation $\upsilon_m \to \upsilon_m + \partial_m \alpha$ (where α is a scalar quantity) and the fields λ and D are invariant.

Below, we present powers of V in this gauge:

$$V = -\theta\sigma^m\bar{\theta}\upsilon_m(x) + i\theta\theta\bar{\theta}\bar{\lambda}(x) - i\bar{\theta}\bar{\theta}\theta\lambda(x) + \frac{1}{2}\theta\theta\bar{\theta}\bar{\theta}D(x) \tag{2.72}$$

$$V^2 = -\frac{1}{2}\theta\theta\bar{\theta}\bar{\theta}\upsilon_m\upsilon^m \tag{2.73}$$

$$V^3 = 0. \tag{2.74}$$

It is worth mentioning that to compute the terms V^2 and V^3, we zero terms with products of three or more parameters of θ or/and $\bar{\theta}$ due to antisymetrization of them.

We use the variables $y^m = x^m + i\theta\sigma^m\bar{\theta}$ and $y^{\dagger m} = x^m - i\theta\sigma^m\bar{\theta}$ in order to simplify the computation. Then, V takes the form:

$$\begin{aligned} V &= -\theta\sigma^m\bar{\theta}\upsilon_m(y) + i\theta\theta\bar{\theta}\bar{\lambda}(y) - i\bar{\theta}\bar{\theta}\theta\lambda(y) \\ &\quad + \frac{1}{2}\theta\theta\bar{\theta}\bar{\theta}[D(y) - i\partial_m\upsilon^m(y)] \\ &= -\theta\sigma^m\bar{\theta}\upsilon_m(y^\dagger) - i\bar{\theta}\bar{\theta}\theta\lambda(y^\dagger) + i\theta\theta\bar{\theta}\bar{\lambda}(y^\dagger) \\ &\quad + \frac{1}{2}\theta\theta\bar{\theta}\bar{\theta}[D(y^\dagger) + i\partial_m\upsilon^m(y^\dagger)]. \end{aligned} \tag{2.75}$$

Note that the vector superfield V can be considered as the supersymetric generalization of the Yang-Mills potential. The next step is to find a quantity that would be the supersymmetric generalization of the electromagnetic or gluon field strength. In this section, we study the abelian case and the aforementioned quantities are the fields W_a and $\bar{W}_{\dot{a}}$ which are defined as:

$$W_a = -\frac{1}{4}\bar{D}\bar{D}D_a V \tag{2.76}$$

$$\bar{W}_{\dot{a}} = -\frac{1}{4}DD\bar{D}_{\dot{a}}V. \tag{2.77}$$

The above fields are chiral and antichiral superfields, respectively since they satisfy the following conditions:

$$\begin{aligned} \bar{D}_{\dot{b}} W_a &= 0 \\ D_b \bar{W}_{\dot{a}} &= 0. \end{aligned} \tag{2.78}$$

The tensor W_a is gauge invariant:

$$\begin{aligned} W_a &\to -\frac{1}{4}\bar{D}\bar{D}D_a(V+\Phi+\Phi^\dagger) \\ &= W_a - \frac{1}{4}\bar{D}\{\bar{D}, D_a\}\Phi = W_a. \end{aligned} \tag{2.79}$$

Likewise, we can prove that the tensor $\bar{W}_{\dot{a}}$ is also gauge invariant.

Now, using the Eqs.(2.75), (2.76) and (2.77) and the definitions of the operators D_a and $\bar{D}_{\dot{a}}$, we present:

$$\begin{aligned} W_a = &-i\lambda_a(y) + [\delta_a{}^b D(y) - \frac{i}{2}(\sigma^m\bar{\sigma}^n)_a{}^b(\partial_m \upsilon_n(y) - \partial_n \upsilon_m(y))]\theta_b \\ &+ \theta\theta\sigma_{a\dot{a}}{}^m \partial_m \bar{\lambda}^{\dot{a}}(y)\,, \end{aligned} \tag{2.80}$$

and

$$\begin{aligned} \bar{W}_{\dot{a}} = &\, i\bar{\lambda}_{\dot{a}}(y^\dagger) + [\epsilon_{\dot{a}\dot{b}} D(y^\dagger) + \frac{i}{2}\epsilon_{\dot{a}\dot{c}}(\bar{\sigma}^m\sigma^n)^{\dot{c}}{}_{\dot{b}}(\partial_m \upsilon_n(y^\dagger) - \partial_n \upsilon_m(y^\dagger))]\bar{\theta}^{\dot{b}} \\ &- \epsilon_{\dot{a}\dot{b}}\bar{\theta}\bar{\theta}\bar{\sigma}^{m\dot{b}a}\partial_m \lambda_a(y^\dagger). \end{aligned} \tag{2.81}$$

We observe that these superfields contain only the gauge invariant fields D, λ_a and $\upsilon_{mn} = \partial_m \upsilon_n - \partial_n \upsilon_m$. Furthermore, they satisfy the additional constraint:

$$D^a W_a = \bar{D}_{\dot{a}} \bar{W}^{\dot{a}}. \tag{2.82}$$

The most general Lagrangian density for a free vector field, which is gauge invariant, is:

$$L = \frac{1}{4}(W^a W_a \mid_{\theta\theta} + \bar{W}_{\dot{a}}\bar{W}^{\dot{a}} \mid_{\bar{\theta}\bar{\theta}}). \tag{2.83}$$

The above Lagrangian density contains $\theta\theta$ components of chiral superfields and thus, they transform into spacetime derivatives. Consequently, the corresponding action is invariant under an infinitesimal supersymmetric transformation. Furthermore, the

Lagrangian density of the Eq. (2.83) consists only scalar quantities so it is invariant under Lorentz transformations. It is also invariant under gauge transformations as the chiral superfields W_a and $\bar{W}_{\dot{a}}$ are invariant under this transformation.

The Lagrangian density can be written in terms of the component fields as:

$$L = \frac{i}{2}(\partial_m \lambda)\sigma^m \bar{\lambda} - \frac{i}{2}\lambda\sigma^m(\partial_m \bar{\lambda}) + \frac{1}{2}D^2 - \frac{1}{4}\upsilon^{mn}\upsilon_{mn}. \tag{2.84}$$

The first two terms remind the terms that appear in Dirac equation and the last term reminds the kinetic term of a photon or a gluon field. Computing the equations of motion, we observe that the vector field υ_m satisfies Maxwell equations, the field $D = 0$ and the field λ satisfy the following equation:

$$\partial_m \lambda \sigma^m = 0. \tag{2.85}$$

Therefore, in this theory there are a gauge field and a field with spin $\frac{1}{2}$, which is the superpartner of the gauge field and it is called gaugino. Gaugino has no mass as we expected and it is free since in the Lagrangian density there are no interaction terms.

2.6 Supersymmetric QCD in the Continuum

In this section, we study the Lagrangian density of Supersymmetric QCD (SQCD) in the continuum. This Lagrangian density consists interaction terms between chiral and vector superfields. Chiral and vector superfields correspond to matter and gauge fields, respectively. In this theory, we have a spinor field ψ and its superpartner, the field A (both with mass m), which originate from the scalar multiplet. We have also a vector field υ_μ, which corresponds to the vector potential, and a spinor field λ that is the superpartner of υ_μ [44–47].

In order to construct a renormalizable supersymmetric generalization of the Lagrangian density of QCD, we have to multiply superfields so as the dimensionality of their products be less or equal than 4. This Lagrangian density must also be Lorentz invariant and invariant under the following supersymmetric gauge

transformations [48]:

$$\begin{aligned} \Phi'_{+} &= e^{-i\Lambda}\Phi_{+} \\ \Phi'_{-} &= \Phi_{-}e^{i\Lambda} \\ e^{2g\,V'} &= e^{-i\Lambda^{\dagger}}e^{2g\,V}e^{i\Lambda}, \end{aligned} \tag{2.86}$$

where $\Lambda_{ij} = \Lambda^a T^a_{ij}$ is an arbitrary chiral superfield and T^a are the generators of the non-abelian group. These generators obey the following equations:

$$\mathrm{Tr}(T^{\alpha}T^{\beta}) = k\,\delta^{\alpha\,\beta}\,, k > 0 \tag{2.87}$$

$$[T_a, T_b] = i f_{abc} T_c\,, \tag{2.88}$$

where f_{abc} are the structure constants of the algebra, which are completely antisymmetric. Note that, the vector superfield can also be expressed in terms of these generators $V_{ij} = V^a T^a_{ij}$.

The most general Lagrangian density, which is renormalizable, Lorentz invariant as well as invariant under supersymmetric gauge transformations, is:

$$\begin{aligned} \mathcal{L}_{SQCD} = \frac{1}{16kg^2}\mathrm{Tr}(W^a W_a \mid_{\theta\theta} + \bar{W}_{\dot{a}}\bar{W}^{\dot{a}} \mid_{\bar{\theta}\bar{\theta}}) + \Phi^{\dagger}_{+}e^{2gV}\Phi_{+} \mid_{\theta\theta\bar{\theta}\bar{\theta}} \\ + \Phi_{-}e^{-2gV}\Phi^{\dagger}_{-} \mid_{\theta\theta\bar{\theta}\bar{\theta}} + m(\Phi_{-}\Phi_{+} \mid_{\theta\theta} + \Phi^{\dagger}_{+}\Phi^{\dagger}_{-} \mid_{\bar{\theta}\bar{\theta}})\,, \end{aligned} \tag{2.89}$$

where the supersymmetric field strength is defined now as:

$$W_a = -\frac{1}{4}\bar{\mathcal{D}}\bar{\mathcal{D}}\,e^{-2g\,V}\,\mathcal{D}_a\,e^{2g\,V}\,, \tag{2.90}$$

and it transforms covarianlty:

$$W'_a = e^{-i\Lambda}W_a e^{i\Lambda}. \tag{2.91}$$

It is worth mentioning that the Lagrangian density of Eq. (2.89) looks non-renormalizable since it contains the term with e^{2gV} that consists all the powers of the vector superfield V. However, it can be evaluated in the Wess-Zumino gauge. Consequently, the term can be expanded as:

$$e^{2gV} = 1 + 2gV + \frac{(2gV)^2}{2}\,, \tag{2.92}$$

as the higher powers of V are zero in this special gauge.

In the context of $\mathcal{N} = 1$ supersymmetry in 4 dimensions, the SQCD Lagrangian is composed of several components for each flavor of matter fields. These components include two complex scalar fields referred to as squarks, denoted as A_+ and A_-, a Dirac spinor representing quarks, denoted as ψ_+, ψ_-, and two auxiliary complex scalar fields, F_+ and F_-. Additionally, the Lagrangian incorporates a gauge field representing gluons, denoted as u_μ, a Majorana spinor representing gluinos, denoted as λ, and an extra real auxiliary field, D. Beginning with Eq. (2.89) and extracting the relevant components of the superfields (including appropriate powers of θ and $\bar{\theta}$), we derive the continuum Lagrangian density for $\mathcal{N} = 1$ SQCD in 4 dimensions in the framework of the Wess-Zumino gauge:

$$\begin{aligned}\mathcal{L}_{\text{SQCD}} = &-\frac{1}{4}u^{\alpha}_{\mu\nu}u^{\mu\nu\alpha} + \frac{1}{2}D^{\alpha}D^{\alpha} - i\bar{\lambda}^{\alpha}\bar{\sigma}^{\mu}\mathcal{D}_{\mu}\lambda^{\alpha} \\ &- \mathcal{D}_{\mu}A_+^{\dagger}\mathcal{D}^{\mu}A_+ - \mathcal{D}_{\mu}A_-^{\dagger}\mathcal{D}^{\mu}A_- - i\bar{\psi}_+\bar{\sigma}^{\mu}\mathcal{D}_{\mu}\psi_+ - i\bar{\psi}_-\bar{\sigma}^{\mu}\mathcal{D}_{\mu}\psi_- + F_+^{\dagger}F_+ + F_-F_-^{\dagger} \\ &+ i\sqrt{2}g(A_+^{\dagger}\lambda^{\alpha}T^{\alpha}\psi_+ - \bar{\psi}_+\bar{\lambda}^{\alpha}\ T^{\alpha}A_+ + A_-\bar{\lambda}^{\alpha}T^{\alpha}\bar{\psi}_- - \psi_-\lambda^{\alpha}T^{\alpha}A_-) \\ &+ g(A_+^{\dagger}D^{\alpha}T^{\alpha}A_+ - A_-D^{\alpha}T^{\alpha}A_-^{\dagger}) \\ &+ m(A_-F_+ + F_-A_+ - \psi_-\psi_+ + A_+^{\dagger}F_-^{\dagger} + F_+^{\dagger}A_-^{\dagger} - \bar{\psi}_+\bar{\psi}_-)\,,\end{aligned} \tag{2.93}$$

where:

$$\begin{aligned}\mathcal{D}_{\mu}A_+ &= \partial_{\mu}A_+ + ig\,u_{\mu}^{\alpha}\,T^{\alpha}\,A_+ \\ \mathcal{D}_{\mu}A_-^{\dagger} &= \partial_{\mu}A_-^{\dagger} + ig\,u_{\mu}^{\alpha}\,T^{\alpha}\,A_-^{\dagger} \\ \mathcal{D}_{\mu}A_- &= \partial_{\mu}A_- - ig\,A_-\,T^{\alpha}\,u_{\mu}^{\alpha} \\ \mathcal{D}_{\mu}A_+^{\dagger} &= \partial_{\mu}A_+^{\dagger} - ig\,A_+^{\dagger}T^{\alpha}\,u_{\mu}^{\alpha} \\ \mathcal{D}_{\mu}\psi_+ &= \partial_{\mu}\psi_+ + ig\,u_{\mu}^{\alpha}\,T^{\alpha}\,\psi_+ \\ \mathcal{D}_{\mu}\psi_- &= \partial_{\mu}\psi_- - ig\,\psi_-\,T^{\alpha}\,u_{\mu}^{\alpha} \\ \mathcal{D}_{\mu}\lambda &= \partial_{\mu}\lambda + ig\,[u_{\mu},\lambda] \\ u_{\mu\nu} &= \partial_{\mu}u_{\nu} - \partial_{\nu}u_{\mu} + ig\,[u_{\mu},u_{\nu}].\end{aligned} \tag{2.94}$$

In this Lagrangian density, there is a gluonic tensor $u^{\alpha}_{\mu\nu}$ that consists the gluon field u^{α}_{μ}. Furthermore, there is a field λ^{α}, the gluino that has spin $\frac{1}{2}$ and it is the superpartner of gluon. The gluino field λ^{α}, the gluon field v^{α}_{μ} and the auxiliary field D^{α}, which are

the component fields of the vector superfield, carry color indices since they are in the adjoint representation of the non-abelian group. Components of the chiral superfield, which are the auxiliary field F, the quark field ψ and the squark field A, are in the fundamental representation of the non-abelian group. Note that the indices coming from the color in fundamental representation and the Dirac indices are left implicit. On contrary, the color in the adjoint representation is shown explicitly. For the SQCD theory, this group is SU(3) and thus the indices α run from 1 to 8. In the Eq. (2.93), the squark field A is a particle with 0 spin and it is the superpartner of quark ψ.

Below, we represent the transformation of every component field that relates each particle with its superpartner and preserves the SQCD action unchanged:

$$\begin{aligned}
\delta_\xi A_+ &= \sqrt{2}\xi\psi_+\,, \\
\delta_\xi A_- &= \sqrt{2}\psi_-\xi\,, \\
\delta_\xi \psi_{+a} &= i\sqrt{2}\sigma^\mu_{a\dot{b}}\bar{\xi}^{\dot{b}}\mathcal{D}_\mu A_+ + \sqrt{2}\xi_a F_+\,, \\
\delta_\xi \psi^a_- &= -i\sqrt{2}\bar{\xi}_{\dot{b}}\bar{\sigma}^{\dot{b}a\mu}\mathcal{D}_\mu A_- + \sqrt{2}F_-\xi^a\,, \\
\delta_\xi F_+ &= i\sqrt{2}\bar{\xi}\bar{\sigma}^\mu\mathcal{D}_\mu\psi_+ + 2igT^\alpha A_+\bar{\xi}\bar{\lambda}^\alpha\,, \\
\delta_\xi F_- &= -i\sqrt{2}\mathcal{D}_\mu\psi_-\sigma^\mu\bar{\xi} - 2igA_-T^\alpha\bar{\xi}\bar{\lambda}^\alpha\,, \\
\delta_\xi u^\alpha_\mu &= -i\bar{\lambda}^\alpha\bar{\sigma}^\mu\xi + i\bar{\xi}\bar{\sigma}^\mu\lambda^\alpha\,, \\
\delta_\xi \lambda^\alpha &= \sigma^{\mu\nu}\xi u^\alpha_{\mu\nu} + i\xi\ D^\alpha\,, \\
\delta_\xi D^\alpha &= -\xi\sigma^\mu\mathcal{D}_\mu\bar{\lambda}^\alpha - \mathcal{D}_\mu\lambda^\alpha\sigma^\mu\bar{\xi}\,,
\end{aligned} \tag{2.95}$$

where ξ and $\bar{\xi}$ are Majorana spinor parameters. It is worth mentioning that these transformations are not linear as we are in the Wess-Zumino gauge. In order to make them linear, we have to reintroduce those field components which are absent in the WZ gauge.

Eq. (2.93) can be represented in 4 dimensions using Dirac notation and in the Weyl basis as shown below:

$$\begin{aligned}
\mathcal{L}_{\text{SQCD}} &= -\frac{1}{4}u^\alpha_{\mu\nu}u^{\mu\nu\alpha} + \frac{1}{2}D^\alpha D^\alpha + \frac{i}{2}\bar{\lambda}^\alpha_M\gamma^\mu\mathcal{D}_\mu\lambda^\alpha_M \\
&- \mathcal{D}_\mu A^\dagger_+\mathcal{D}^\mu A_+ - \mathcal{D}_\mu A_-\mathcal{D}^\mu A^\dagger_- + i\bar{\psi}_D\gamma^\mu\mathcal{D}_\mu\psi_D + F^\dagger_+F_+ + F_-F^\dagger_- \\
&- i\sqrt{2}g(A^\dagger_+\bar{\lambda}^\alpha_M T^\alpha P_+\psi_D - \bar{\psi}_D P_-\lambda^\alpha_M T^\alpha A_+ + A_-\bar{\lambda}^\alpha_M T^\alpha P_-\psi_D - \bar{\psi}_D P_+\lambda^\alpha_M T^\alpha A^\dagger_-) \\
&+ g(A^\dagger_+ D^\alpha T^\alpha A_+ - A_- D^\alpha T^\alpha A^\dagger_-) \\
&+ m(A_-F_+ + F_-A_+ + \bar{\psi}_D\psi_D + A^\dagger_+F^\dagger_- + F^\dagger_+A^\dagger_-),
\end{aligned} \tag{2.96}$$

where $P_\pm = \frac{1\pm\gamma_5}{2}$, $\gamma_5 = i\gamma^0\gamma^1\gamma^2\gamma^3$, $\lambda_M = \begin{pmatrix} \lambda_a \\ \bar{\lambda}^{\dot{a}} \end{pmatrix}$ and $\psi_D^T = \begin{pmatrix} \psi_{+a} \\ \bar{\psi}_-^{\dot{a}} \end{pmatrix}$.

We can remove the auxiliary fields by either using their equations of motion (in the classical case) or by performing functional integration over them (in the quantum case). In either scenario, the action of SQCD in Minkowski space assumes the following form:

$$\begin{aligned}
\mathcal{S}_{\rm SQCD} &= \int d^4x \Big[-\frac{1}{4} u^\alpha_{\mu\nu} u^{\mu\nu\alpha} + \frac{i}{2}\bar{\lambda}^\alpha_M \gamma^\mu \mathcal{D}_\mu \lambda^\alpha_M \\
&- \mathcal{D}_\mu A_+^\dagger \mathcal{D}^\mu A_+ - \mathcal{D}_\mu A_- \mathcal{D}^\mu A_-^\dagger + i\bar{\psi}_D \gamma^\mu \mathcal{D}_\mu \psi_D \\
&- i\sqrt{2} g (A_+^\dagger \bar{\lambda}^\alpha_M T^\alpha P_+ \psi_D - \bar{\psi}_D P_- \lambda^\alpha_M T^\alpha A_+ + A_- \bar{\lambda}^\alpha_M T^\alpha P_- \psi_D - \bar{\psi}_D P_+ \lambda^\alpha_M T^\alpha A_-^\dagger) \\
&- \frac{1}{2} g^2 (A_+^\dagger T^\alpha A_+ - A_- T^\alpha A_-^\dagger)^2 + m(\bar{\psi}_D \psi_D - m A_+^\dagger A_+ - m A_- A_-^\dagger) \Big] . \qquad (2.97)
\end{aligned}$$

The above action remains invariant under the following supersymmetric transformations:

$$\begin{aligned}
\delta_\xi A_+ &= -\sqrt{2}\bar{\xi}_M P_+ \psi_D \,, \\
\delta_\xi A_- &= -\sqrt{2}\bar{\psi}_D P_+ \xi_M \,, \\
\delta_\xi (P_+\psi_D) &= i\sqrt{2}(\mathcal{D}_\mu A_+) P_+ \gamma^\mu \xi_M - \sqrt{2} m P_+ \xi_M A_-^\dagger \,, \\
\delta_\xi (P_-\psi_D) &= i\sqrt{2}(\mathcal{D}_\mu A_-)^\dagger P_- \gamma^\mu \xi_M - \sqrt{2} m A_+ P_- \xi_M \,, \\
\delta_\xi u^\alpha_\mu &= -i\bar{\xi}_M \gamma^\mu \lambda^\alpha_M , \\
\delta_\xi \lambda^\alpha_M &= \frac{1}{4} u^\alpha_{\mu\nu} [\gamma^\mu, \gamma^\nu] \xi_M - 2ig\gamma^5 \xi_M (A_+^\dagger T^\alpha A_+ - A_- T^\alpha A_-^\dagger) \,. \qquad (2.98)
\end{aligned}$$

The parts of the continuum and lattice SQCD actions that are associated with the quark and the squark fields (Eqs. (2.97) and (3.2), respectively) involve a summation over flavor indices; these flavor indices are implicit within our expressions. A double summation over flavors is also implicit in the 4-squark term of the action (last line of Eqs. (2.97) and (3.2)). Note that matter fields are in the fundamental representation of the gauge group, as in ordinary QCD; also, in the interest of studying the simplest manifestly renormalizable supersymmetric extension of QCD, we have not included any additional superpotential terms in the SQCD Lagrangian.

Following a Wick rotation, the derived expression for the Euclidean action in Dirac notation, denoted as $\mathcal{S}^E_{\rm SQCD}$, is as follows:

$$\begin{aligned}\mathcal{S}^E_{\rm SQCD} &= \int d^4x \Big[\frac{1}{4}u^\alpha_{\mu\nu}u^\alpha_{\mu\nu} + \frac{1}{2}\bar\lambda^\alpha_M\gamma^E_\mu\mathcal{D}_\mu\lambda^\alpha_M \\ &+ \mathcal{D}_\mu A^\dagger_+\mathcal{D}_\mu A_+ + \mathcal{D}_\mu A_-\mathcal{D}_\mu A^\dagger_- + \bar\psi_D\gamma^E_\mu\mathcal{D}_\mu\psi_D \\ &+ i\sqrt{2}g(A^\dagger_+\bar\lambda^\alpha_M T^\alpha P^E_+\psi_D - \bar\psi_D P^E_-\lambda^\alpha_M T^\alpha A_+ + A_-\bar\lambda^\alpha_M T^\alpha P^E_-\psi_D - \bar\psi_D P^E_+\lambda^\alpha_M T^\alpha A^\dagger_-) \\ &+ \frac{1}{2}g^2(A^\dagger_+T^\alpha A_+ - A_-T^\alpha A^\dagger_-)^2 - m(\bar\psi_D\psi_D - mA^\dagger_+A_+ - mA_-A^\dagger_-)\Big], \qquad (2.99)\end{aligned}$$

where $P^E_\pm = \frac{1\pm\gamma^E_5}{2}$, $\gamma^E_5 = \gamma^E_1\gamma^E_2\gamma^E_3\gamma^E_4$. Euclidean γ matrices are defined as: $\gamma^E_4 = \gamma^0$, $\gamma^E_i = -i\gamma_i$ and they satisfy: $\{\gamma_\mu, \gamma_\nu\} = 2\delta_{\mu\,\nu}$.

As in the case with the quantization of ordinary gauge theories, additional infinities will appear upon functionally integrating over gauge orbits. The standard remedy is to introduce a gauge-fixing term in the Lagrangian, along with a compensating Faddeev-Popov ghost term. The resulting Lagrangian, though no longer gauge invariant, is still invariant under BRST transformations [49]. This procedure of gauge fixing guarantees that Green's functions of gauge invariant objects will be gauge independent to all orders in perturbation theory.

The supersymmetric generalization of covariant gauge fixing term is shown below [50]:

$$\begin{aligned}S^{SUSY}_{GF} &= -\frac{1}{8\,\alpha}\int d^4x\left(\bar{\mathcal{D}}^2V\right)\left(\mathcal{D}^2V\right)|_{\theta\theta\bar\theta\bar\theta} \qquad (2.100)\\ &= -\frac{1}{8\,\alpha\,k}\int d^4x{\rm Tr}(4M\Box M + 4N\Box N + 4(D+\Box C)^2 + 4(\partial_\mu u^\mu)^2 \\ &\quad -8\lambda\Box\chi - 8\bar\lambda\Box\bar\chi - 8i\bar\lambda\bar\sigma^\mu\partial_\mu\lambda - 8i\bar\chi\bar\sigma^\mu\partial_\mu\Box\chi).\end{aligned}$$

We note that this gauge fixing term does not break supersymmetry due to the fact that it is a $\theta\theta\bar\theta\bar\theta$ term. Therefore, if we use a regulator which strives to preserve exact supersymmetry at all intermediate steps of the calculation of renormalized Green's functions, it is a reasonable choice. However, having in mind that the renormalized theory does not depend on the choice of the gauge fixing term, and that many regularizations, especially the lattice regularization, violate supersymmetry at intermediate steps, we choose the standard covariant gauge fixing term, proportional to $(\partial_\mu u^\mu)^2$, which breaks supersymmetry as well. Actually, this simpler choice is most often used also in continuum perturbative calculations of supersymmetric models. We present this simpler gauge fixing term and the ghost contribution arising from the

Faddeev-Popov gauge fixing procedure:

$$\mathcal{S}^E_{GF} = \frac{1}{\alpha}\int d^4x \mathrm{Tr}\left(\partial^\mu u_\mu\right)^2, \tag{2.101}$$

where α is the gauge parameter ($\alpha = 1(0)$ corresponds to Feynman (Landau) gauge), and

$$\mathcal{S}^E_{Ghost} = -2\int d^4x \mathrm{Tr}\left(\bar{c}\,\partial^\mu D_\mu c\right), \quad \mathcal{D}_\mu c = \partial_\mu c - ig\,[u_\mu, c], \tag{2.102}$$

where the ghost field, c, is a Grassmann scalar which transforms in the adjoint representation of the gauge group. We note that the term S^E_{GF} is quadratic in terms of u_μ, thereby contributing to the tree-level gluon propagator. In addition, S^E_{Ghost} involves an interaction between gluon and ghost fields.

The corresponding continuum action has the form:

$$\mathcal{S}^E_{\mathrm{total}} = \mathcal{S}^E_{\mathrm{SQCD}} + \mathcal{S}^E_{GF} + \mathcal{S}^E_{Ghost}. \tag{2.103}$$

Figure 2.1 illustrates all vertices of the action of SQCD of the Eq. (2.103) [48]. Four of these vertices exist also in the non-supersymmetric case (1, 5, 10, 16). The algebraic expression for each vertex, V_i ($i = 1, \ldots, 16$), has the following form:

$$V_1(k_1,k_2,k_3) = ig(2\pi)^4\delta(k_1-k_2+k_3)\gamma_{\mu_1}T^{\alpha_1}_{a_2a_3} \tag{2.104}$$

$$V_2(k_1,k_2,k_3) = g(2\pi)^4\delta(k_1-k_2+k_3)(k_{2\,\mu_1}+k_{3\,\mu_1})T^{\alpha_1}_{a_2a_3} \tag{2.105}$$

$$V_3(k_1,k_2,k_3) = -g(2\pi)^4\delta(k_1+k_2-k_3)(k_{2\,\mu_1}+k_{3\,\mu_1})T^{\alpha_1}_{a_3a_2} \tag{2.106}$$

$$V_4(k_1,k_2,k_3) = \frac{1}{2}g(2\pi)^4\delta(k_1-k_2+k_3)\gamma_{\mu_1}f^{\alpha_1\alpha_2\alpha_3} \tag{2.107}$$

$$V_5(k_1,k_2,k_3) = -ig(2\pi)^4\delta(k_1-k_2+k_3)k_{2\,\mu}f^{\alpha_1\,\alpha_2\,\alpha_3} \tag{2.108}$$

$$V_6(k_1,k_2,k_3) = -i\sqrt{2}g(2\pi)^4\delta(k_1-k_2+k_3)\frac{1-\gamma_5}{2}T^{\alpha_1}_{a_2a_3} \tag{2.109}$$

$$V_7(k_1,k_2,k_3) = -i\sqrt{2}g(2\pi)^4\delta(k_1-k_2+k_3)\frac{1+\gamma_5}{2}T^{\alpha_1}_{a_2a_3} \tag{2.110}$$

$$V_8(k_1,k_2,k_3) = i\sqrt{2}g(2\pi)^4\delta(k_1-k_2+k_3)\frac{1+\gamma_5}{2}T^{\alpha_1}_{a_3\,a_2} \tag{2.111}$$

$$V_9(k_1,k_2,k_3) = i\sqrt{2}g(2\pi)^4\delta(k_1-k_2+k_3)\frac{1-\gamma_5}{2}T^{\alpha_1}_{a_3a_2} \tag{2.112}$$

$$V_{10}(k_1,k_2,k_3) = -\frac{i}{2}g(2\pi)^4\delta(k_1+k_2+k_3)f^{\alpha_1\,\alpha_2\,\alpha_3}\delta_{\mu_1\mu_2}(k_{2\,\mu_3}-k_{1\,\mu_3}) \tag{2.113}$$

$$V_{11}(k_1,k_2,k_3,k_4) = \frac{1}{2}g^2(2\pi)^4\delta(k_1+k_2-k_3-k_4)T^{\alpha}_{a_1\,a_3}T^{\alpha}_{a_2\,a_4} \tag{2.114}$$

$$V_{12}(k_1,k_2,k_3,k_4) = \frac{1}{2}g^2(2\pi)^4\delta(k_1+k_2-k_3-k_4)T^{\alpha}_{a_3\,a_1}T^{\alpha}_{a_4\,a_2} \tag{2.115}$$

$$V_{13}(k_1,k_2,k_3,k_4) = -g^2(2\pi)^4\delta(k_1-k_2+k_3-k_4)T^{\alpha}_{a_1\,a_2}T^{\alpha}_{a_4\,a_3} \tag{2.116}$$

$$V_{14}(k_1,k_2,k_3,k_4) = g^2(2\pi)^4\delta(k_1+k_2-k_3+k_4)(T^{\alpha_1}T^{\alpha_2})_{a_3\,a_4}\delta_{\mu_1\,\mu_2} \tag{2.117}$$

$$V_{15}(k_1,k_2,k_3,k_4) = g^2(2\pi)^4\delta(k_1+k_2+k_3-k_4)(T^{\alpha_1}T^{\alpha_2})_{a_4\,a_3}\delta_{\mu_1\,\mu_2} \tag{2.118}$$

$$V_{16}(k_1,k_2,k_3,k_4) = \frac{1}{4}g^2(2\pi)^4\delta(k_1+k_2+k_3+k_4)f^{\alpha_1\,\alpha_2\,\alpha}f^{\alpha\,\alpha_3\,\alpha_4}\delta_{\mu_1\,\mu_3}\delta_{\mu_2\,\mu_4}, \tag{2.119}$$

where k_j denote momenta; $\alpha_j(a_j)$ are color indices in the adjoint(fundamental) representation; μ_j are Lorentz indices. A factor of $\int d^4k/(2\pi)^4\tilde{X}(k)$ is understood for each field X appearing in the vertex; saturation of the vertices' indices (Dirac, color, Lorentz) with those of the corresponding external fields is also implied. All these vertices are intended to be symmetrized over identical fields before contraction among the fields and creation of Feynman diagrams.

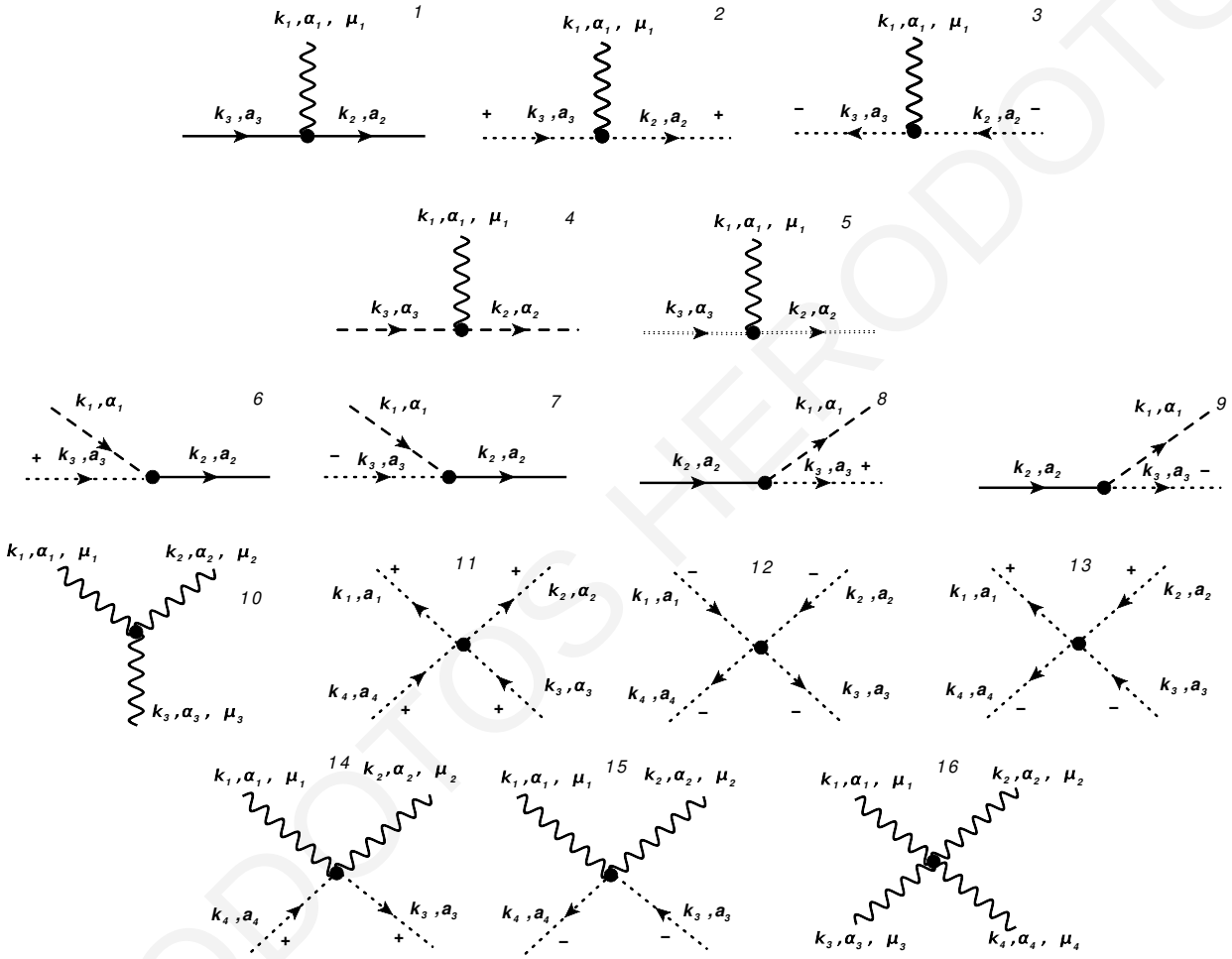

FIGURE 2.1: Vertices of the supersymmetric QCD action $\mathcal{S}^E_{\rm total}$. A wavy (solid) line represents gluons (quarks). A dotted (dashed) line corresponds to squarks (gluinos). The "double dashed" line represents the ghost field. Squark lines are further marked with a $+(-)$ sign, to denote an A_+ (A_-) field. An arrow entering (exiting) a vertex denotes a $\lambda, \psi, A_+, A_-^\dagger$ $(\bar{\lambda}, \bar{\psi}, A_+^\dagger, A_-)$ field.

Chapter 3

Supersymmetry on the Lattice

3.1 Motivation and Challenges

Unbroken SUSY dictates equal fermionic and bosonic degrees of freedom within supermultiplets. However, SUSY particles have remained elusive [51], necessitating the nonperturbative study of the SUSY breaking mechanism [43, 52]. Supersymmetric models of strongly coupled theories are a very promising models for new physics Beyond the SM and lattice investigations of supersymmetric extensions of QCD are becoming within reach. However, there are several well-known obstacles arising from the breaking of SUSY in a regularized theory on the lattice [13], including the necessity for fine tuning of the theory's bare Lagrangian [14–16].

The only way to obtain nonperturbative information for strong interacting systems is the study of QCD on the lattice. In recent years nonperturbative information for supersymmetric theories through lattice simulations is also extracted and there are many motivations for this. We can obtain nonperturbative information by supersymmetric lattice field theories that cannot be obtained by other means. From Beyond Standard Model physics side, if we want to understand mechanisms for supersymmetry breaking and why supersymmetry is not observed in low energy scales, we should study supersymmetry on the lattice. Due to asymptotic freedom, we have confinement in low energy scales so the gauge coupling of the supersymmetric action is high and hence we cannot perform a perturbative study in these energy regimes.

In addition, it is possible for a theory, which is well-defined in the perturbation theory, to arise a nonperturbative anomaly. Specifically, there is a nonperturbative, supersymmetric anomaly which can be studied only on the lattice as it is referred to [53]. Furthermore, Monte Carlo simulations on the lattice can be used as a tool to study actions which consist nonholomorphic quantities that are related to supersymmetry-breaking soft-terms that determine spectra and couplings in supersymmetric extensions to the Standard Model [14]. Another motivation for studying supersymmetry on the lattice is for better understand of dynamical supersymmetry breaking. A good formalism of the supersymmetric Yang-Mills theory (SYM) on the lattice would help us to understand the strong interactions which split the superpartners from the observed Standard Model spectrum. Moreover, for specific supersymmetric theories there are many quantities that are known precisely and thus, when they are calculated again on the lattice, the lattice analytic methods and simulations can be improved. For example, we can study the chiral symmetry breaking for $\mathcal{N} = 2$ SYM [54].

An additional significant incentive for delving into nonperturbative explorations of supersymmetric theories stems from theoretical conjectures concerning confinement mechanisms and their connections to Gauge/Gravity duality; in particular, to string/M-theory. These have their foundations in the enhanced symmetries of supersymmetric gauge theories and it would be interesting to extend and relate them to QCD or Yang-Mills theory. This requires more general insights into the nonperturbative regime of supersymmetric theories. Numerical lattice simulations would be an ideal nonperturbative first-principles tool to investigate gauge theories with SUSY. However, it is unavoidable to break SUSY in any non-trivial theory on the lattice. In general, fine tuning is required to restore supersymmetry in the continuum limit (see, e.g., Ref. [55]), which can be guided by signals provided by the SUSY Ward identities [56, 57]. The analysis of SUSY Ward identities requires the renormalization of the supercurrent [58], which can mix due to broken supersymmetry with other operators of the same or lower dimension. Even though lattice breaks $\mathcal{N} = 1$ supersymmetry explicitly [12], it is the best method at present to obtain quantitative results. There are also other theories with extended supersymmetry [59–61], which preserve some supercharges on the lattice; however in this work we focus on $\mathcal{N} = 1$ supersymmetric QCD (SQCD) which is more realistic in the sense that it is directly related to extensions of the SM.

As we referred, many notorious problems arise when formulating supersymmetric models on the lattice. Unfortunately, the lattice discretization of spacetime breaks supersymmetry for three main reasons [15]. At first, as we can observe from Eq. (2.2), the supersymmetric algebra closes on the generator of infinitesimal spacetime translations by the following anti-commutation relation:

$$\{Q_a, \bar{Q}_{\dot{b}}\} = 2\sigma^m_{a\dot{b}} P_m \,, \tag{3.1}$$

where Q_a and $\bar{Q}_{\dot{b}}$ are the spinorial generators of supersymmetry transformations. However, on the lattice there only discrete translations; there is an absent of infinitesimal translations and thus, supersymmetry breaks.

The second main reason of the supersymmetry breaking on the lattice is the fact that bosonic and fermionic fields are discretized on the lattice in different way. Specifically, in the standard discretization gauginos, which are fermionic fields, are defined on the lattice sites whilst gauge fields, which are bosonic fields, are defined on the links of the lattice. A naïve lattice formulation would produce too many fermions on the lattice and a lattice formulation without fermion doubling and with continuous chiral symmetry have been shown not to exist. Therefore, supersymmetry and chiral symmetry breaking is inevitable.

Finally, knowing that a derivative operator that obeys Leibniz rule is required for supersymmetry, we conclude that supersymmetry breaks on the lattice [11]. The reason for this is the fact that the derivative operators in discrete spacetime are finite-difference operators which do not obey Leibniz rule. Only non-local derivative and product operators can obey Leibniz rule on the lattice and many recent researches make an effort to construct formulations that balance locality and supersymmetry [62–64].

Using the lattice as a regulator requires not only breaking of supersymmetry but also breaking of symmetries, including Lorentz/rotational symmetry and chiral symmetry. However, our requirement is that all of these symmetries should only be recovered at the continuum limit [12]. In the absence of anomalies, in order to achieve this, we introduce the appropriate counterterms to the regularised Lagrangian so as to fine-tune the bare parameters since these parameters receive divergent non-supersymmetric corrections in the continuum limit. Nevertheless, some fine-tuning problems arise in theories with scalar fields regarding the scalars' mass terms. These problems are similar to that of the Higgs boson in the Standard Model. Fermion masses, Yukawa and quartic couplings

have to be fine-tuned as well and thus, they imply a high-dimensional parameter space which makes numerical lattice calculations difficult. In addition, the aforementioned counterterms can diverge with inverse powers of the lattice spacing.

However, there are some ways to reduce the amount of the parameters that need fine-tuning and thus, supersymmetry on the lattice can be analyzed numerically much easier. The first one is to consider lower-dimensional systems of supersymmetric theories. In other words, we should study theories with fewer than four spacetime dimensions by reviewing dimensional reduction. Now, in many cases, not only does the system have smaller number of degrees of freedom but supersymmetry can be also restored in the continuum limit only by a one-loop calculation.

Another way to make the numerical analysis easier is to consider the special case of minimal ($\mathcal{N} = 1$) SYM where there are no scalar fields. SYM action contains only one gauge field and its superpartner gaugino, which is a massless Majorana fermion in the adjoint representation of the gauge group. Therefore, only one parameter, the gaugino mass, has to be fine-tuned in order to obtain the correct continuum limit. If we use Ginsparg-Wilson (overlap or domain-wall) lattice fermions, we can even avoid this single fine-tuning [65]. Nevertheless, the Ginsparg-Wilson lattice fermions are not used due to high computational expense and thus, the current researches concentrate on the fine-tuning of the gaugino mass so as to keep computational costs under control. In general, we can exploit some symmetries of the action so as to reduce the number of counterterms significantly. Furthermore, we can study another special case of maximal ($\mathcal{N} = 4$) SYM, for which a closed supersymmetry subalgebra can be preserved on the lattice.

Therefore, we conclude that asymptotically free supersymmetric gauge theories can be studied nonperturbatively on the lattice. Nevertheless, we must evoke both perturbative and nonperturbative methods in order to achieve a reliable renormalization of the theory. Firstly, we should start on very small lattices and perform calculations perturbatively so as to get a good idea where to begin for weak bare couplings. These calculations are important ingredients in extracting nonperturbative information for supersymmetric theories through lattice simulations. Consequently, after the perturbative calculations, we should perform nonperturbative calculations by doing simulations into stronger coupling regimes.

3.2 Supersymmetric QCD on the Lattice and its Symmetries

In this section we concentrate on $\mathcal{N} = 1$ supersymmetry on the lattice in the Wess-Zumino (WZ) gauge. In this gauge, the SQCD Lagrangian contains the following fields: the gluon together with the gluino and one real auxiliary scalar; in addition, for each quark flavor, a Dirac fermion, two squarks and two complex auxiliary scalars. The squark fields, which are the superpartners of quarks, are complex scalar bosons whilst the gluino field, which is the superpartner of gluon, is a Majorana fermion. Note that, supersymmetry requires that the renormalized masses for quark and squark fields have to be the same.

From this point on, we switch to Euclidean space. In our lattice calculation, we extend Wilson's formulation of the QCD action, to encompass SUSY partner fields as well. In this standard discretization quarks (ψ), squarks ($A_\pm$) and gluinos (λ) live on the lattice sites, and gluons (u_μ) live on the links of the lattice: $U_\mu(x) = e^{igaT^\alpha u_\mu^\alpha(x+a\hat{\mu}/2)}$; α is a color index in the adjoint representation of the gauge group. This formulation leaves no SUSY generators intact, and it also breaks chiral symmetry; hence, the need for fine-tuning will arise in numerical simulations of SQCD. For Wilson-type quarks and gluinos, the Euclidean action $\mathcal{S}^L_{\rm SQCD}$ on the lattice becomes:

$$\begin{aligned}
\mathcal{S}^L_{\rm SQCD} &= a^4 \sum_x \Big[\frac{N_c}{g^2} \sum_{\mu,\nu} \left(1 - \frac{1}{N_c} \mathrm{Tr} U_{\mu\nu} \right) + \sum_\mu \mathrm{Tr} \left(\bar{\lambda} \gamma_\mu \mathcal{D}_\mu \lambda \right) - a \frac{r}{2} \mathrm{Tr} \left(\bar{\lambda} \mathcal{D}^2 \lambda \right) \\
&+ \sum_\mu \Big(\mathcal{D}_\mu A_+^\dagger \mathcal{D}_\mu A_+ + \mathcal{D}_\mu A_- \mathcal{D}_\mu A_-^\dagger + \bar{\psi} \gamma_\mu \mathcal{D}_\mu \psi \Big) - a \frac{r}{2} \bar{\psi} \mathcal{D}^2 \psi \\
&+ i\sqrt{2} g (A_+^\dagger \bar{\lambda}^\alpha T^\alpha P_+ \psi - \bar{\psi} P_- \lambda^\alpha T^\alpha A_+ + A_- \bar{\lambda}^\alpha T^\alpha P_- \psi - \bar{\psi} P_+ \lambda^\alpha T^\alpha A_-^\dagger) \\
&+ \frac{1}{2} g^2 (A_+^\dagger T^\alpha A_+ - A_- T^\alpha A_-^\dagger)^2 - m(\bar{\psi}\psi - m A_+^\dagger A_+ - m A_- A_-^\dagger) \Big] , \qquad (3.2)
\end{aligned}$$

where: $P_\pm = (1 \pm \gamma_5)/2$, $U_{\mu\nu}(x) = U_\mu(x) U_\nu(x + a\hat{\mu}) U_\mu^\dagger(x + a\hat{\nu}) U_\nu^\dagger(x)$, a is the lattice spacing, and a summation over flavors is understood in the last three lines of Eq. (3.2). The 4-vector x is restricted to the values $x = na$, with n being an integer 4-vector. Therefore, the integration of momentum, following a Fourier transformation, is confined to the initial Brillouin zone (BZ) $[-\pi/a, \pi/a]^4$, and considering the summation over x ensures momentum conservation at every vertex. The terms proportional to the Wilson parameter, r, eliminate the problem of fermion doubling, at the expense of breaking chiral invariance. In the limit $a \to 0$ the lattice action reproduces the continuum

(Euclidean) one. As we will describe below, the bare coupling for the Yukawa terms (third line of Eq. (3.2)) and the bare coupling for the four-squark interactions (fourth line of Eq. (3.2)) need not coincide with the gauge coupling g; this requirement will be imposed on the respective renormalized values.

The definitions of the covariant derivatives are as follows:

$$\mathcal{D}_\mu\lambda(x) \equiv \frac{1}{2a}\Big[U_\mu(x)\lambda(x+a\hat{\mu})U_\mu^\dagger(x) - U_\mu^\dagger(x-a\hat{\mu})\lambda(x-a\hat{\mu})U_\mu(x-a\hat{\mu})\Big] \tag{3.3}$$

$$\mathcal{D}^2\lambda(x) \equiv \frac{1}{a^2}\sum_\mu\Big[U_\mu(x)\lambda(x+a\hat{\mu})U_\mu^\dagger(x) - 2\lambda(x) + U_\mu^\dagger(x-a\hat{\mu})\lambda(x-a\hat{\mu})U_\mu(x-a\hat{\mu})\Big] \tag{3.4}$$

$$\mathcal{D}_\mu\psi(x) \equiv \frac{1}{2a}\Big[U_\mu(x)\psi(x+a\hat{\mu}) - U_\mu^\dagger(x-a\hat{\mu})\psi(x-a\hat{\mu})\Big] \tag{3.5}$$

$$\mathcal{D}^2\psi(x) \equiv \frac{1}{a^2}\sum_\mu\Big[U_\mu(x)\psi(x+a\hat{\mu}) - 2\psi(x) + U_\mu^\dagger(x-a\hat{\mu})\psi(x-a\hat{\mu})\Big] \tag{3.6}$$

$$\mathcal{D}_\mu A_+(x) \equiv \frac{1}{a}\Big[U_\mu(x)A_+(x+a\hat{\mu}) - A_+(x)\Big] \tag{3.7}$$

$$\mathcal{D}_\mu A_+^\dagger(x) \equiv \frac{1}{a}\Big[A_+^\dagger(x+a\hat{\mu})U_\mu^\dagger(x) - A_+^\dagger(x)\Big] \tag{3.8}$$

$$\mathcal{D}_\mu A_-(x) \equiv \frac{1}{a}\Big[A_-(x+a\hat{\mu})U_\mu^\dagger(x) - A_-(x)\Big] \tag{3.9}$$

$$\mathcal{D}_\mu A_-^\dagger(x) \equiv \frac{1}{a}\Big[U_\mu(x)A_-^\dagger(x+a\hat{\mu}) - A_-^\dagger(x)\Big]. \tag{3.10}$$

In Eqs. (3.7)-(3.10) in order to avoid a "doubling" problem for squarks we do not use the symmetric derivative; note, however, that the symmetries of the action are the same for both types of derivatives.

A discrete version of a gauge-fixing term, together with the compensating ghost field term, must be added to the action, in order to avoid divergences from the integration over gauge orbits; these terms are the same as in the non-supersymmetric case. Below, we present this appropriate gauge-fixing term:

$$S_{GF}^L = \frac{1}{2\alpha}a^2\sum_x\sum_\mu \mathrm{Tr}\left(u_\mu(x+a\hat{\mu}/2) - u_\mu(x-a\hat{\mu}/2)\right)^2 , \tag{3.11}$$

and the compensating ghost field term:

$$\begin{aligned} S^L_{Ghost} &= 2a^2 \sum_x \sum_\mu \mathrm{Tr}\{(\bar{c}(x+a\hat{\mu}) - \bar{c}(x))(c(x+a\hat{\mu}) - c(x) \\ &+ ig[u_\mu(x+a\hat{\mu}/2), c(x)] + \frac{1}{2} ig[u_\mu(x+a\hat{\mu}/2), c(x+a\hat{\mu}) - c(x)] \\ &- \frac{1}{12} g^2 [u_\mu(x+a\hat{\mu}/2), [u_\mu(x+a\hat{\mu}/2), c(x+a\hat{\mu}) - c(x)]])\} + \mathcal{O}(g^3). \end{aligned} \tag{3.12}$$

It is worth mentioning that in simulations there is no need for gauge fixing since functional integration is performed over a finite number of degrees of freedom (d.o.f.), each of which ranges within the compact domain of the group manifold. However, in perturbation theory, where an infinite number of d.o.f. takes values over the noncompact algebra, gauge fixing is necessary in order to avoid divergences from the integration over gauge orbits.

Similarly, a standard "measure" term must be added to the action, in order to account for the Jacobian in the change of integration variables: $U_\mu \to u_\mu$:

$$S^L_M = \frac{g^2 N_c}{12} a^2 \sum_x \sum_\mu \mathrm{Tr}\,(u_\mu(x+a\hat{\mu}/2))^2 + \mathcal{O}(g^4). \tag{3.13}$$

Therefore, the total lattice action of SQCD is:

$$\mathcal{S}^L_{\text{total}} = \mathcal{S}^L_{\text{SQCD}} + \mathcal{S}^L_{GF} + \mathcal{S}^L_{Ghost} + S^L_M. \tag{3.14}$$

Note that computations on the lattice are much more complicated than continuum computations. One main reason for this is that there are more vertices stemming from the discretized action and thus, they lead to more Feynman diagrams; what is harder, the propagators and vertices, with which one builds the Feynman diagrams, are also more complicated on the lattice than they are in the continuum, which can lead to expressions containing a very large number of terms.

At this point, we present the tree-level propagators on the lattice as they have been calculated in [48]:

$$\text{Quark Propagator :} \qquad \frac{1}{i\not{q} + \frac{2r}{a}\sum_\mu \sin^2(aq_\mu/2) - m}$$

$$\text{Gluon Propagator :} \qquad \frac{1}{\hat{q}^2}\left(\delta_{\mu\nu} - (1-\alpha)\frac{\hat{q}_\mu \hat{q}_\nu}{\hat{q}^2}\right)$$

$$\text{Ghost Propagator :} \qquad \frac{1}{\hat{q}^2}$$

$$\text{Squark Propagator :} \qquad \frac{1}{\hat{q}^2 + m^2}$$

$$\text{Gluino Propagator :} \qquad \frac{2}{i\mathring{\not{q}} + \frac{2r}{a}\sum_\mu \sin^2(aq_\mu/2)},$$

where:

$$\mathring{\not{q}} = \frac{1}{a}\sum_\mu \gamma_\mu \sin(aq_\mu)$$
$$\hat{q}_\mu = \frac{2}{a}\sin\frac{aq_\mu}{2}, \quad \hat{q}^2 = \sum_\mu \hat{q}_\mu^2.$$

Below, we also illustrate the algebraic expressions of the vertices of the lattice action of SQCD of the Eq. (3.14) in momentum space [48]. The additional vertices on the lattice are presented in Fig. 3.1. In these expressions we have rescaled all momenta k_i to the range $[-\pi, \pi]$ and omitted overall powers of a.

$$V_1(k_1,k_2,k_3) = ig(2\pi)^4\delta(k_1-k_2+k_3)T^{\alpha_1}_{a_2a_3}\left(\gamma_{\mu_1}\cos\left(\frac{(k_2+k_3)_{\mu_1}}{2}\right) - ir\sin\left(\frac{(k_2+k_3)_{\mu_1}}{2}\right)\right) \quad (3.15)$$

$$V_2(k_1,k_2,k_3) = 2g(2\pi)^4\delta(k_1-k_2+k_3)T^{\alpha_1}_{a_2a_3}\sin\left(\frac{(k_2+k_3)_{\mu_1}}{2}\right) \quad (3.16)$$

$$V_3(k_1,k_2,k_3) = -2g(2\pi)^4\delta(k_1-k_2+k_3)T^{\alpha_1}_{a_3a_2}\sin\left(\frac{(k_2+k_3)_{\mu_1}}{2}\right) \quad (3.17)$$

$$V_4(k_1,k_2,k_3) = \frac{1}{2}g(2\pi)^4\delta(k_1-k_2+k_3)f^{\alpha_1\alpha_2\alpha_3}\left(\gamma_{\mu_1}\cos\left(\frac{(k_2+k_3)_{\mu_1}}{2}\right) - ir\sin\left(\frac{(k_2+k_3)_{\mu_1}}{2}\right)\right) \quad (3.18)$$

$$V_5(k_1,k_2,k_3) = -2\,i\,g\,(2\pi)^4\delta(k_1-k_2+k_3)\,f^{\alpha_1\alpha_2\alpha_3}\cos\left(\frac{k_{3\,\mu_1}}{2}\right)\sin\left(\frac{k_{2\,\mu_1}}{2}\right) \quad (3.19)$$

$$V_6(k_1,k_2,k_3) = -i\sqrt{2}g(2\pi)^4\delta(k_1-k_2+k_3)\frac{1-\gamma_5}{2}T^{\alpha_1}_{a_2a_3} \quad (3.20)$$

$$V_7(k_1,k_2,k_3) = -i\sqrt{2}g(2\pi)^4\delta(k_1-k_2-k_3)\frac{1+\gamma_5}{2}T^{\alpha_1}_{a_2a_3} \quad (3.21)$$

$$V_8(k_1,k_2,k_3) = i\sqrt{2}g(2\pi)^4\delta(-k_1+k_2-k_3)\frac{1+\gamma_5}{2}T^{\alpha_1}_{a_3a_2} \quad (3.22)$$

$$V_9(k_1,k_2,k_3) = i\sqrt{2}g(2\pi)^4\delta(-k_1+k_2+k_3)\frac{1-\gamma_5}{2}T^{\alpha_1}_{a_3a_2} \tag{3.23}$$

$$V_{10}(k_1,k_2,k_3) = ig(2\pi)^4\delta(k_1+k_2+k_3)\delta_{\mu_1\,\mu_2}f^{\alpha_1\alpha_2\alpha_3}\cos\left(\frac{k_{3\,\mu_1}}{2}\right)\sin\left(\frac{(k_1-k_2)_{\mu_3}}{2}\right) \tag{3.24}$$

$$V_{11}(k_1,k_2,k_3,k_4) = \frac{1}{2}g^2(2\pi)^4\delta(k_1+k_2-k_3-k_4)T^{\alpha}_{a_1\,a_3}T^{\alpha}_{a_2\,a_4} \tag{3.25}$$

$$V_{12}(k_1,k_2,k_3,k_4) = \frac{1}{2}g^2(2\pi)^4\delta(k_1+k_2-k_3-k_4)T^{\alpha}_{a_3\,a_1}T^{\alpha}_{a_4\,a_2} \tag{3.26}$$

$$V_{13}(k_1,k_2,k_3,k_4) = -g^2(2\pi)^4\delta(k_1-k_2+k_3-k_4)T^{\alpha}_{a_1\,a_2}T^{\alpha}_{a_4\,a_3} \tag{3.27}$$

$$V_{14}(k_1,k_2,k_3,k_4) = g^2(2\pi)^4\delta(k_1+k_2-k_3+k_4)\delta_{\mu_1\,\mu_2}(T^{\alpha_1}T^{\alpha_2})_{a_3\,a_4}\cos\left(\frac{(k_3+k_4)_{\mu_1}}{2}\right) \tag{3.28}$$

$$V_{15}(k_1,k_2,k_3,k_4) = g^2(2\pi)^4\delta(k_1+k_2-k_3+k_4)\delta_{\mu_1\,\mu_2}(T^{\alpha_1}T^{\alpha_2})_{a_4\,a_3}\cos\left(\frac{(k_3+k_4)_{\mu_1}}{2}\right) \tag{3.29}$$

$$\begin{aligned}V_{16}(k_1,k_2,k_3,k_4) &= -g^2(2\pi)^4\delta(k_1+k_2+k_3+k_4)\mathrm{Tr}(T^{\alpha_1}T^{\alpha_2}T^{\alpha_3}T^{\alpha_4})\times\\
&\Big[\delta_{\mu_1\mu_2\mu_3\mu_4}\left(\frac{2}{3}-\frac{2}{3}\sum_\rho\cos(k_{1\,\rho})+\frac{1}{2}\sum_\rho\cos(k_1+k_2)_\rho\right)\\
&+\delta_{\mu_1\mu_2\mu_3}\left(-\frac{4}{3}\sin\left(\frac{k_{4\,\mu_1}}{2}\right)\sin\left(\frac{k_{4\,\mu_4}}{2}\right)+2\sin\left(\frac{k_{4\,\mu_1}}{2}\right)\sin\left(\frac{(2k_1+k_4)_{\mu_4}}{2}\right)+2\sin\left(\frac{k_{4\,\mu_1}}{2}\right)\sin\left(\frac{(2k_3+k_4)_{\mu_4}}{2}\right)\right)\\
&+\delta_{\mu_1\mu_2}\delta_{\mu_3\mu_4}\left(\cos\left(\frac{(k_3+k_4)_{\mu_1}}{2}\right)\cos\left(\frac{(k_3+k_4)_{\mu_3}}{2}\right)-2\cos\left(\frac{(k_3-k_4)_{\mu_1}}{2}\right)\cos\left(\frac{(k_3+k_4)_{\mu_3}}{2}\right)\right)\\
&+\delta_{\mu_1\mu_3}\delta_{\mu_2\mu_4}\left(\cos\left(\frac{(k_1-k_3)_{\mu_2}}{2}\right)\cos\left(\frac{(k_2-k_4)_{\mu_1}}{2}\right)\right)\Big]\end{aligned} \tag{3.30}$$

$$\begin{aligned}V_{17}(k_1,k_2,k_3,k_4) &= \frac{1}{2}g^2(2\pi)^4\delta(k_1+k_2-k_3+k_4)\delta_{\mu_1\,\mu_2}(T^{\alpha_1}T^{\alpha_2})_{a_3a_4}\times\\
&\left(-i\gamma_{\mu_1}\sin\left(\frac{(k_3+k_4)_{\mu_1}}{2}\right)+r\cos\left(\frac{(k_3+k_4)_{\mu_1}}{2}\right)\right)\end{aligned} \tag{3.31}$$

$$\begin{aligned}V_{18}(k_1,k_2,k_3,k_4) &= \frac{1}{4}g^2(2\pi)^4\delta(k_1+k_2-k_3+k_4)\delta_{\mu_1\,\mu_2}f^{\alpha_1\alpha_3\alpha}f^{\alpha_2\alpha_4\alpha}\times\\
&\left(-i\gamma_{\mu_1}\sin\left(\frac{(k_3+k_4)_{\mu_1}}{2}\right)+r\cos\left(\frac{(k_3+k_4)_{\mu_1}}{2}\right)\right)\end{aligned} \tag{3.32}$$

$$V_{19}(k_1,k_2,k_3,k_4) = -\frac{1}{3}g^2\delta_{\mu_1\,\mu_2}(2\pi)^4\delta(k_1+k_2-k_3+k_4)f^{\alpha_1\alpha_3\alpha}f^{\alpha_2\alpha_4\alpha}\sin\left(\frac{k_{3\,\mu_1}}{2}\right)\sin\left(\frac{k_{4\,\mu_1}}{2}\right) \tag{3.33}$$

$$V_{20}(k_1,k_2) = \frac{1}{12}N_c\,g^2\delta_{\mu_1\,\mu_2}(2\pi)^4\delta(k_1+k_2)\mathrm{Tr}(T^{\alpha_1}\,T^{\alpha_2}). \tag{3.34}$$

The Eq. (3.14) represents the most general lattice action for SQCD consistent with the symmetries that the lattice preserve. The gauge group of the action depends on the number of color of the theory, N_c, and hence the gauge group is $SU(N_c)$. The action also depends on the number of flavors, N_f. We could write down an action with non zero gluino mass for numerical stability and then extrapolate to chiral limit $m_\lambda \to 0$. Obviously, this chiral limit coincides with the supersymmetric limit.

As in the continuum, the matter fields, which are the quark and squark fields, are in the fundamental representation of the gauge group whereas the gauge fields, which are the gluon and gluino fields, are in adjoint representation of the gauge group. Although

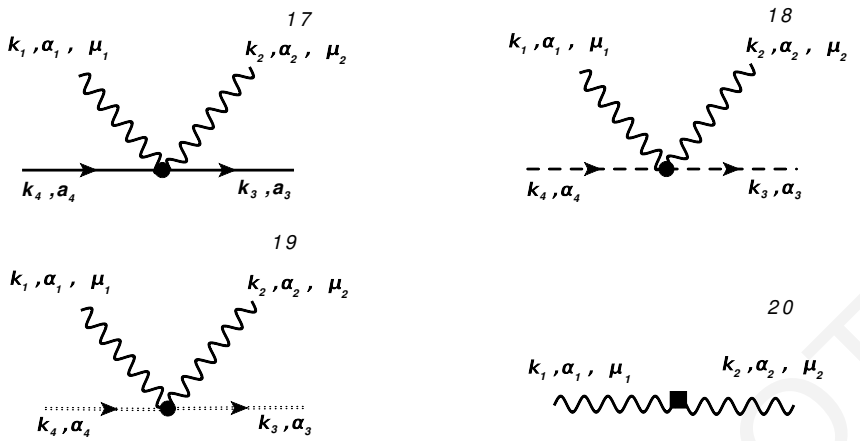

FIGURE 3.1: Additional vertices of SQCD on the lattice. We have the same notation as in Fig. 2.1. The solid box of the vertex 20 comes from the measure part of the lattice action.

the action is not gauge invariant due to the gauge-fixing and ghost field terms, it is invariant under the BRS transformations which are presented below [48, 49, 66]:

$$\begin{aligned}
u_\mu^\alpha &\rightarrow u_\mu^\alpha + (\partial_\mu c^a + g c_{\alpha\beta\gamma} c^\beta A_\mu^\gamma)\ \xi \\
\lambda &\rightarrow \lambda + g c^\alpha \lambda^\beta f^{\beta\alpha\gamma} T^\gamma\ \xi \\
c^\alpha &\rightarrow c^\alpha - \frac{g}{2} f^{\alpha\beta\gamma} c^\beta c^\gamma\ \xi \\
\bar{c}^\alpha &\rightarrow \bar{c}^\alpha + \partial_\mu u_\mu^\alpha\ \xi \\
\psi &\rightarrow \psi + i g T^\alpha c^\alpha \psi\ \xi \\
\bar{\psi} &\rightarrow \bar{\psi} + i g \bar{\psi} T^\alpha c^\alpha\ \xi \\
A_+ &\rightarrow A_+ - i g c^\alpha T^\alpha A_+\ \xi \\
A_+^\dagger &\rightarrow A_+^\dagger + i g A_+^\dagger c^\alpha T^\alpha\ \xi \\
A_- &\rightarrow A_- + i g A_- c^\alpha T^\alpha\ \xi \\
A_-^\dagger &\rightarrow A_-^\dagger - i g c^\alpha T^\alpha A_-^\dagger\ \xi\,,
\end{aligned} \tag{3.35}$$

where ξ is an infinitesimal Grassmann variable.

Parity ($\mathcal{P}$) and charge conjugation ($\mathcal{C}$) are symmetries of the continuum theory that are preserved exactly in the lattice formulation. Their definitions are presented below:

$$\mathcal{P}: \begin{cases} U_0(x) \to U_0(x_{\mathcal{P}})\,, \qquad U_k(x) \to U_k^{\dagger}(x_{\mathcal{P}} - a\hat{k})\,, \qquad k = 1,2,3 \\ \psi(x) \to \gamma_0 \psi(x_{\mathcal{P}}) \\ \bar{\psi}(x) \to \bar{\psi}(x_{\mathcal{P}})\gamma_0 \\ \lambda^{\alpha}(x) \to \gamma_0 \lambda^{\alpha}(x_{\mathcal{P}}) \\ \bar{\lambda}^{\alpha}(x) \to \bar{\lambda}^{\alpha}(x_{\mathcal{P}})\gamma_0 \\ A_{\pm}(x) \to A_{\mp}^{\dagger}(x_{\mathcal{P}}) \\ A_{\pm}^{\dagger}(x) \to A_{\mp}(x_{\mathcal{P}}) \end{cases} \tag{3.36}$$

where $x_{\mathcal{P}} = (-\mathbf{x}, x_0)$.

$$\mathcal{C}: \begin{cases} U_{\mu}(x) \to U_{\mu}^{\star}(x)\,, \quad \mu = 0,1,2,3 \\ \psi(x) \to -C\bar{\psi}(x)^T \\ \bar{\psi}(x) \to \psi(x)^T C^{\dagger} \\ \lambda(x) \to C\bar{\lambda}(x)^T \\ \bar{\lambda}(x) \to -\lambda(x)^T C^{\dagger} \\ A_{\pm}(x) \to A_{\mp}(x) \\ A_{\pm}^{\dagger}(x) \to A_{\mp}^{\dagger}(x) \end{cases} \tag{3.37}$$

where ^{T} means transpose (also in the $SU(N_c)$ generators implicit in the gluino fields). The matrix C satisfies: $(C\gamma_{\mu})^T = C\gamma_{\mu}$, $C^T = -C$ and $C^{\dagger}C = 1$. In four dimensions, in a standard basis for γ matrices, in which $\gamma_0,\ \gamma_2$ ($\gamma_1,\ \gamma_3$) are symmetric (antisymmetric), $C = -\mathrm{i}\gamma_0\gamma_2$.

Further symmetries of the continuum action, at the classical level, are $\mathcal{R}$ and χ. The $U(1)_R$ symmetry, $\mathcal{R}$, rotates the quark and gluino fields in opposite direction:

$$\mathcal{R}: \begin{cases} \psi(x) \to e^{i\theta\gamma_5}\psi(x) \\ \bar{\psi}(x) \to \bar{\psi}(x)e^{i\theta\gamma_5} \\ \lambda(x) \to e^{-i\theta\gamma_5}\lambda(x) \\ \bar{\lambda}(x) \to \bar{\lambda}(x)e^{-i\theta\gamma_5} \end{cases} \tag{3.38}$$

$\mathcal{R}$-symmetry does not commute with the SUSY transformation. The $U(1)_A$ symmetry, χ, rotates the squark and the quark fields in the same direction as follows:

$$\chi : \begin{cases} \psi(x) \to e^{i\theta'\gamma_5}\psi(x) \\ \bar{\psi}(x) \to \bar{\psi}(x)e^{i\theta'\gamma_5} \\ A_{\pm}(x) \to e^{i\theta'}A_{\pm}(x) \\ A^{\dagger}_{\pm}(x) \to e^{-i\theta'}A^{\dagger}_{\pm}(x) \end{cases} \tag{3.39}$$

However, the two terms with the Wilson parameter of the lattice action break these two symmetries in order to remedy the fermion doubling problem.

Chapter 4

Fine-tuning of the Yukawa and Quartic Couplings in SQCD

4.1 Introduction

As we mentioned in the previous chapter, there are several obstacles arising from the breaking of supersymmetry in a regularized theory on the lattice, including the necessity for fine-tuning of the theory's bare Lagrangian. We address these problems via perturbative calculations, to one loop and to the lowest order in the lattice spacing so as to restore supersymmetry in the continuum limit. The quantities, which we calculate in this chapter, are important ingredients in extracting nonperturbative information for supersymmetric theories through lattice simulations. Furthermore, the renormalization factors are necessary ingredients in relating lattice matrix elements to physical amplitudes.

Note that the coupling constants appearing in the lattice action are not all identical. The gauge invariance of the lattice SQCD action dictates that some of the action's interaction terms will share the same coupling constant, g (gauge coupling). This is particularly applicable to the kinematic terms containing covariant derivatives, resulting in gluons coupling with quarks, squarks, gluinos, and other gluons, all governed by the same gauge coupling constant. The Yukawa interactions involving quarks, squarks, and gluinos, as well as the four-squark interactions, have the potential to feature distinct couplings, at the quantum level. Furthermore, new terms may also emerge, necessitating careful fine-tuning on the lattice. By exploiting the

symmetries of the Wilson lattice action, we can predict these potentially novel interaction terms. Moreover, with the actual computation we can understand if they will arise at the quantum level, and more importantly we can determine their renormalizations to certain perturbative order. It is desirable to employ a lattice discretization that preserves as many continuum symmetries as possible, thereby reducing the number of relevant parameters requiring fine-tuning.

In this chapter, we investigate the fine-tuning of parameters in $\mathcal{N} = 1$ Supersymmetric QCD, discretized on a Euclidean lattice with the gauge group $SU(N_c)$ and N_f flavors in the fundamental representation. Specifically, we study the renormalization of the Yukawa (gluino-squark-quark interactions) and the quartic (four-squark interactions) couplings. To deduce the renormalization factors and the coefficients of the counterterms we compute, perturbatively to one-loop and to the lowest order in the lattice spacing, the relevant three-point and four-point Green's functions using both dimensional and lattice regularizations.

Note that in Refs. [48] and [66], the first lattice perturbative computations in the context of SQCD were presented; apart from the Yukawa and the quartic couplings [67, 68], the renormalization of all parameters and fields appearing in Eq. (3.2) have been extracted by using Wilson gluons and fermions. The results in Refs. [48] and [66] will find further use in the present work.

4.2 Fine-Tuning of the Yukawa Couplings

4.2.1 Computational Setup

In some previous works [69–71], the mixing of certain composite operators upon renormalization was studied. The symmetries of the action play a crucial role to identify the candidate mixing operators. Similarly, in this work, we examine the transformation properties of Yukawa-type operators (gauge-invariant operators of dimension-four, composed of one gluino, one quark, and one squark field) under both parity $\mathcal{P}$ and charge conjugation $\mathcal{C}$, and we have determined which specific linear combinations of them remain unchanged. All potential Yukawa terms and their transformation properties are detailed in Table 4.1. Note that all operators that we consider here are flavor singlets.

Operators	$\mathcal{C}$	$\mathcal{P}$
$A_+^\dagger \bar{\lambda} P_+ \psi$	$-\bar{\psi} P_+ \lambda A_-^\dagger$	$A_- \bar{\lambda} P_- \psi$
$\bar{\psi} P_- \lambda A_+$	$-A_- \bar{\lambda} P_- \psi$	$\bar{\psi} P_+ \lambda A_-^\dagger$
$A_- \bar{\lambda} P_- \psi$	$-\bar{\psi} P_- \lambda A_+$	$A_+^\dagger \bar{\lambda} P_+ \psi$
$\bar{\psi} P_+ \lambda A_-^\dagger$	$-A_+^\dagger \bar{\lambda} P_+ \psi$	$\bar{\psi} P_- \lambda A_+$
$A_+^\dagger \bar{\lambda} P_- \psi$	$-\bar{\psi} P_- \lambda A_-^\dagger$	$A_- \bar{\lambda} P_+ \psi$
$\bar{\psi} P_+ \lambda A_+$	$-A_- \bar{\lambda} P_+ \psi$	$\bar{\psi} P_- \lambda A_-^\dagger$
$A_- \bar{\lambda} P_+ \psi$	$-\bar{\psi} P_+ \lambda A_+$	$A_+^\dagger \bar{\lambda} P_- \psi$
$\bar{\psi} P_- \lambda A_-^\dagger$	$-A_+^\dagger \bar{\lambda} P_- \psi$	$\bar{\psi} P_+ \lambda A_+$

TABLE 4.1: Gluino-squark-quark dimension-4 operators which are gauge invariant and flavor singlet. All matter fields carry an implicit flavor index.

The transformation properties of the Yukawa terms, as shown in Table 4.1, allow two distinct linear combinations of Yukawa-type operators:

$$Y_1 \equiv A_+^\dagger \bar{\lambda} P_+ \psi - \bar{\psi} P_- \lambda A_+ + A_- \bar{\lambda} P_- \psi - \bar{\psi} P_+ \lambda A_-^\dagger \,, \tag{4.1}$$

$$Y_2 \equiv A_+^\dagger \bar{\lambda} P_- \psi - \bar{\psi} P_+ \lambda A_+ + A_- \bar{\lambda} P_+ \psi - \bar{\psi} P_- \lambda A_-^\dagger \,. \tag{4.2}$$

The first combination aligns with the third line of Eq. (3.2). However, at the quantum level, the second combination may emerge, having a potentially different Yukawa coupling. All terms within each of the combinations in Eqs. (4.1) and (4.2) are multiplied by a Yukawa coupling, denoted as g_{Y_1} and g_{Y_2}, respectively. In the classical continuum limit, g_{Y_1} corresponds to g, while g_{Y_2} vanishes.

Both Yukawa terms commute with $\mathcal{R}$. However the quark mass terms do not. Thus, if we insist on a theory with massive quarks, $\mathcal{R}$ is not a symmetry. χ leaves invariant each of the four constituents of the Yukawa term (Eq. (4.1)), but it changes the constituents of the "mirror" Yukawa term (i.e. a term with all P_+ and P_- interchanged) by phases $e^{2i\theta'}$ and $e^{-2i\theta'}$.

Thus the continuum action is classically invariant separately under χ and $\mathcal{R}$ (for massless quarks), or under $\chi \times \mathcal{R}$ (where the phases in χ and $\mathcal{R}$ are chosen to be opposite, so that quarks are left unchanged) for massive quarks. The lattice action with Ginsparg-Wilson (GW) gluinos, even in the presence of Wilson quarks and/or a quark mass, will also be classically invariant under $\chi \times \mathcal{R}$ (with opposite phases:

$\theta = -\theta'$); it is interesting to study how this symmetry will develop an anomaly in the quantum level. The structure of counterterms on the lattice becomes simpler if both GW gluinos and GW quarks is employed: Even in such a case, terms proportional to the tree-level Green's functions of the mirror Yukawa will appear in lattice Green's functions, just as they do in the continuum Green's functions, as a consequence of the anomalous symmetries; however, these terms will coincide in the bare lattice and continuum Green's functions, and no further lattice counterterms [such as our Eq. (4.43)] will be required. Another interesting feature of the SQCD action which can be investigated on the lattice, making use of GW gluinos and massless GW quarks, is the conservation of an anomaly-free combination of $\chi \times \mathcal{R}$, taking into account the values of the parameters N_c and N_f [72] which enter the phases of χ and $\mathcal{R}$.

In our investigation, we compute perturbatively the relevant three-point Green's functions with external gluino, quark and squark fields, using both the Dimensional Regularization (DR) and the Lattice Regularization (LR). In DR the regulator, ϵ, is defined by $D \equiv 4 - 2\epsilon$; in the LR the lattice spacing, a, serves as regulator for the UV divergences. Each Green's function which contributes to the one-loop expression of the Yukawa couplings, consists of three Feynman diagrams shown in Fig. 4.1. The renormalizations of fundamental fields and the gauge coupling are a prerequisite for the renormalization of the Yukawa coupling, since renormalization conditions in 3-point-vertex corrections (with external gluino, quark and squark fields) involve these quantities. More specifically, combining the results for the bare Green's functions on the lattice with the renormalized Green's functions (obtained in $\overline{\rm MS}$ via DR), and using the renormalization factors for the gluino, quark, squark fields as well as the renormalization of the gauge coupling, we extract the renormalization and counterterms of the Yukawa couplings appropriate to the lattice regularization and the $\overline{\rm MS}$ renormalization scheme.

Before we turn our attention to the calculation, notice that there exist several prescriptions [73, 74] for defining γ_5 in D dimensions, such as the naïve dimensional regularization (NDR) [75], the t'Hooft-Veltman (HV) [76], the $DRED$ [77] and the $DR\overline{EZ}$ prescriptions (see, e.g., Ref. [78]). These prescriptions are linked via finite conversion relations [79]. In our calculation, we apply the NDR and HV prescriptions. The latter does not violate Ward identities involving pseudoscalar and axial-vector operators in D dimensions [75]. The Dirac matrices, γ_μ, are Hermitian in

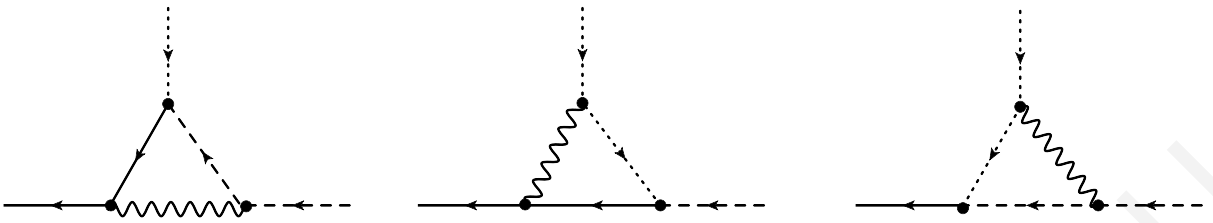

FIGURE 4.1: One-loop Feynman diagrams leading to the fine-tuning of g_{Y_1} and g_{Y_2}. A wavy (solid) line represents gluons (quarks). A dotted (dashed) line corresponds to squarks (gluinos). In the above diagrams the directions of the external line depend on the particular Green's function under study. An arrow entering (exiting) a vertex denotes a $\lambda, \psi, A_+, A_-^\dagger$ ($\bar{\lambda}, \bar{\psi}, A_+^\dagger, A_-$) field. Squark lines could be further marked with a $+(-)$ sign, to denote an A_+ (A_-) field.

D-dimensional Euclidean space and satisfy the following relations:

$$\eta_{\mu\nu}\eta_{\mu\nu} = D, \qquad \{\gamma_\mu, \gamma_\nu\} = 2\delta_{\mu\nu}\mathbb{1}. \tag{4.3}$$

In NDR, the definition of γ_5 satisfies:

$$\{\gamma_5, \gamma_\mu\} = 0, \ \forall\mu, \tag{4.4}$$

whereas in HV it satisfies:

$$\{\gamma_5, \gamma_\mu\} = 0, \ \mu = 1,2,3,4, \qquad [\gamma_5, \gamma_\mu] = 0, \ \mu > 4. \tag{4.5}$$

NDR is known to be an inconsistent regularization; in particular, a calculation of the triangle diagram does not reproduce the axial anomaly, leading to the incorrect result that the axial current is conserved. Thus, our use of NDR will serve only to highlight its effect on Green's functions such as Eqs. (4.14)-(4.19), pointing out how some opposite chirality terms are absent in NDR. Our end results [see Eqs. (4.42)-(4.43)] will employ the HV prescription ($c_{\rm hv} = 1$).

4.2.2 Renormalization in Dimensional Regularization

At this point we will present our one-loop results for the bare three-point Green's functions and the renormalization factors of the Yukawa couplings in the $\overline{\rm MS}$ scheme, using both dimensional (DR) and lattice (LR) regularizations [80]. For the renormalization of g_{Y_1} and g_{Y_2}, we impose renormalization conditions which result in the cancellation of divergences of the corresponding bare three-point amputated

Green's functions with external gluino-squark-quark fields. The application of the renormalization factors on the bare Green's functions leads to the renormalized Green's functions, which are independent of the regulator (ϵ in DR, a in LR).

Given that we are interested in the $\overline{\rm MS}$ renormalization of the Yukawa couplings, and that $\overline{\rm MS}$ is a mass-independent renormalization scheme, we are free to treat all particles (in particular, quarks and squarks) as massless. In the next section [81], regarding the quartic (4-squark) couplings in SQCD, we choose instead to treat quarks and squarks as massive, in order to avoid the emergence of spurious infrared divergences. A mass-independent scheme allows us to make use of techniques for evaluating Feynman diagrams which have been developed to very high perturbative order (see, e.g., [82–87]). Still perturbative calculations become exceedingly complicated on the lattice, and consequently, calculations beyond two loops are practically unfeasible.

The calculation of the amputated tree-level Green's functions is straightforward and their expressions are[1]:

$$\langle \lambda^{\alpha_1}(q_1) A_+(q_3) \bar{\psi}(q_2) \rangle^{\rm tree} = -\frac{i}{2}\, g_{Y_1}\, (2\pi)^4 \delta(q_1 - q_2 + q_3)\, (1+\gamma_5)\, T^{\alpha_1}/\sqrt{2} \quad (4.6)$$

$$\langle \psi(q_2) A_+^\dagger(q_3) \bar{\lambda}^{\alpha_1}(q_1) \rangle^{\rm tree} = \frac{i}{2}\, g_{Y_1}\, (2\pi)^4 \delta(q_1 - q_2 + q_3)\, (1-\gamma_5)\, T^{\alpha_1}/\sqrt{2} \quad (4.7)$$

$$\langle \lambda^{\alpha_1}(q_1) A_-^\dagger(q_3) \bar{\psi}(q_2) \rangle^{\rm tree} = -\frac{i}{2}\, g_{Y_1}\, (2\pi)^4 \delta(q_1 - q_2 + q_3)\, (1-\gamma_5)\, T^{\alpha_1}/\sqrt{2} \quad (4.8)$$

$$\langle \psi(q_2) A_-(q_3) \bar{\lambda}^{\alpha_1}(q_1) \rangle^{\rm tree} = \frac{i}{2}\, g_{Y_1}\, (2\pi)^4 \delta(q_1 - q_2 + q_3)\, (1+\gamma_5)\, T^{\alpha_1}/\sqrt{2}, \quad (4.9)$$

where our conventions for Fourier transformations are:

$$\tilde{\psi}(q) = \int d^4x\, e^{-iq\cdot x}\, \psi(x), \quad (4.10)$$

$$\tilde{A}_\pm(q) = \int d^4x\, e^{\mp iq\cdot x}\, A_\pm(x), \quad (4.11)$$

$$\tilde{u}_\mu(q) = \int d^4x\, e^{-iq\cdot x}\, u_\mu(x), \quad (4.12)$$

$$\tilde{\lambda}(q) = \int d^4x\, e^{-iq\cdot x}\, \lambda(x). \quad (4.13)$$

[1]Note that the indices coming from the color in fundamental representation and the Dirac indices are left implicit. On the contrary, the color in the adjoint representation is shown explicitly.

The procedure of calculating the renormalization in the $\overline{\text{MS}}$ scheme entails performing first the perturbative calculations of the Green's function in DR; this is unavoidable by the very nature of the $\overline{\text{MS}}$ scheme. The comparison with the same Green's functions calculated in LR will lead to the lattice renormalizations in the $\overline{\text{MS}}$ scheme.

The calculations presented in this section could ideally be performed using generic external momenta. However, for convenience of computation, we are free to make appropriate choices of these momenta; the resulting renormalization factors will not be affected at all. By inspection of the propagators and vertices in the diagrams of Fig. 4.1, we conclude that no superficial infrared divergences will be generated, if any one of the three external momenta is set to zero; in what follows, we calculate the corresponding diagrams by setting to zero only one of these momenta. The choice of the external momenta for Green's functions will not affect their pole parts in DR or their logarithmic dependence on the lattice spacing in LR. Therefore, the three choices for each three-point Green's function will provide a useful consistency check.

There are, in total, 4 different gluino-squark-quark Green's functions, depending on whether the external squark field is $A_+/A_+^\dagger/A_-/A_-^\dagger$. We present first the four Green's functions for the three choices of external momentum in DR. To avoid heavy notation we have omitted Dirac/flavor/color indices[2] on the Green's functions of Eqs. (4.14)-(4.19).

$$\langle\lambda^{\alpha_1}(0)A_+(q_3)\bar{\psi}(q_2)\rangle^{DR,1\text{loop}} = -\langle\psi(q_2)A_-(q_3)\bar{\lambda}^{\alpha_1}(0)\rangle^{DR,1\text{loop}} = -i\,(2\pi)^4\delta(q_2-q_3)\frac{g_{Y_1}g^2}{16\pi^2}\frac{1}{4\sqrt{2}N_c}T^{\alpha_1}\times$$
$$\left[-3(1+\gamma_5)+((1+\alpha)(1+\gamma_5)+8\gamma_5 c_{\text{hv}})N_c^2+(1+\gamma_5)(-\alpha+(3+2\alpha)N_c^2)\left(\frac{1}{\epsilon}+\log\left(\frac{\bar{\mu}^2}{q_2^2}\right)\right)\right] \tag{4.14}$$

$$\langle\lambda^{\alpha_1}(q_1)A_+(q_3)\bar{\psi}(0)\rangle^{DR,1\text{loop}} = -\langle\psi(0)A_-(q_3)\bar{\lambda}^{\alpha_1}(q_1)\rangle^{DR,1\text{loop}} = -i\,(2\pi)^4\delta(q_1+q_3)\frac{g_{Y_1}g^2}{16\pi^2}\frac{1}{4\sqrt{2}N_c}T^{\alpha_1}\times$$
$$\left[((4+\alpha)(1+\gamma_5)+8\gamma_5 c_{\text{hv}})N_c^2+(1+\gamma_5)(-\alpha+(3+2\alpha)N_c^2)\left(\frac{1}{\epsilon}+\log\left(\frac{\bar{\mu}^2}{q_1^2}\right)\right)\right] \tag{4.15}$$

$$\langle\lambda^{\alpha_1}(q_1)A_+(0)\bar{\psi}(q_2)\rangle^{DR,1\text{loop}} = -\langle\psi(q_2)A_-(0)\bar{\lambda}^{\alpha_1}(q_1)\rangle^{DR,1\text{loop}} = -i\,(2\pi)^4\delta(q_1-q_2)\frac{g_{Y_1}g^2}{16\pi^2}\frac{1}{4\sqrt{2}N_c}T^{\alpha_1}\times$$
$$\left[-\alpha(1+\gamma_5)+((4+3\alpha)(1+\gamma_5)+8\gamma_5 c_{\text{hv}})N_c^2+(1+\gamma_5)(-\alpha+(3+2\alpha)N_c^2)\left(\frac{1}{\epsilon}+\log\left(\frac{\bar{\mu}^2}{q_1^2}\right)\right)\right] \tag{4.16}$$

[2]The color indices in the adjoint representation are shown explicitly.

$$\langle\psi(q_2)A_+^\dagger(q_3)\bar{\lambda}^{\alpha_1}(0)\rangle^{DR,1\text{loop}} = -\langle\lambda^{\alpha_1}(0)A_-^\dagger(q_3)\bar{\psi}(q_2)\rangle^{DR,1\text{loop}} = -i\,(2\pi)^4\delta(q_2-q_3)\frac{g_{Y_1}g^2}{16\pi^2}\frac{1}{4\sqrt{2}N_c}T^{\alpha_1}\times$$
$$\left[3(1-\gamma_5)-((1+\alpha)(1-\gamma_5)-8\gamma_5 c_{\rm hv})N_c^2-(1-\gamma_5)(-\alpha+(3+2\alpha)N_c^2)\left(\frac{1}{\epsilon}+\log\left(\frac{\bar{\mu}^2}{q_2^2}\right)\right)\right] \tag{4.17}$$

$$\langle\psi(0)A_+^\dagger(q_3)\bar{\lambda}^{\alpha_1}(q_1)\rangle^{DR,1\text{loop}} = -\langle\lambda^{\alpha_1}(q_1)A_-^\dagger(q_3)\bar{\psi}(0)\rangle^{DR,1\text{loop}} = -i\,(2\pi)^4\delta(q_1+q_3)\frac{g_{Y_1}g^2}{16\pi^2}\frac{1}{4\sqrt{2}N_c}T^{\alpha_1}\times$$
$$\left[(-(4+\alpha)(1-\gamma_5)N_c^2+8\gamma_5 c_{\rm hv})N_c^2-(1-\gamma_5)(-\alpha+(3+2\alpha)N_c^2)\left(\frac{1}{\epsilon}+\log\left(\frac{\bar{\mu}^2}{q_1^2}\right)\right)\right] \tag{4.18}$$

$$\langle\psi(q_2)A_+^\dagger(0)\bar{\lambda}^{\alpha_1}(q_1)\rangle^{DR,1\text{loop}} = -\langle\lambda^{\alpha_1}(q_1)A_-^\dagger(0)\bar{\psi}(q_2)\rangle^{DR,1\text{loop}} = -i\,(2\pi)^4\delta(q_1-q_2)\frac{g_{Y_1}g^2}{16\pi^2}\frac{1}{4\sqrt{2}N_c}T^{\alpha_1}\times$$
$$\left[\alpha(1-\gamma_5)+(-(4+3\alpha)(1-\gamma_5)+8\gamma_5 c_{\rm hv})N_c^2-(1-\gamma_5)(-\alpha+(3+2\alpha)N_c^2)\left(\frac{1}{\epsilon}+\log\left(\frac{\bar{\mu}^2}{q_1^2}\right)\right)\right], \tag{4.19}$$

where $c_{\rm hv}=0\,(1)$ for the NDR (HV) prescription of γ_5. The pole parts do not depend on $c_{\rm hv}$. Further, in the NDR prescription, all one-loop bare Green's functions are proportional to the tree-level ones. The above one-loop Green's functions indeed confirm that the pole parts are the same for different choices of the external momenta and that they are proportional to the tree-level value. In HV, the fact that the first quantum corrections (one-loop) of these Green's functions have finite parts which are not proportional to their tree-level counterparts [i.e., in addition to terms with $(1\pm\gamma_5)$, they contain also terms with $(1\mp\gamma_5)$], is a consequence of the chiral anomaly; the same finite parts will necessarily appear also in LR. The need for introducing appropriate counterterms, which connect $\overline{\rm MS}$ renormalized Green's functions to SUSY invariant Green's functions, is indicated by the supersymmetric Ward Identities [88]. The value of the coefficients multiplying these counterterms requires a purely continuum calculation, including Eqs. (4.14)-(4.19); the same coefficients can be applied to the renormalization functions extracted in LR. The appearance of such counterterms, which are crucial to restore all SUSY relations among couplings, was extensively discussed within the algebraic renormalization approach to SUSY theories [89–91].

Note that the terms in Eqs. (4.14)-(4.19) involving multiplication by $c_{\rm hv}\gamma_5$ can be equivalently expressed as: $\frac{1}{2}c_{\rm hv}\left((1+\gamma_5)-(1-\gamma_5)\right)$. Terms with reversed chirality account for the mirror Yukawa interactions; given that they are pole free, they will

have no effect on a straightforward $\overline{\rm MS}$ renormalization. However, if one opts for a renormalization scheme in which these terms are absent, one must add a finite Y_2 counterterm to the action of the form:

$$\mathcal{L}^{\rm ct}_{Y_2} \equiv i\,\sqrt{2}\,g_{Y_2}Y_2, \;\; \text{where}: g_{Y_2} = 2g^3 N_c\, c_{\rm hv}/(16\pi^2) + \mathcal{O}(g^5). \tag{4.20}$$

This term, as well as Eqs. (4.14)-(4.19), become relevant in our lattice calculations as they contribute to finite fine-tuning terms in the lattice action.

The difference between the renormalized Green's functions and the corresponding Green's functions regularized on the lattice allows us to deduce the one-loop lattice renormalizations factors. The renormalization factors of the fields and the gauge coupling constant can be found in Ref. [48]. For the sake of completeness we present their definition here:

$$\psi \equiv \psi^B = Z_\psi^{-1/2}\,\psi^R, \tag{4.21}$$
$$u_\mu \equiv u_\mu^B = Z_u^{-1/2}\,u_\mu^R, \tag{4.22}$$
$$\lambda \equiv \lambda^B = Z_\lambda^{-1/2}\,\lambda^R, \tag{4.23}$$
$$c \equiv c^B = Z_c^{-1/2}\,c^R, \tag{4.24}$$
$$g \equiv g^B = Z_g^{-1}\,\mu^\epsilon\,g^R, \tag{4.25}$$

where B stands for the bare and R for renormalized quantities and μ is an arbitrary scale with dimensions of inverse length. For one-loop calculations, the distinction between g^R and g^B is inessential in many cases; we will simply use g in those cases. The Yukawa coupling is renormalized as follows:

$$g_{Y_1} \equiv g^B_{Y_1} = Z^{-1}_{Y_1} Z_g^{-1} \mu^\epsilon g^R, \tag{4.26}$$

where at the lowest perturbative order $Z_g Z_{Y_1} = 1$, and the renormalized Yukawa coupling coincides with the gauge coupling.

In DR, we are interested in getting rid of the pole parts in bare continuum Green's functions; this requires not only the renormalization factors of the fields and of the gauge coupling, Z_g, but also a further factor Z_{Y_1} for the bare Yukawa coupling. Note also that the components of the squark fields may mix at the quantum level, via a 2×2 mixing matrix (Z_A). We define the renormalization mixing matrix for the squark fields

as follows:

$$\begin{pmatrix} A_+^R \\ A_-^{R\dagger} \end{pmatrix} = \left(Z_A^{1/2}\right) \begin{pmatrix} A_+^B \\ A_-^{B\dagger} \end{pmatrix}. \tag{4.27}$$

In Ref. [48] we found that in the DR and $\overline{\rm MS}$ scheme this 2×2 mixing matrix is diagonal. On the lattice, this matrix is non-diagonal, leading to a mixing of the components A_+ and A_- with $A_-^\dagger$ and $A_+^\dagger$, respectively. Consequently, the renormalization conditions on the lattice become more intricate. As we referred, we focus on the $\overline{\rm MS}$ scheme, using both DR and LR regularizations. Given that SUSY is broken by either regulator and that SUSY-noninvariant gauge fixing is employed, it is anticipated that a nontrivial fine-tuning for the Yukawa coupling will be necessary.

Taking as an example the Green's function in DR with external squark field A_+, the renormalization condition up to g^2 will be given by:

$$\langle\lambda(q_1)A_+(q_3)\bar\psi(q_2)\rangle\Big|^{\overline{\rm MS}} = Z_\psi^{-1/2}Z_\lambda^{-1/2}(Z_A^{-1/2})_{++}\langle\lambda(q_1)A_+(q_3)\bar\psi(q_2)\rangle\Big|^{\rm bare}. \tag{4.28}$$

All appearances of coupling constants in the right-hand side of Eq. (4.28) must be expressed in terms of their renormalized values, via Eqs. (4.25)-(4.26). The left-hand side of Eq. (4.28) is just the $\overline{\rm MS}$ (free of pole parts) renormalized Green's function. Similar to Eq. (4.28), the other renormalization conditions which involve the external squark fields $A_+^\dagger, A_-, A_-^\dagger$ are understood. The renormalization factors $Z = \mathbb{1} + \mathcal{O}(g^2)$ should more properly be denoted as $Z^{X,Y}$, where X is the regularization and Y the renormalization scheme.

For the sake of clarity and comprehensiveness, the updated expressions for the renormalization factors of the fields and of the gauge coupling in DR which are involved in the right-hand side of Eq. (4.28) are[3]:

$$Z_\psi^{DR,\overline{\rm MS}} = 1 + \frac{g^2\,C_F}{16\,\pi^2}\frac{1}{\epsilon}\,(1+\alpha) \tag{4.29}$$

$$Z_{A_\pm}^{DR,\overline{\rm MS}} = 1 + \frac{g^2\,C_F}{16\,\pi^2}\frac{1}{\epsilon}\,(-1+\alpha) \tag{4.30}$$

$$Z_\lambda^{DR,\overline{\rm MS}} = 1 + \frac{g^2}{16\,\pi^2}\frac{1}{\epsilon}\,(\alpha\,N_c + N_f) \tag{4.31}$$

$$Z_g^{DR,\overline{\rm MS}} = 1 + \frac{g^2}{16\,\pi^2}\frac{1}{\epsilon}\left(\frac{3}{2}N_c - \frac{1}{2}N_f\right), \tag{4.32}$$

[3]The expressions for $Z_\psi, Z_{A_\pm}, Z_\lambda$ and Z_g (Eqs. (4.29)-(4.32), Eqs. (4.36)-(4.39)) appeared also in Ref. [48]; however, a factor of $1/2$ was missing in diagrams involving open internal gluino lines. For a more detailed explanation, see Appendix A.

where $C_F = (N_c^2 - 1)/(2\,N_c)$ is the quadratic Casimir operator in the fundamental representation. The expressions in Eqs. (4.29)-(4.32) take carefully into account the effect of the Majorana nature of gluinos in the functional integral. In Appendix A, we provide a more comprehensive discussion and treatment of the gluino field; in particular, we focus on the effect of Yukawa terms in SQCD, which are clearly absent in pure SUSY Yang-Mills.

Substituting Eqs. (4.29)-(4.32) in Eq. (4.28), and by virtue of the fact that the counterterm Eq. (4.20) contains no pole parts, we extract the value of $Z_{Y_1}^{DR,\overline{\rm MS}}$; this value is the same for all gluino-squark-quark Green's functions and for all choices of the external momenta which we have considered:

$$Z_{Y_1}^{DR,\overline{\rm MS}} = 1 + \mathcal{O}(g^4)\,. \tag{4.33}$$

Eq. (4.33) means that, at the quantum-level, the renormalization of the Yukawa coupling in DR is not affected by one-loop corrections. This observation has important implications for our understanding of the renormalization scheme in SQCD. It shows also that the corresponding renormalization on the lattice will be finite. Although, the mirror Yukawa term does not appear in $\overline{\rm MS}$ renormalization using DR, a finite admixture of this term will arise in $\overline{\rm MS}$ on the lattice. We expect that the $\overline{\rm MS}$ renormalization factors of gauge invariant quantities will turn out to be gauge-independent also on the lattice, as was the case of $Z_{Y_1}^{DR,\overline{\rm MS}}$.

4.2.3 Renormalization in Lattice Regularization

We now turn to the lattice regularization. As emphasized earlier, even though the renormalization of the squark fields in the $\overline{\rm MS}$ scheme and in DR is diagonal, on the lattice it is not; the mixing between the squark components $(A_+,\, A_-^\dagger)$ (and, similarly, $(A_+^\dagger,\, A_-)$) appears on the lattice through the 2×2 symmetric matrix Z_A, whose nondiagonal matrix elements are nonzero. The renormalization conditions are not as simple as is shown in Eq. (4.28); instead, they involve the following pairs of Green's functions:

$$\begin{aligned} &\langle \lambda(q_1) A_+(q_3) \bar{\psi}(q_2) \rangle \quad \text{with} \quad \langle \lambda(q_1) A_-^\dagger(q_3) \bar{\psi}(q_2) \rangle \\ &\langle \psi(q_2) A_+^\dagger(q_3) \bar{\lambda}(q_1) \rangle \quad \text{with} \quad \langle \psi(q_2) A_-(q_3) \bar{\lambda}(q_1) \rangle \end{aligned} \tag{4.34}$$

The appearance of the mirror Yukawa coupling, g_{Y_2}, is another feature of the use of Wilson gluinos, which increases the degree of difficulty on the lattice. The $\chi \times \mathcal{R}$ symmetry is broken by using Wilson discretization and thus lattice bare Green's functions are not invariant under $\chi \times \mathcal{R}$ at the quantum level. This difficulty may be avoided with chirality preserving actions, but the implementation of these actions in numerical simulations is very time consuming.

Thus, in the calculation of bare Green's functions on the lattice, one-loop spurious contributions will arise, which will need to be removed by introducing mirror Yukawa counterterms in the action. The renormalization condition is the following:

$$\langle \lambda(q_1) A_+(q_3) \bar{\psi}(q_2) \rangle \Big|^{\overline{\rm MS}} = Z_\psi^{-1/2} Z_\lambda^{-1/2} \langle \lambda(q_1) ((Z_A^{-1/2})_{++} A_+(q_3) + (Z_A^{-1/2})_{+-} A_-^\dagger(q_3)) \bar{\psi}(q_2) \rangle \Big|^{\rm bare} . \tag{4.35}$$

It is understood that the bare couplings on the right-hand side of this equation must be converted into the corresponding renormalized ones, making use of Z_g and Z_{Y_1}; a mirror Yukawa term also contributes, with a coupling constant g_{Y_2} which will be determined in what follows. Eq. (4.35) consists of two types of contributions with opposite chiralities; matching each of these to the $\overline{\rm MS}$ expressions found in DR, Eqs. (4.14)-(4.16), amounts to two separate conditions, which will be used to determine the two unknowns Z_{Y_1} and g_{Y_2}. Analogous equations hold for the other gluino-squark-quark Green's functions and may be calculated for consistency checks.

To offer a self-contained presentation, we revisit a collection of lattice results outlined in Ref. [48]:

$$Z_\psi^{LR,\overline{\rm MS}} = 1 + \frac{g^2 C_F}{16\pi^2} \left(-16.7235 + 3.7920\alpha - (1+\alpha) \log\left(a^2 \bar{\mu}^2\right) \right), \tag{4.36}$$

$$\begin{aligned} \left(Z_A^{1/2}\right)^{LR,\overline{\rm MS}} = \mathbb{1} - \frac{g^2 C_F}{16\pi^2} \Bigg\{ & \left[16.9216 - 3.7920\alpha - (1-\alpha) \log\left(a^2 \bar{\mu}^2\right) \right] \begin{pmatrix} 1 & 0 \\ 0 & 1 \end{pmatrix} \\ & -0.1623 \begin{pmatrix} 0 & 1 \\ 1 & 0 \end{pmatrix} \Bigg\}, \end{aligned} \tag{4.37}$$

$$\begin{aligned} Z_\lambda^{LR,\overline{\rm MS}} = 1 - \frac{g^2}{16\pi^2} \Bigg[& N_c \left(16.6444 - 3.7920\alpha + 2\alpha \log\left(a^2 \bar{\mu}^2\right) \right) \\ & + N_f \left(0.07907 + 2 \log\left(a^2 \bar{\mu}^2\right) \right) \Bigg], \end{aligned} \tag{4.38}$$

$$Z_g^{LR,\overline{\rm MS}} = 1+\frac{g^2}{16\,\pi^2}\left[-9.8696\frac{1}{N_c}+N_c\left(12.8904-\frac{3}{2}\log\left(a^2\,\bar{\mu}^2\right)\right)\right.$$
$$\left.-N_f\left(0.4811-\frac{1}{2}\log(a^2\,\bar{\mu}^2)\right)\right]. \tag{4.39}$$

The lattice three-point Green's functions involve the same Feynman diagrams as in Fig. 4.1. At first perturbative order, $\mathcal{O}(g^2)$, Eq. (4.35) and its counterparts involve only the difference between the one-loop $\overline{\rm MS}$-renormalized and bare lattice Green's functions. Having checked that alternative choices of the external momenta give the same results for these differences, we present them only for zero gluino momentum. Additionally, we should mention that the errors on our lattice expressions are smaller than the last shown digit and the Wilson parameter, r was set to its default value: $r=1$.

$$\begin{aligned}
&\langle\lambda^{\alpha_1}(0)A_+(q_3)\bar{\psi}(q_2)\rangle^{\overline{\rm MS},1{\rm loop}}-\langle\lambda^{\alpha_1}(0)A_+(q_3)\bar{\psi}(q_2)\rangle^{LR,1{\rm loop}}\\
&=-\langle\psi(q_2)A_-(q_3)\bar{\lambda}^{\alpha_1}(0)\rangle^{\overline{\rm MS},1{\rm loop}}+\langle\psi(q_2)A_-(q_3)\bar{\lambda}^{\alpha_1}(0)\rangle^{LR,1{\rm loop}}\\
&=i\,(2\pi)^4\delta(q_2-q_3)\frac{g_{Y_1}g^2}{16\pi^2}\frac{1}{8\sqrt{2}N_c}T^{\alpha_1}\times\left[-3.7920\alpha(1+\gamma_5)+(1+\gamma_5)(\alpha-(3+2\alpha)N_c^2)\log\left(a^2\bar{\mu}^2\right)\right.\\
&\qquad\left.+(-3.6920+5.9510\gamma_5+7.5840\alpha(1+\gamma_5)-8\gamma_5 c_{\rm hv})N_c^2\right],
\end{aligned}\tag{4.40}$$

$$\begin{aligned}
&\langle\psi(q_2)A_+^\dagger(q_3)\bar{\lambda}^{\alpha_1}(0)\rangle^{\overline{\rm MS},1{\rm loop}}-\langle\psi(q_2)A_+^\dagger(q_3)\bar{\lambda}^{\alpha_1}(0)\rangle^{LR,1{\rm loop}}\\
&=-\langle\lambda^{\alpha_1}(0)A_-^\dagger(q_3)\bar{\psi}(q_2)\rangle^{\overline{\rm MS},1{\rm loop}}+\langle\lambda^{\alpha_1}(0)A_-^\dagger(q_3)\bar{\psi}(q_2)\rangle^{LR,1{\rm loop}}\\
&=i\,(2\pi)^4\delta(q_2-q_3)\frac{g_{Y_1}g^2}{16\pi^2}\frac{1}{8\sqrt{2}N_c}T^{\alpha_1}\times\left[3.79201\alpha(1-\gamma_5)+(1-\gamma_5)(-\alpha+(3+2\alpha)N_c^2)\log\left(a^2\bar{\mu}^2\right)\right.\\
&\qquad\left.+(3.6920+5.9510\gamma_5-7.5840\alpha(1-\gamma_5)-8\gamma_5 c_{\rm hv})N_c^2\right].
\end{aligned}\tag{4.41}$$

As expected, the above expressions are momentum-independent, and they are linear combinations of the tree-level expressions stemming from the Yukawa vertex and its mirror; also, all corresponding decimal coefficients between Eqs. (4.40) and (4.41) coincide, and we have checked that they are the same for any other choice of external momenta, as they should. Thus, we are led to a unique result for ${Z_{Y_1}}^{LR,\overline{\rm MS}}$ and also for ${g_{Y_2}}^{LR,\overline{\rm MS}}$. By combining the lattice expressions with the $\overline{\rm MS}$-renormalized Green's functions calculated in the continuum (see Eq. (4.35)), we find for the renormalization

factors:

$$Z_{Y_1}{}^{LR,\overline{\rm MS}} = 1 + \frac{g^2}{16\,\pi^2}\left(\frac{1.45833}{N_c} + 2.40768 N_c + 0.520616 N_f\right), \tag{4.42}$$

$$g_{Y_2}{}^{LR,\overline{\rm MS}} = \frac{g^3}{16\,\pi^2}\left(\frac{-0.040580}{N_c} + 0.45134 N_c\right). \tag{4.43}$$

We note that the above factors are gauge independent in the $\overline{\rm MS}$ scheme, as expected from the principles of renormalization and gauge invariance. Furthermore, the multiplicative renormalization $Z_{Y_1}^{LR,\overline{\rm MS}}$ and the coefficient $g_{Y_2}^{LR,\overline{\rm MS}}$ of the mirror Yukawa counterterm are finite as one can predict from the continuum calculation. These findings shed light on the fine-tunings for the lattice SQCD action. They suggest that while the renormalization process in $\overline{\rm MS}$ is well-behaved on the lattice, it still exhibits an intriguing connection with the mirror Yukawa term through $g_{Y_2}^{LR,\overline{\rm MS}}$.

4.3 Fine-Tuning and Counterterms for the Quartic Couplings

4.3.1 Computational Setup

As previously mentioned the coupling constants appearing in the lattice action are not all identical. In the previous section we study the fine-tuning of the Yukawa interaction, an interaction between quarks, squarks and gluinos. In this section our focus shifts to investigating the fine-tuning of the quartic couplings, which characterize the four-squark interactions. Our methodology involves calculations of Green's functions with four external squarks, extending up to one loop and to the lowest order in the lattice spacing. These Green's functions are not only crucial for understanding the perturbative aspects of the theory but also play a pivotal role in unraveling nonperturbative insights into supersymmetric theories. For instance, they are instrumental in studying phenomena such as the supersymmetric phase transition through the analysis of the four-squark effective potential [50].

In this section, we present our one-loop calculations for the bare 4-point Green's functions and the renormalization factors of the quartic couplings in the $\overline{\rm MS}$ scheme, employing both dimensional regularization (DR) and lattice regularization (LR). To renormalize the quartic couplings, we impose specific renormalization conditions,

ensuring the cancellation of divergences in the corresponding bare 4-point amputated Green's functions with four external squark fields. Applying these renormalization factors to the bare Green's functions yields the renormalized Green's functions, which are independent of the regulator (ϵ in DR, a in LR).

To identify the four external squark fields, we consider gauge symmetry constraints. Consequently, we determine that two squark fields must belong to the fundamental representation, while the other two must belong to the antifundamental representation; ignoring flavor indices, there are ten possibilities for choosing the four external fields:

$$\begin{aligned}
&(A_+^\dagger A_+)(A_+^\dagger A_+), \quad (A_- A_-^\dagger)(A_- A_-^\dagger), \\
&(A_+^\dagger A_+)(A_- A_-^\dagger), \quad (A_+^\dagger A_-^\dagger)(A_+^\dagger A_-^\dagger), \quad (A_- A_+)(A_- A_+), \quad (A_- A_+)(A_+^\dagger A_-^\dagger), \\
&(A_+^\dagger A_+)(A_+^\dagger A_-^\dagger), \quad (A_+^\dagger A_+)(A_- A_+), \quad (A_- A_-^\dagger)(A_+^\dagger A_-^\dagger), \quad (A_- A_-^\dagger)(A_- A_+).
\end{aligned} \tag{4.44}$$

Pairs of squark fields in parenthesis denote color-singlet combinations. Noting that the Green's function with the four external squark fields $(A_+^\dagger A_+)(A_- A_-^\dagger)$ yields identical outcomes as the Green's function with the four external squark fields $(A_- A_+)(A_+^\dagger A_-^\dagger)$. We also notice that only the four external squark fields of the first three terms from Eq. (4.44) appear in the SQCD action.

By requiring that the above terms must be also invariant under symmetries of the SQCD action; one must further take into account $\mathcal{C}$ and $\mathcal{P}$ to construct combinations which are invariant under these symmetries. There are five combinations as shown in Table 4.2.

Operators	$\mathcal{C}$	$\mathcal{P}$
$\lambda_1(A_+^\dagger\, T^\alpha\, A_+ + A_-\, T^\alpha\, A_-^\dagger)^2/2$	+	+
$\lambda_2[(A_+^\dagger A_-^\dagger)^2 + (A_- A_+)^2]$	+	+
$\lambda_3(A_+^\dagger A_+)(A_- A_-^\dagger)$	+	+
$\lambda_4(A_+^\dagger A_-^\dagger)(A_- A_+)$	+	+
$\lambda_5(A_+^\dagger A_-^\dagger + A_- A_+)(A_+^\dagger A_+ + A_- A_-^\dagger)$	+	+

TABLE 4.2: Dimension-4 operators which are gauge invariant and flavor singlets. All operators appearing in this table are eigenstates of charge conjugation, $\mathcal{C}$, and parity, $\mathcal{P}$, with eigenvalue 1. In the above operators, squark fields carry flavor indices. The symbols λ_i are five quartic couplings.

When applying the transformation $\chi \times \mathcal{R}$ to the combinations listed in Table 4.2, $(A_+^\dagger A_-^\dagger)^2 + (A_- A_+)^2$ and $(A_+^\dagger A_-^\dagger + A_- A_+)(A_+^\dagger A_+ + A_- A_-^\dagger)$ are not invariant; however, due to the potential anomaly in $\chi \times \mathcal{R}$ symmetry, they may appear in our one-loop computations.

The first combination in Table 4.2 aligns with the first term of the fourth line of Eq. (3.2). However, at the quantum level, the other combinations may emerge, having a potentially different quartic couplings, denoted as λ_{2-5}. In the classical continuum limit, λ_1 corresponds to g, while λ_{2-5} vanishes.

4.3.2 Renormalization in Dimensional Regularization

Below, we present the amputated tree-level Green's functions, whose Feynman diagrams are shown in Fig. 4.2, with four external squarks:

$$\begin{aligned}\langle A_{+\,f_1}^{\dagger\alpha_1}(q_1) A_{+\,f_2}^{\dagger\alpha_2}(q_2)\, A_{+\,f_3}^{\alpha_3}(q_3) A_{+\,f_4}^{\alpha_4}(q_4)\rangle^{\text{tree}} &= \frac{1}{2N_c}\, g^2\,(-1-\alpha)\times \\ &\Big[\delta_{f_1 f_3}\delta_{f_2 f_4}(-\delta^{\alpha_1\alpha_3}\delta^{\alpha_2\alpha_4} + N_c\,\delta^{\alpha_1\alpha_4}\delta^{\alpha_2\alpha_3}) \\ &+ \delta_{f_1 f_4}\delta_{f_2 f_3}(-\delta^{\alpha_1\alpha_4}\delta^{\alpha_2\alpha_3} + N_c\,\delta^{\alpha_1\alpha_3}\delta^{\alpha_2\alpha_4})\Big]\end{aligned} \tag{4.45}$$

$$\begin{aligned}\langle A_{-\,f_1}^{\dagger\alpha_1}(q_1) A_{-\,f_2}^{\dagger\alpha_2}(q_2)\, A_{-\,f_3}^{\alpha_3}(q_3) A_{-\,f_4}^{\alpha_4}(q_4)\rangle^{\text{tree}} &= \frac{1}{2N_c}\, g^2\,(-1-\alpha)\times \\ &\Big[\delta_{f_1 f_3}\delta_{f_2 f_4}(-\delta^{\alpha_3\alpha_1}\delta^{\alpha_4\alpha_2} + N_c\,\delta^{\alpha_4\alpha_1}\delta^{\alpha_3\alpha_2}) \\ &+ \delta_{f_1 f_4}\delta_{f_2 f_3}(-\delta^{\alpha_4\alpha_1}\delta^{\alpha_3\alpha_2} + N_c\,\delta^{\alpha_3\alpha_1}\delta^{\alpha_4\alpha_2})\Big]\end{aligned} \tag{4.46}$$

$$\langle A_{+\,f_1}^{\dagger\alpha_1}(q_1) A_{+\,f_2}^{\alpha_2}(q_2)\, A_{-\,f_3}^{\dagger\alpha_3}(q_3) A_{-\,f_4}^{\alpha_4}(q_4)\rangle^{\text{tree}} = \frac{1}{2N_c}\, g^2\,(1-\alpha)\delta_{f_1 f_2}\delta_{f_3 f_4}\,(N_c\,\delta^{\alpha_1\alpha_3}\delta^{\alpha_4\alpha_2} - \delta^{\alpha_1\alpha_2}\delta^{\alpha_4\alpha_3})\,, \tag{4.47}$$

where f_i are the flavour indices of the external squark fields. The rest of the tree-level Green's functions with four external squarks are zero.

The tree-level values of quartic couplings which satisfy SUSY are:

$$\lambda_1 = g^2,\;\; \lambda_2 = \lambda_3 = \lambda_4 = \lambda_5 = 0\,. \tag{4.48}$$

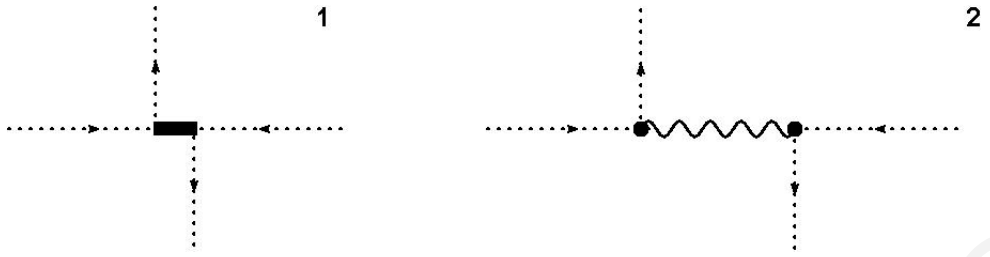

FIGURE 4.2: Tree-level Feynman diagrams with four external squark fields. The second diagram can have mirror variants. A wavy line represents gluons and a dotted line corresponds to squarks. Squark lines could be further marked with a $+(-)$ sign, to denote an A_+ (A_-) field. The 4-squark vertex of the action has been denoted by a solid rectangle, in order to indicate the squark-antisquark pairing; all remaining vertices are denoted by a solid circle.

These couplings receive quantum corrections, coming from the Feynman diagrams which are one-particle irreducible (1PI) and one-particle reducible (1PR) and are shown in Figs. 4.3 and 4.4, respectively. Note that here we introduce a non-zero mass for quarks and squarks in order to avoid IR divergences. It is worth mentioning that the Majorana nature of gluinos manifests itself in some diagrams, in which $\lambda - \lambda$ as well as $\bar{\lambda} - \bar{\lambda}$ propagators appear. The Majorana condition is the following:

$$(\bar{\lambda}^{\alpha})^T = C\lambda^{\alpha}\,, \tag{4.49}$$

and the tree-level propagators that relate $\lambda - \lambda$ and $\bar{\lambda} - \bar{\lambda}$ are:

$$\langle \lambda^{\alpha_1}(q_1)\lambda^{\alpha_2}(q_2)\rangle^{\text{tree}} = 2i\,\delta^{\alpha_1\alpha_2}\delta(q_1+q_2)\frac{1}{\not{q}_1}C^{\dagger} \tag{4.50}$$

$$\langle \bar{\lambda}^{\alpha_1}(q_1)\bar{\lambda}^{\alpha_2}(q_2)\rangle^{\text{tree}} = -2i\,C\,\delta^{\alpha_1\alpha_2}\delta(q_1+q_2)\frac{1}{\not{q}_2}\,. \tag{4.51}$$

In order to obtain the renormalized quartic couplings, we impose renormalization conditions which result in the cancellation of divergences in the corresponding bare four-point Green's functions with external squark fields and thus, the renormalization factors are defined in such a way as to remove all divergences.

Note that in order to compute the four-point Green's functions, we have to symmetrize over identical external fields. As in the case of the Yukawa coupling [80], for convenience of computation, we are free to make appropriate choices of the external momenta. Having checked that no superficial IR divergences are generated,

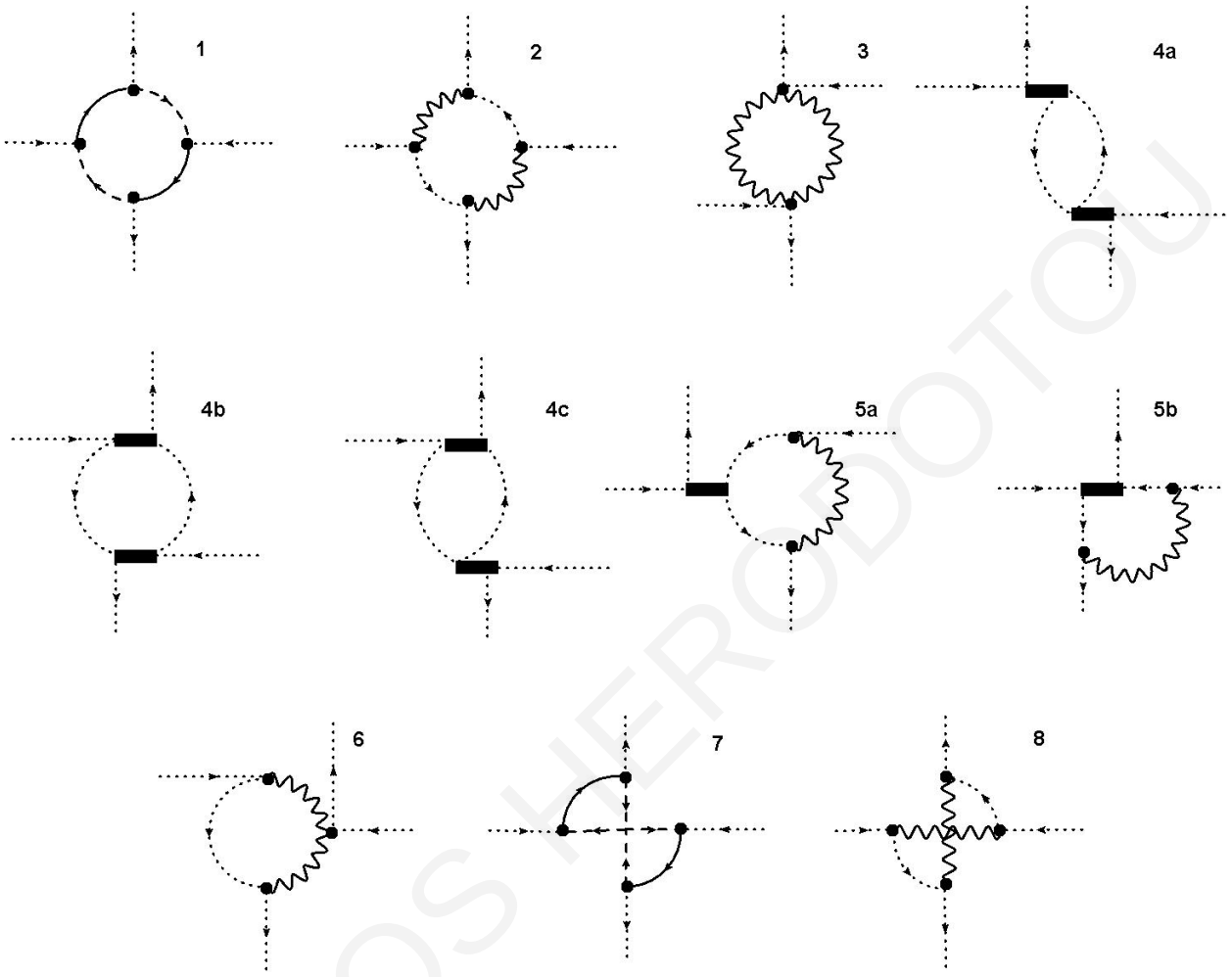

FIGURE 4.3: One-loop 1PI Feynman diagrams leading to the fine-tuning of the quartic couplings. A wavy (solid) line represents gluons (quarks). A dotted (dashed) line corresponds to squarks (gluinos). In the above diagrams the directions of the external line depend on the particular Green's function under study. An arrow entering (exiting) a vertex denotes a $\lambda, \psi, A_+, A_-^\dagger$ ($\bar{\lambda}, \bar{\psi}, A_+^\dagger, A_-$) field. The 4-squark vertex of the action has been denoted by a solid rectangle, in order to indicate the squark-antisquark pairing; all remaining vertices are denoted by a solid circle. Squark lines could be further marked with a $+(-)$ sign, to denote an A_+ (A_-) field. All diagrams can have mirror variants. In diagrams 4 and 5, there are additional variants in which two external outgoing (or incoming) lines stem from a 4-squark vertex.

we compute the diagrams by setting the 2 external momenta of the squark fields in the fundamental representation to zero.

The choice of the external momenta for Green's functions does not affect their pole parts in DR or their logarithmic dependence on the lattice spacing in LR. Since the

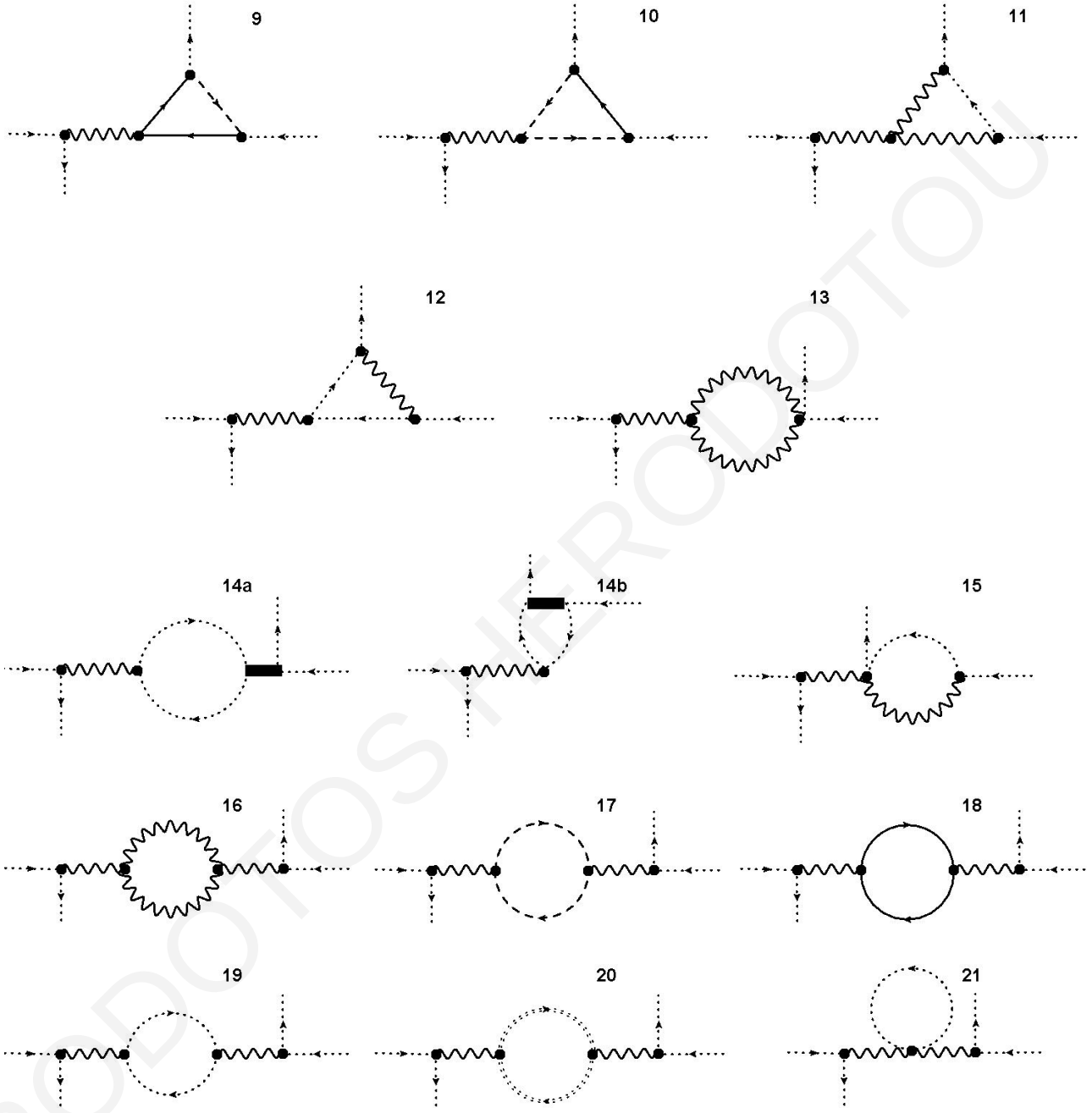

FIGURE 4.4: One-loop 1PR Feynman diagrams leading to the fine-tuning of the quartic couplings. Notation is identical to that of Figure 4.3. Note that the "double dashed" line is the ghost field. All diagrams can have mirror variants. Unlike gluon tadpoles which vanish in dimensional regularization, the massive squark tadpole gives a nonzero contribution (diagram 21).

difference between the $\overline{\text{MS}}$-renormalized and the corresponding bare Green's function enters in the extraction of the one-loop renormalization of the quartic couplings, we

present below this difference:

$$\langle A^{\dagger\alpha_1}_{+\,f_1}(q_1)A^{\dagger\alpha_2}_{+\,f_2}(q_2)\,A^{\alpha_3}_{+\,f_3}(q_3)A^{\alpha_4}_{+\,f_4}(q_4)\rangle^{\overline{\rm MS},1{\rm loop}} - \langle A^{\dagger\alpha_1}_{+\,f_1}(q_1)A^{\dagger\alpha_2}_{+\,f_2}(q_2)\,A^{\alpha_3}_{+\,f_3}(q_3)A^{\alpha_4}_{+\,f_4}(q_4)\rangle^{DR,1{\rm loop}}$$
$$= \frac{g^4}{64\,\pi^2\,N_c^2}\,\frac{1}{\epsilon}\Bigg[\Bigg(2+4\,N_c^2+\alpha\,(-2\alpha+3\,(1+\alpha)\,N_c^2)-2\,N_c\,N_f\Bigg)\times$$
$$\Bigg(\delta_{f_1f_3}\delta_{f_2f_4}(-\delta^{\alpha_1\alpha_3}\delta^{\alpha_2\alpha_4}+N_c\,\delta^{\alpha_1\alpha_4}\delta^{\alpha_2\alpha_3})$$
$$+\,\delta_{f_1f_4}\delta_{f_2f_3}(-\delta^{\alpha_1\alpha_4}\delta^{\alpha_2\alpha_3}+N_c\,\delta^{\alpha_1\alpha_3}\delta^{\alpha_2\alpha_4})\Bigg)\Bigg] \tag{4.52}$$

$$\langle A^{\dagger\alpha_1}_{-\,f_1}(q_1)A^{\dagger\alpha_2}_{-\,f_2}(q_2)\,A^{\alpha_3}_{-\,f_3}(q_3)A^{\alpha_4}_{-\,f_4}(q_4)\rangle^{\overline{\rm MS},1{\rm loop}} - \langle A^{\dagger\alpha_1}_{-\,f_1}(q_1)A^{\dagger\alpha_2}_{-\,f_2}(q_2)\,A^{\alpha_3}_{-\,f_3}(q_3)A^{\alpha_4}_{-\,f_4}(q_4)\rangle^{DR,1{\rm loop}}$$
$$= \frac{g^4}{64\,\pi^2\,N_c^2}\,\frac{1}{\epsilon}\Bigg[\Bigg(2+4\,N_c^2+\alpha\,(-2\alpha+3\,(1+\alpha)\,N_c^2)-2\,N_c\,N_f\Bigg)\times$$
$$\Bigg(\delta_{f_1f_3}\delta_{f_2f_4}(-\delta^{\alpha_3\alpha_1}\delta^{\alpha_4\alpha_2}+N_c\,\delta^{\alpha_4\alpha_1}\delta^{\alpha_3\alpha_2})$$
$$+\,\delta_{f_1f_4}\delta_{f_2f_3}(-\delta^{\alpha_4\alpha_1}\delta^{\alpha_3\alpha_2}+N_c\,\delta^{\alpha_3\alpha_1}\delta^{\alpha_4\alpha_2})\Bigg)\Bigg] \tag{4.53}$$

$$\langle A^{\dagger\alpha_1}_{+\,f_1}(q_1)A^{\alpha_2}_{+\,f_2}(q_2)\,A^{\dagger\alpha_3}_{-\,f_3}(q_3)A^{\alpha_4}_{-\,f_4}(q_4)\rangle^{\overline{\rm MS},1{\rm loop}} - \langle A^{\dagger\alpha_1}_{+\,f_1}(q_1)A^{\alpha_2}_{+\,f_2}(q_2)\,A^{\dagger\alpha_3}_{-\,f_3}(q_3)A^{\alpha_4}_{-\,f_4}(q_4)\rangle^{DR,1{\rm loop}}$$
$$= \frac{g^4}{64\,\pi^2\,N_c^2}\,\frac{1}{\epsilon}\Bigg[\Bigg(-2-4\,N_c^2+\alpha\,(4-N_c^2+\alpha\,(-2+3\,N_c^2))+2\,N_c\,N_f\Bigg)\times$$
$$\delta_{f_1f_2}\delta_{f_3f_4}\Bigg(N_c\,\delta^{\alpha_1\alpha_3}\delta^{\alpha_4\alpha_2}-\delta^{\alpha_1\alpha_2}\delta^{\alpha_4\alpha_3})\Bigg)\Bigg] \tag{4.54}$$

$$\langle A_{+\,f_1}(q_1)A_{-\,f_2}(q_2)A_{+\,f_3}(q_3)A_{-\,f_4}(q_4)\rangle^{\overline{\rm MS},1{\rm loop}} - \langle A_{+\,f_1}(q_1)A_{-\,f_2}(q_2)A_{+\,f_3}(q_3)A_{-\,f_4}(q_4)\rangle^{DR,1{\rm loop}} = 0 \tag{4.55}$$

$$\langle A^{\dagger}_{-\,f_1}(q_1)A^{\dagger}_{+\,f_2}(q_2)A^{\dagger}_{-\,f_3}(q_3)A^{\dagger}_{+\,f_4}(q_4)\rangle^{\overline{\rm MS},1{\rm loop}} - \langle A^{\dagger}_{-\,f_1}(q_1)A^{\dagger}_{+\,f_2}(q_2)A^{\dagger}_{-\,f_3}(q_3)A^{\dagger}_{+\,f_4}(q_4)\rangle^{DR,1{\rm loop}} = 0 \tag{4.56}$$

$$\langle A_{+\,f_1}(q_1)A^{\dagger}_{+\,f_2}(q_2)A_{+\,f_3}(q_3)A_{-\,f_4}(q_4)\rangle^{\overline{\rm MS},1{\rm loop}} - \langle A_{+\,f_1}(q_1)A^{\dagger}_{+\,f_2}(q_2)A_{+\,f_3}(q_3)A_{-\,f_4}(q_4)\rangle^{DR,1{\rm loop}} = 0 \tag{4.57}$$

$$\langle A_{+\,f_1}(q_1)A^{\dagger}_{+\,f_2}(q_2)A^{\dagger}_{-\,f_3}(q_3)A^{\dagger}_{+\,f_4}(q_4)\rangle^{\overline{\rm MS},1{\rm loop}} - \langle A_{+\,f_1}(q_1)A^{\dagger}_{+\,f_2}(q_2)A^{\dagger}_{-\,f_3}(q_3)A^{\dagger}_{+\,f_4}(q_4)\rangle^{DR,1{\rm loop}} = 0 \tag{4.58}$$

$$\langle A^{\dagger}_{-\,f_1}(q_1)A_{-\,f_2}(q_2)A_{+\,f_3}(q_3)A_{-\,f_4}(q_4)\rangle^{\overline{\rm MS},1{\rm loop}} - \langle A^{\dagger}_{-\,f_1}(q_1)A_{-\,f_2}(q_2)A_{+\,f_3}(q_3)A_{-\,f_4}(q_4)\rangle^{DR,1{\rm loop}} = 0 \tag{4.59}$$

$$\langle A^{\dagger}_{-\,f_1}(q_1)A_{-\,f_2}(q_2)A^{\dagger}_{-\,f_3}(q_3)A^{\dagger}_{+\,f_4}(q_4)\rangle^{\overline{\rm MS},1{\rm loop}} - \langle A^{\dagger}_{-\,f_1}(q_1)A_{-\,f_2}(q_2)A^{\dagger}_{-\,f_3}(q_3)A^{\dagger}_{+\,f_4}(q_4)\rangle^{DR,1{\rm loop}} = 0. \tag{4.60}$$

Note that in the case of finite bare Green's functions, the $\overline{\text{MS}}$-renormalized Green's functions coincide with the bare ones in DR.

For the renormalization conditions, we recall the definitions of the renormalization factor of the gauge coupling in Eq. (4.25) and of the renormalization mixing matrix for the squark fields in Eq. (4.27). As noted earlier, this 2×2 renormalization matrix is diagonal in the DR and $\overline{\text{MS}}$ scheme whereas it is non diagonal and the component $A_+(A_-)$ mixes with $A_-^\dagger(A_+^\dagger)$ on the lattice.

We also revisit the renormalization factor of the gauge parameter Z_α, which is defined as follows:

$$\alpha^R = Z_\alpha^{-1}\, Z_u\, \alpha^B, \tag{4.61}$$

By calculating the gluon self energy, it is found to be transverse, reflecting the gauge invariance of the theory. Since there is no longitudinal part for the gluon self energy, Z_α receives no one-loop contribution. Z_u is the renormalization factor of the gluon field and its definition is shown in Eq. (4.22).

In DR, we are interested in getting rid of the pole parts in bare continuum Green's functions; this requires not only the renormalization factors of the fields, of the gauge coupling, Z_g, and of the gauge parameter, Z_α, but requires a special treatment of the bare quartic coupling multiplying also with Z_{λ_1}. The quartic coupling is renormalized as follows:

$$\lambda_1 = Z_{\lambda_1}^{-1} Z_g^{-2} \mu^{2\epsilon}\, (g^R)^2. \tag{4.62}$$

At the lowest perturbative order, it holds that $Z_g Z_{\lambda_1} = 1$, and consequently, the renormalized quartic coupling aligns with the gauge coupling.

Considering the example of the Green's function in DR with four external squark fields A_+ and $A_+^\dagger$, the renormalization condition up to g^2 is expressed as follows:

$$\langle A_+(q_1) A_+^\dagger(q_2) A_+(q_3) A_+^\dagger(q_4)\rangle\Big|^{\overline{\text{MS}}} = (Z_A^{-2})_{++} \langle A_+(q_1) A_+^\dagger(q_2) A_+(q_3) A_+^\dagger(q_4)\rangle\Big|^{\text{bare}}. \tag{4.63}$$

As in the case of the Yukawa coupling renormalization, all appearances of coupling constants, and the gauge parameter in the right-hand side of Eq. (4.63) must be

expressed in terms of their renormalized values, via Eq. (4.25), Eq. (4.62), and Eq. (4.61).

The renormalization factors in DR which appear in the right-hand side of the renormalization condition are shown bellow [48]:

$$Z_{A_\pm}^{DR,\overline{\rm MS}} = 1 + \frac{g^2\, C_F}{16\,\pi^2}\frac{1}{\epsilon}\,(-1+\alpha) \tag{4.64}$$

$$Z_{g}^{DR,\overline{\rm MS}} = 1 + \frac{g^2}{16\,\pi^2}\frac{1}{\epsilon}\left(\frac{3}{2}N_c - \frac{1}{2}N_f\right) \tag{4.65}$$

$$Z_{u}^{DR,\overline{\rm MS}} = 1 + \frac{g^2}{16\,\pi^2}\frac{1}{\epsilon}\left[\left(\frac{\alpha}{2} - \frac{3}{2}\right)N_c + N_f\right] \tag{4.66}$$

$$Z_{\alpha}^{DR,\overline{\rm MS}} = 1 + \mathcal{O}(g^4)\,, \tag{4.67}$$

where $C_F = (N_c^2-1)/(2\,N_c)$ is the quadratic Casimir operator in the fundamental representation.

Utilizing Eq. (4.63) for all bare Green's functions that have pole parts (see Eqs. (4.52) - (4.54)), we obtain the same value for the renormalization factor of $\lambda_1^{DR,\overline{\rm MS}}$:

$$Z_{\lambda_1}{}^{DR,\overline{\rm MS}} = 1 + \mathcal{O}(g^4). \tag{4.68}$$

It is noteworthy that we obtain the same value for the renormalization factor of $\lambda_1^{\rm DR,\overline{MS}}$ by setting the momenta of the squark fields that lie to the antifundamental representation to zero instead of those in the fundamental representation.

Eq. (4.68) implies that, at the quantum level, the renormalization of the quartic coupling in DR remains unaffected by one-loop corrections. This observation carries significant implications for our comprehension of the renormalization scheme in SQCD. Furthermore, it indicates that the corresponding renormalization on the lattice will be finite. While terms proportional to λ_2 - λ_5 do not manifest in the $\overline{\rm MS}$ renormalization using DR, a finite mixture of these terms may emerge in $\overline{\rm MS}$ on the lattice. We anticipate that the $\overline{\rm MS}$ renormalization factors of gauge-invariant quantities will also be gauge-independent on the lattice, mirroring the behavior of $Z_{\lambda_1}^{\rm DR,\overline{MS}}$.

4.3.3 Renormalization in Lattice Regularization

Shifting our focus to LR, it is crucial to note that despite the diagonal nature of the renormalization matrix of the squark fields in the $\overline{\text{MS}}$ scheme and in DR, such simplicity does not carry over to the lattice. On the lattice, the mixing between squark components arises through the matrix Z_A, where the non-diagonal matrix elements are nonzero. Therefore, the renormalization conditions are not as straightforward as depicted in Eq. (4.63).

Taking into account the additional vertices on the lattice, we need to include additional one-loop Feynman diagrams to accurately calculate the fine-tuning of the quartic couplings on the lattice. These additional diagrams are illustrated in Fig. 4.5.

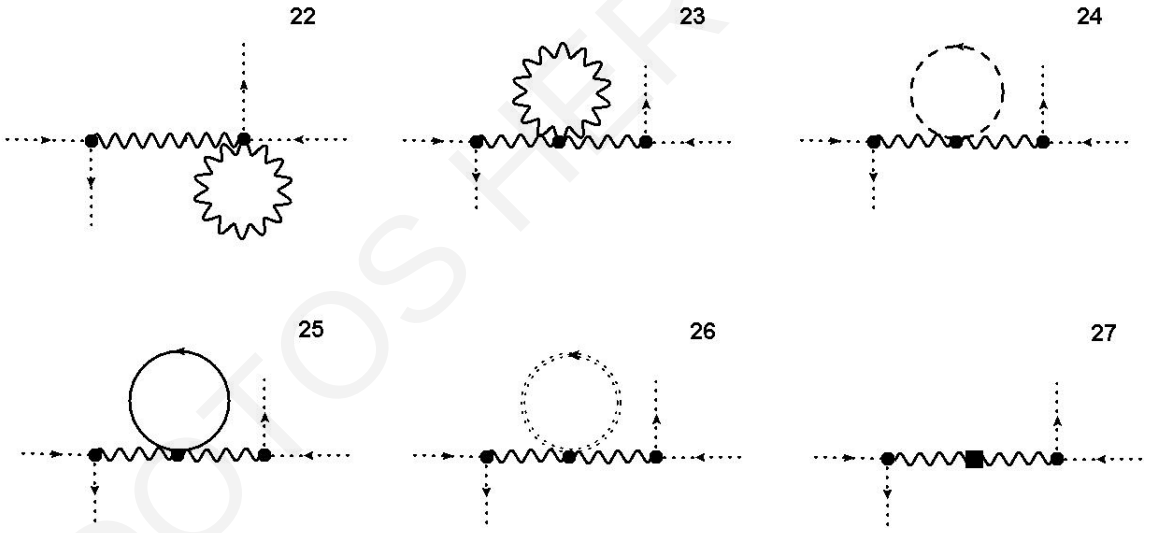

FIGURE 4.5: Additional one-loop Feynman diagrams leading to the fine-tuning of the quartic couplings on the lattice. Notation is identical to that of Fig. 4.3. Note that the "double dashed" line is the ghost field and the solid box in diagram 27 comes from the measure part of the lattice action.

Now, on the lattice the renormalization condition up to g^2 will be given by:

$$\begin{aligned}\langle A_+(q_1)A_+^\dagger(q_2)A_+(q_3)A_+^\dagger(q_4)\rangle\Big|^{\overline{\text{MS}}} =&\langle((Z_A^{-1/2})_{++}+(Z_A^{-1/2})_{+-})A_+(q_1)\\ &((Z_A^{-1/2})^\dagger_{++}+(Z_A^{-1/2})^\dagger_{+-})A_+^\dagger(q_2)\\ &((Z_A^{-1/2})_{++}+(Z_A^{-1/2})_{+-})A_+(q_3)\\ &((Z_A^{-1/2})^\dagger_{++}+(Z_A^{-1/2})^\dagger_{+-})A_+^\dagger(q_4)\rangle\Big|^{\text{bare}}. \qquad (4.69)\end{aligned}$$

As in the case of DR, all appearances of coupling constants, and of the gauge parameter in the right-hand side of Eq. (4.69) must be expressed in terms of their renormalized values. Analogous equations hold for the other Green's functions which involve the other matrix elements.

To provide a comprehensive overview, we revisit a collection of lattice results discussed in Ref. [48]:

$$\left(Z_A^{1/2}\right)^{LR,\overline{\rm MS}} = \mathbb{1} - \frac{g^2\,C_F}{16\,\pi^2}\left\{\left[16.9216 - 3.7920\alpha - (1-\alpha)\log\left(a^2\,\bar{\mu}^2\right)\right]\begin{pmatrix}1 & 0\\ 0 & 1\end{pmatrix} - 0.1623\begin{pmatrix}0 & 1\\ 1 & 0\end{pmatrix}\right\}, \tag{4.70}$$

$$Z_g^{LR,\overline{\rm MS}} = 1 + \frac{g^2}{16\,\pi^2}\left[-9.8696\frac{1}{N_c} + N_c\left(12.8904 - \frac{3}{2}\log\left(a^2\,\bar{\mu}^2\right)\right) - N_f\left(0.4811 - \frac{1}{2}\log(a^2\,\bar{\mu}^2)\right)\right], \tag{4.71}$$

$$Z_u^{LR,\overline{\rm MS}} = 1 + \frac{g^2}{16\,\pi^2}\left[19.7392\frac{1}{N_c} - N_c\left(18.5638 - 1.3863\alpha + \left(-\frac{3}{2} + \frac{\alpha}{2}\right)\log\left(a^2\,\bar{\mu}^2\right)\right) + N_f\left(0.9622 - \log\left(a^2\,\bar{\mu}^2\right)\right)\right], \tag{4.72}$$

$$Z_\alpha^{LR,\overline{\rm MS}} = 1 + \mathcal{O}(g^4). \tag{4.73}$$

The computation of all four-point Green's functions on the lattice is currently in progress [67, 68].

4.4 Possible Extensions

The perturbative renormalization of the Yukawa and quartic couplings completes the one-loop fine-tuning of the SQCD action on the lattice, paving the way for numerical simulations of SQCD. The results of this work will be particularly relevant for the setup and the calibration of lattice numerical simulations of SQCD. In the coming years, it is expected that simulations of supersymmetric theories will become ever more feasible and precise. It would be highly interesting to apply these fine-tunings in Monte Carlo simulations of the SQCD action.

A natural extension of this work would be the perturbative calulations of all fine-tunings in SQCD on the lattice using chirally invariant actions. In particular, the overlap action can be used for gluino and quark fields, in order to ensure correct chiral properties. There is clear risk involved in simulating overlap fermions, since this is very expensive in CPU time. On the other hand, the number of parameters which need fine-tuning is minimized, and this is a significant advantage for these kind of calculations. Nevertheless, fixing the correct values of these parameters still entails calculating a plethora of Green's functions.

Chapter 5

Gauge-invariant Renormalization of Four-quark Operators in Lattice QCD

The remarkable success of the SM in accurately describing electroweak and strong interactions at the fundamental level lies in the fact that the SM Lagrangian incorporates all pertinent operators with dimensions ≤ 4. These operators are constructed using the elementary particle fields that have already been observed and adhere to the principles of Lorentz invariance and gauge symmetry. The potential influence of higher-dimensional ($D > 4$) effective operators, not encompassed within the SM Lagrangian, is anticipated to be inherently small. This is due to their suppression by negative powers of the high-energy scale M, characterizing physics beyond the SM, expressed as M^{4-D}, with allowances for logarithmic correction. In this framework, operators with a dimension of $D = 6$, such as the four-quark operators, assume a particular significance, as their impact is suppressed by M^{-2}.

Furthermore by the high precision achieved in experimental CKM matrix element measurements, the study of four-quark operators becomes even more pertinent in the context of potential discoveries at the Large Hadron Collider (LHC), such as new tetraquarks [92–95]. Thus it is important to explore their properties numerically on the lattice; this calls for a detailed investigation of the corresponding four-quark operators.

Phenomenological bag parameters are other important lattice quantities associated with four-quark operators [96]. For instance, the kaon bag parameter, B_K, is defined as [97–103]:

$$\frac{8}{3}m_K^2 f_K^2 B_K(\mu) = \langle \bar{K}^0|\mathcal{O}|K^0\rangle, \tag{5.1}$$

where m_K is the kaon mass, f_K is the decay constant, μ is the renormalization scale and the relevant four-quark operator, $\mathcal{O}$, is:

$$\mathcal{O} = \bar{\psi}_s\gamma_\mu(1-\gamma_5)\psi_d\,\bar{\psi}_s\gamma_\mu(1-\gamma_5)\psi_d, \tag{5.2}$$

where s and d stand for strange and down quarks. B_K must be calculated nonperturbatively, and this nonperturbative calculation requires the renormalization of the four-quark operator within a continuum renormalization scheme, such as the widely used $\overline{\text{MS}}$ scheme. This ensures compatibility with experimental data and facilitates comparison with phenomenology. In the literature, determinations of B_K are known to high precision [102, 103], and the results are all consistent.

Calculating matrix elements of four-quark operators in lattice QCD offers insights into a wide range of phenomena, including weak decays of hadrons [104] and electroweak interactions. Moreover, the renormalization of four-fermion operators find utility in models of new physics beyond the SM. In these cases, the complete basis of 4-fermion operators plays a role in determining neutral meson mixing amplitudes. This holds true, for example, in SUSY models [105].

In this chapter, we focus on the renormalization of four-quark operators which involved in flavor-changing $\Delta F = 2$ processes. The main objective laid out in this work is the study of four-quark operators under renormalization using both GIRS and $\overline{\text{MS}}$ schemes. In particular, we provide the conversion matrices between GIRS and $\overline{\text{MS}}$. On one hand, the conversion matrices depend on both scales. On the other hand, the conversion matrices are regularization-independent, and thus we can compute them in dimensional regularization, where perturbative computation can be performed more readily and to higher-loop order. For this purpose, we calculate the first quantum corrections for the two-point and three-point Green's functions using coordinate space in DR, where we regularize the theory in $D \equiv 4 - 2\epsilon$ dimensions. By imposing the renormalization conditions on these bare one-loop Green's functions we compute the perturbative renormalization constants for a complete basis of $\Delta F = 2$ four-quark operators, and we determine their gauge invariant mixing patterns. In

particular, the theoretical foundation of our study is based on the most general weak effective Hamiltonian, describing parity-even and parity-odd four-quark operators. The interplay of these operators during renormalization underline the complexity of the investigation.

In the following sections, we detail GIRS scheme, discussing both its merits and its drawbacks. We outline the formulation, presenting the definitions of the operators along with their property symmetries, providing the necessary Green's functions for studying four-quark operator renormalization in GIRS, specifying the implied renormalization conditions, and establishing the definition of the conversion matrices between GIRS and $\overline{\text{MS}}$. Afterwards, we describe our methodology for computing the two-point and three-point GIRS Green's functions using dimensional regularization. Subsequently, we provide perturbative results for these Green's functions, along with the mixing matrices and the conversion matrices between GIRS and $\overline{\text{MS}}$, in DR. Lastly, we summarize our findings and outline potential calculations for future work.

5.1 Gauge Invariant Renormalization Scheme (GIRS)

Gauge Invariant Renormalization Scheme (GIRS) was initially developed in Ref. [9] as an extension of the coordinate space (X-space) renormalization approach [10, 106–109]. Its purpose was to ensure applicability in both continuum and lattice regularizations, thus enabling connections with continuum schemes. GIRS is a gauge-invariant and mass-independent method for renormalizing composite operators on the lattice. This approach focuses on Green's functions of products of gauge-invariant operators at different spacetime points in order to avoid potential contact singularities. These Green's functions can be calculated nonperturbatively in numerical simulations without requiring to fix a specific gauge, allowing for a fully nonperturbative renormalization process to this "intermediate" scheme.

As of now, the utilization of the X-space scheme on the lattice remains relatively limited. Primarily, its application has focused on the multiplicative renormalization of fermion bilinear operators. However, studies involving more complex operators, like the four-fermion operators, have been explored in works such as [110].

In GIRS we examine two-point Green's functions of the form:

$$\langle \mathcal{O}_1(x)\mathcal{O}_2(y)\rangle, \qquad (x \neq y), \tag{5.3}$$

where $\mathcal{O}_1(x)$ and $\mathcal{O}_2(y)$ denote gauge-invariant operators situated at distinct spacetime points. Frequently, the renormalization factors of these operators in GIRS can be determined solely by studying two-point Green's functions. However, in some cases, as in this work, the analysis of three-point Green's functions becomes necessary.

GIRS scheme offers several advantages that simplify its implementation in lattice simulations [9]:

- The Green's functions in GIRS are gauge-invariant. Therefore, when mixing occurs, the number of operators involved in the mixing is reduced as we exclude gauge-variant operators, such as operators that are invariant under BRST symmetry and operators that vanish by the equations of motion. These gauge-variant operators include ghost fields and/or gauge-fixing terms which are defined in perturbation theory and it can be challenging to study in a nonperturbative context. Consequently, excluding the aforementioned operators is advantageous when investigating the nonperturbative renormalization of gauge-invariant operators through lattice simulations.

- By utilizing GIRS, no gauge fixing is required and thus, we can evade issues of fixing a covariant gauge on the lattice [111, 112]. Furthermore, we can conduct calculations perturbatively in a gauge where the momentum-loop integrals are more straightforward, such as the Feynman gauge, since Green's functions in GIRS do not depend on the gauge-fixing parameter.

- When mixing does not occur, perturbative computations within the GIRS framework can be carried out using Feynman diagrams with only one external momentum. This approach, known as a massless renormalization scheme, allows for the application of established techniques developed for evaluating such diagrams to very high perturbative orders. (see, e.g., [82–87, 113]).

- In order to obtain the conversion factors from GIRS to $\overline{\text{MS}}$, you can perform only continuum perturbative calculations since GIRS renormalization functions can be determined entirely non-perturbatively, without relying on lattice perturbation theory.

- In contrast to standard renormalization schemes in momentum space, in GIRS contact terms are naturally excluded ($x \neq y$).

Certainly, GIRS has its drawbacks as well:

- The absence of contact terms in GIRS comes at the cost of introducing exponentials in Feynman integrals, which can complicate their computation.
- Calculations within GIRS, at a specific order in perturbation theory, necessitate diagrams with an additional loop compared to other schemes.
- When mixing arises, it often requires the study of Green's functions with more than two external points. While this complexity is not unique to GIRS and exists in other schemes as well, it still presents a challenge.

As previously stated GIRS is an intermediate scheme enabling the direct derivation of renormalization functions through lattice simulations. The primary objective entails acquiring renormalized Green's functions within the $\overline{\text{MS}}$ scheme, widely used for experimental data analysis. To achieve this objective, it is essential to calculate suitable conversion factors between GIRS and $\overline{\text{MS}}$ schemes. These conversion factors are finite and independent of regularization.

5.2 Formulation and Calculation Setup

In this section, we briefly introduce the formulation of our study, along with the notation utilized throughout this project. We provide definitions of the four-quark operators, as well as their transformation properties under parity, charge conjugation and flavor exchange symmetries. These symmetries allow mixing between specific groups of operators, which arise at the quantum level. Furthermore, we describe the required Green's functions for studying the renormalization of four-quark operators in GIRS, the implied renormalization conditions, and we define the conversion matrices between GIRS and $\overline{\text{MS}}$. Note that there are multiple possibilities for defining GIRS, each leading to different conversion matrices and we present one of them in Section 5.3.

Our calculations are performed within the framework of QCD. The action of QCD in Euclidean spacetime is given by:

$$S_{\rm QCD} = \int d^4x \left[\frac{1}{4} F^a_{\mu\nu} F^{a\mu\nu} + \sum_i \bar{\psi}_{f_i} (\gamma_\mu D_\mu + m_{f_i}) \psi_{f_i} \right], \tag{5.4}$$

where $F^a_{\mu\nu}$ represents the gluon field strength tensor, ψ denotes the quark field of flavor, f_i, and D_μ is the covariant derivative, which accounts the interaction of quarks with the gluon (A_μ) fields: $D_\mu\psi = \partial_\mu\psi + igA_\mu\psi$. Index a is the color index in adjoint representation of the gauge group.

Note that we use a mass-idependent scheme, and the masses m_{f_i} are kept zero throughout to preserve the chiral symmetry. In this way we will exclude complicated renormalization patterns for the four-quark operators since this procedure does not allow mixing among operators of different chirality and operators which are multiplied by masses.

5.2.1 Definition of the Four-quark Operators and their Symmetry Properties

We investigate four-quark composite operators of the form:

$$\mathcal{O}_{\Gamma\tilde{\Gamma}}(x) = \bar{\psi}_{f_1}(x)\Gamma\psi_{f_3}(x)\bar{\psi}_{f_2}(x)\tilde{\Gamma}\psi_{f_4}(x), \tag{5.5}$$

where Γ and $\tilde{\Gamma}$ denote products of Dirac matrices:

$$\Gamma, \tilde{\Gamma} \in \{\mathbb{1},\, \gamma_5,\, \gamma_\mu,\, \gamma_\mu\gamma_5,\, \sigma_{\mu\nu},\, \gamma_5\sigma_{\mu\nu}\} \equiv \{S, P, V, A, T, \tilde{T}\}, \qquad \sigma_{\mu\nu} = \frac{1}{2}[\gamma_\mu, \gamma_\nu], \tag{5.6}$$

and f_i represent the flavor indices on quark fields ψ; color and spinor indices are implied. In our study, we focus on four-quark operators with $\Gamma = \tilde{\Gamma}$ and $\Gamma = \tilde{\Gamma}\gamma_5$, which are scalar or pseudoscalar quantities under rotational symmetry.

One complication in the study of these operators is that mixing is allowed among four-quark operators with different Dirac matrices, under renormalization, as dictated by symmetries. In order to study the mixing of the four-quark operators at the quantum level, it is convenient to construct operators with exchanged flavors of their quark fields, which are related to the original operators through the Fierz–Pauli–Kofink identity (the

superscript letter F stands for Fierz) [22]:

$$\mathcal{O}_{\Gamma\tilde{\Gamma}} \equiv (\bar{\psi}_{f_1}\,\Gamma\,\psi_{f_3})(\bar{\psi}_{f_2}\,\tilde{\Gamma}\,\psi_{f_4}) \equiv \sum_x \sum_{a,c} \Big(\bar{\psi}^a_{f_1}(x)\,\Gamma\,\psi^a_{f_3}(x)\Big)\Big(\bar{\psi}^c_{f_2}(x)\,\tilde{\Gamma}\,\psi^c_{f_4}(x)\Big), \quad (5.7)$$

$$\mathcal{O}^F_{\Gamma\tilde{\Gamma}} \equiv (\bar{\psi}_{f_1}\,\Gamma\,\psi_{f_4})(\bar{\psi}_{f_2}\,\tilde{\Gamma}\,\psi_{f_3}) \equiv \sum_x \sum_{a,c} \Big(\bar{\psi}^a_{f_1}(x)\,\Gamma\,\psi^a_{f_4}(x)\Big)\Big(\bar{\psi}^c_{f_2}(x)\,\tilde{\Gamma}\,\psi^c_{f_3}(x)\Big), \quad (5.8)$$

where Dirac indices are implicit, and color indices are denoted by Latin letters a, c.

In order to study the renormalization of the four-quark operators, we considered the symmetries of the QCD action, with 4 degenerate quarks: Parity $\mathcal{P}$, Charge conjugation $\mathcal{C}$, Flavor exchange symmetry $\mathcal{S}\equiv(\psi_{f_3} \leftrightarrow \psi_{f_4})$, Flavor Switching symmetries $\mathcal{S}'\equiv(\psi_{f_1} \leftrightarrow \psi_{f_3}, \psi_{f_2} \leftrightarrow \psi_{f_4})$ and $\mathcal{S}''\equiv(\psi_{f_1} \leftrightarrow \psi_{f_4}, \psi_{f_3} \leftrightarrow \psi_{f_2})$ [114]. Operators which have the same behavior under these symmetries can mix. The parity $\mathcal{P}$ and charge conjugation $\mathcal{C}$ transformations on quarks and antiquarks are defined in the Eqs. (3.36) and (3.37), respectively.

Referring to [114–116], we derive the complete basis of dimension-six, four-quark operators that undergo mixing during renormalization. This derivation is based in general symmetry principles, particularly those stemming from the flavor symmetries, which are also preserved on the lattice. Note that, four-quark operators, which involved in flavor-changing $\Delta F = 2$ processes, can mix only with other dimension-six operators with the same quantum numbers and not with lower dimensional operators as they do not have the same four-flavor content.

In Table 5.1, we illustrate the transformations of the four-quark operators $\mathcal{O}_{\Gamma\tilde{\Gamma}}$ under $\mathcal{P}$, $\mathcal{CS}'$, $\mathcal{CS}''$, $\mathcal{CPS}'$ and $\mathcal{CPS}''$. It is worth mentioning that the Parity Violating operators, which does not obey $\mathcal{CS}''$ symmetry, have been symmetrized or antisymmetrized to generate eigenstates of $\mathcal{CS}''$. For the Fierz four-quark operators $\mathcal{O}^F_{\Gamma\tilde{\Gamma}}$, we must exchange the columns $\mathcal{CS}' \to \mathcal{CS}''$ and $\mathcal{CPS}' \to \mathcal{CPS}''$.

The new basis of operators can be further decomposed into smaller independent bases according to the discrete symmetries $\mathcal{P}$, $\mathcal{S}$, $\mathcal{CPS}'$ and $\mathcal{CPS}''$. Following the notation of Ref. [115], the 20 operators of Table 5.1 (including the Fierz operators) are classified into 4 categories:

(a) Parity Conserving ($\mathcal{P} = +1$) operators with $\mathcal{S} = +1$: $Q_i^{S=+1}$, $\quad (i = 1, 2, \ldots, 5)$,

(b) Parity Conserving ($\mathcal{P} = +1$) operators with $\mathcal{S} =$ -1: $Q_i^{S=-1}$, $\quad (i = 1, 2, \ldots, 5)$,

	$\mathcal{P}$	$\mathcal{CS}'$	$\mathcal{CS}''$	$\mathcal{CPS}'$	$\mathcal{CPS}''$
$\mathcal{O}_{VV}$	+	+	+	+	+
$\mathcal{O}_{AA}$	+	+	+	+	+
$\mathcal{O}_{PP}$	+	+	+	+	+
$\mathcal{O}_{SS}$	+	+	+	+	+
$\mathcal{O}_{TT}$	+	+	+	+	+
$\mathcal{O}_{[VA+AV]}$	−	−	−	+	+
$\mathcal{O}_{[VA-AV]}$	−	−	+	+	−
$\mathcal{O}_{[SP-PS]}$	−	+	−	−	+
$\mathcal{O}_{[SP+PS]}$	−	+	+	−	−
$\mathcal{O}_{T\tilde{T}}$	−	+	+	−	−

TABLE 5.1: Transformations of the four-quark operators $\mathcal{O}_{\Gamma\tilde{\Gamma}}$ under $\mathcal{P}$, $\mathcal{CS}'$, $\mathcal{CS}''$, $\mathcal{CPS}'$ and $\mathcal{CPS}''$ are noted. The operators $\mathcal{O}_{\tilde{T}T}$ and $\mathcal{O}_{\tilde{T}\tilde{T}}$ are not explicitly shown in the above matrix, as they coincide with $\mathcal{O}_{T\tilde{T}}$ and $\mathcal{O}_{TT}$, respectively. For the Fierz four-quark operators $\mathcal{O}^F_{\Gamma\tilde{\Gamma}}$, we must exchange the columns $\mathcal{CS}' \to \mathcal{CS}''$ and $\mathcal{CPS}' \to \mathcal{CPS}''$ [115].

(c) Parity Violating ($\mathcal{P}$ = -1) operators with $\mathcal{S}$ = +1: $\mathcal{Q}_i^{S=+1}$, $(i = 1, 2, \ldots, 5)$,

(d) Parity Violating ($\mathcal{P}$ = -1) operators with $\mathcal{S}$ = -1: $\mathcal{Q}_i^{S=-1}$, $(i = 1, 2, \ldots, 5)$,

which are given, explicitly, below:

$$\begin{cases} Q_1^{S=\pm1} \equiv \frac{1}{2}\left[\mathcal{O}_{VV} \pm \mathcal{O}^F_{VV}\right] + \frac{1}{2}\left[\mathcal{O}_{AA} \pm \mathcal{O}^F_{AA}\right], \\ Q_2^{S=\pm1} \equiv \frac{1}{2}\left[\mathcal{O}_{VV} \pm \mathcal{O}^F_{VV}\right] - \frac{1}{2}\left[\mathcal{O}_{AA} \pm \mathcal{O}^F_{AA}\right], \\ Q_3^{S=\pm1} \equiv \frac{1}{2}\left[\mathcal{O}_{SS} \pm \mathcal{O}^F_{SS}\right] - \frac{1}{2}\left[\mathcal{O}_{PP} \pm \mathcal{O}^F_{PP}\right], \\ Q_4^{S=\pm1} \equiv \frac{1}{2}\left[\mathcal{O}_{SS} \pm \mathcal{O}^F_{SS}\right] + \frac{1}{2}\left[\mathcal{O}_{PP} \pm \mathcal{O}^F_{PP}\right], \\ Q_5^{S=\pm1} \equiv \frac{1}{2}\left[\mathcal{O}_{TT} \pm \mathcal{O}^F_{TT}\right], \end{cases} \tag{5.9}$$

$$\begin{cases} \mathcal{Q}_1^{S=\pm1} \equiv \frac{1}{2}\left[\mathcal{O}_{VA} \pm \mathcal{O}^F_{VA}\right] + \frac{1}{2}\left[\mathcal{O}_{AV} \pm \mathcal{O}^F_{AV}\right], \\ \mathcal{Q}_2^{S=\pm1} \equiv \frac{1}{2}\left[\mathcal{O}_{VA} \pm \mathcal{O}^F_{VA}\right] - \frac{1}{2}\left[\mathcal{O}_{AV} \pm \mathcal{O}^F_{AV}\right], \\ \mathcal{Q}_3^{S=\pm1} \equiv \frac{1}{2}\left[\mathcal{O}_{PS} \pm \mathcal{O}^F_{PS}\right] - \frac{1}{2}\left[\mathcal{O}_{SP} \pm \mathcal{O}^F_{SP}\right], \\ \mathcal{Q}_4^{S=\pm1} \equiv \frac{1}{2}\left[\mathcal{O}_{PS} \pm \mathcal{O}^F_{PS}\right] + \frac{1}{2}\left[\mathcal{O}_{SP} \pm \mathcal{O}^F_{SP}\right], \\ \mathcal{Q}_5^{S=\pm1} \equiv \frac{1}{2}\left[\mathcal{O}_{T\tilde{T}} \pm \mathcal{O}^F_{T\tilde{T}}\right]. \end{cases} \tag{5.10}$$

Note that there is a summation over all independent Lorentz indices (if any), of the Dirac matrices. The operators of Eqs. (5.9) and (5.10) are grouped together according to their mixing pattern. Therefore, the mixing matrices $Z^{S=\pm1}$ ($\mathcal{Z}^{S=\pm1}$), which renormalize the Parity Conserving (Violating) operators, take the following form:

$$Z^{S=\pm1} = \begin{pmatrix} Z_{11} & Z_{12} & Z_{13} & Z_{14} & Z_{15} \\ Z_{21} & Z_{22} & Z_{23} & Z_{24} & Z_{25} \\ Z_{31} & Z_{32} & Z_{33} & Z_{34} & Z_{35} \\ Z_{41} & Z_{42} & Z_{43} & Z_{44} & Z_{45} \\ Z_{51} & Z_{52} & Z_{53} & Z_{54} & Z_{55} \end{pmatrix}^{S=\pm1}, \quad \mathcal{Z}^{S=\pm1} = \begin{pmatrix} \mathcal{Z}_{11} & 0 & 0 & 0 & 0 \\ 0 & \mathcal{Z}_{22} & \mathcal{Z}_{23} & 0 & 0 \\ 0 & \mathcal{Z}_{32} & \mathcal{Z}_{33} & 0 & 0 \\ 0 & 0 & 0 & \mathcal{Z}_{44} & \mathcal{Z}_{45} \\ 0 & 0 & 0 & \mathcal{Z}_{54} & \mathcal{Z}_{55} \end{pmatrix}^{S=\pm1}. \tag{5.11}$$

The renormalized Parity Conserving (Violating) operators, $\hat{Q}^{S=\pm1}$ ($\hat{\mathcal{Q}}^{S=\pm1}$), are defined as follows:

$$\hat{Q}_l^{S=\pm1} = Z_{lm}^{S=\pm1} \cdot Q_m^{S=\pm1}, \quad \hat{\mathcal{Q}}_l^{S=\pm1} = \mathcal{Z}_{lm}^{S=\pm1} \cdot \mathcal{Q}_m^{S=\pm1}, \tag{5.12}$$

where $l, m = 1, \ldots, 5$ and a sum over m is implied.

In principle, the four-quark operators can also mix with a number of possible lower dimensional operators, which have the same symmetry properties. However, in this work, we focus on operators which change flavor numbers by two units ($\Delta F = 2$); thus, $f_1 \notin \{f_3, f_4\}$ and $f_2 \notin \{f_3, f_4\}$, which forbid such additional mixing.

5.2.2 Green's Functions and Feynman Diagrams

In this work, GIRS is employed for extracting the renormalization matrices $Z^{S=\pm1}$ and $\mathcal{Z}^{S=\pm1}$. In the case of a multiplicatively renormalizable operator, $\mathcal{O}$, a typical condition in GIRS has the following form:

$$(Z_{\mathcal{O}}^{\mathrm{GIRS}})^2 \langle \mathcal{O}(x)\, \mathcal{O}^\dagger(y) \rangle|_{x-y=\bar{z}} = \langle \mathcal{O}(x)\, \mathcal{O}^\dagger(y) \rangle^{\mathrm{tree}}\Big|_{x-y=\bar{z}}, \tag{5.13}$$

where $\bar{z}$ is a nonzero renormalization 4-vector scale. To ensure that discretization effects are manageable and that we can effectively connect with continuum perturbation theory, the scale $\bar{z}$ has to be within the range where the lattice spacing a is much smaller than $\bar{z}$, but $\bar{z}$ itself is much smaller than the inverse of the QCD scale Λ_{QCD}.

Note that the Green's function $\langle \mathcal{O}(x)\, \mathcal{O}(y)^\dagger \rangle$ is gauge independent and thus, a nonperturbative implementation of such a scheme on the lattice avoids gauge fixing

altogether and the numerical simulation becomes more straightforward and statistically robust without the issue of Gribov copies. When operator mixing occurs, we need to consider a set of conditions involving more than one Green's functions of two or more gauge-invariant operators, each of which has a similar form to Eq. (5.13), i.e., the renormalized Green's functions are set to their tree-level values when the operators' space-time separations equal to specific reference scales.

In our study, the determination of the 5×5 mixing matrices of Eq. (5.11) requires the calculation of (i) two-point Green's functions with two four-quark operators and (ii) three-point Green's functions with one four-quark operator and two lower dimensional operators, e.g., quark bilinear operators:

$$\mathcal{O}_\Gamma(x) = \bar{\psi}_{f_1}(x)\Gamma\psi_{f_2}(x). \tag{5.14}$$

All operators are placed at different spacetime points, in a way as to avoid potential contact singularities:

$$G^{\text{2pt}}_{\mathcal{O}_{\Gamma\tilde{\Gamma}};\mathcal{O}_{\Gamma'\tilde{\Gamma}'}}(z) \equiv \langle \mathcal{O}_{\Gamma\tilde{\Gamma}}(x)\, \mathcal{O}^\dagger_{\Gamma'\tilde{\Gamma}'}(y)\rangle, \qquad z \equiv x-y,\ x \neq y, \tag{5.15}$$

$$G^{\text{3pt}}_{\mathcal{O}_{\Gamma'};\mathcal{O}_{\Gamma\tilde{\Gamma}};\mathcal{O}_{\Gamma''}}(z,z') \equiv \langle \mathcal{O}_{\Gamma'}(x)\, \mathcal{O}_{\Gamma\tilde{\Gamma}}(y)\mathcal{O}_{\Gamma''}(w)\rangle, \qquad z \equiv x-y,\ z' \equiv y-w,\ x \neq y \neq w \neq x. \tag{5.16}$$

Two-point Green's functions with one four-quark operator and one bilinear operator are not considered since they vanish when $\Delta F = 2$. In principle, the perturbative calculation of the Green's functions of Eqs. (5.15) and (5.16) can be performed for generic Dirac matrices $\Gamma, \tilde{\Gamma}, \Gamma', \tilde{\Gamma}', \Gamma''$, which do not lead to vanishing result. However, when we construct the renormalization conditions, we specify the Dirac matrices for both four-quark (Q_i and $\mathcal{Q}_i$ combinations) and bilinear operators.

In order to determine a consistent and solvable set of nonperturbative renormalization conditions, we need to examine multiple choices of three-point Green's functions with different bilinear operators. Also, since there is no unique way of selecting solvable conditions in GIRS, a perturbative calculation of all possible Green's functions will be useful for determining conversion factors from different variants of GIRS to $\overline{\text{MS}}$. To this end, we calculate the Green's functions of Eqs. (5.15) and (5.16), up to one-loop order, in DR.

The Feynman diagrams contributing to the two-point Green's functions with two $\Delta F = 2$ four-quark operators, to order $\mathcal{O}(g^0)$ (diagram 1) and $\mathcal{O}(g^2)$ (the remaining diagrams), are shown in Fig. 5.1.

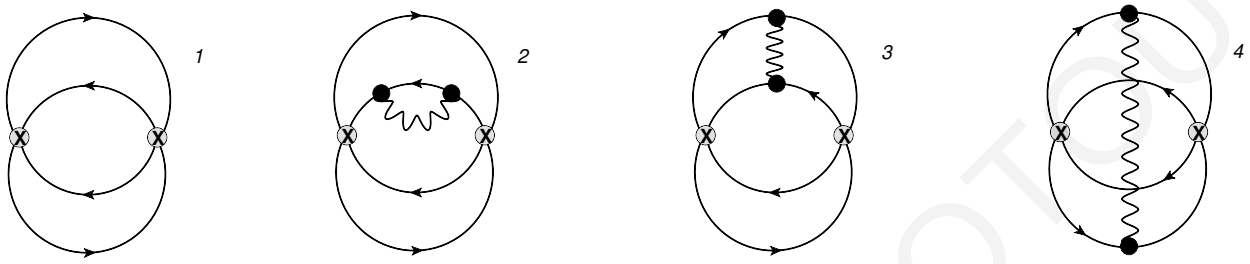

FIGURE 5.1: Feynman diagrams contributing to $\langle \mathcal{O}_{\Gamma\tilde{\Gamma}}(x)\, \mathcal{O}^{\dagger}_{\Gamma'\tilde{\Gamma}'}(y) \rangle$ with two $\Delta F = 2$ four-quark operators, to order $\mathcal{O}(g^0)$ (diagram 1) and $\mathcal{O}(g^2)$ (the remaining diagrams). Wavy (solid) lines represent gluons (quarks). A circled cross denotes insertion of the four-quark operator. Diagrams 2 and 4 have also mirror variants.

The Feynman diagrams contributing to the three-point Green's functions of the product of one $\Delta F = 2$ four-quark operator and two quark bilinear operators are shown in Fig. 5.2.

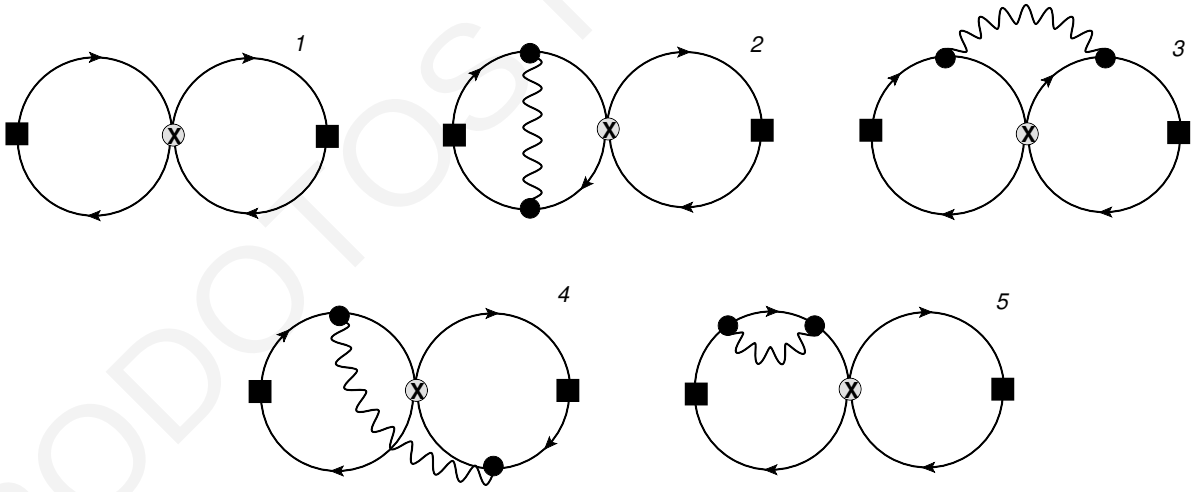

FIGURE 5.2: Feynman diagrams contributing to $\langle \mathcal{O}_{\Gamma'}(x)\, \mathcal{O}_{\Gamma\tilde{\Gamma}}(0) \mathcal{O}_{\Gamma''}(y) \rangle$ with one $\Delta F = 2$ four-quark operator, to order $\mathcal{O}(g^0)$ (diagram 1) and $\mathcal{O}(g^2)$ (the remaining diagrams). Notation is identical to that of Figure 5.1. The solid squares denote the quark bilinear operators. Diagrams 2-5 have also mirror variants.

In Appendix B, we depict diagrams that are absent for $\Delta F = 2$ four-quark operators but contribute to the Green's functions involving products of four-quark operators with $\Delta F < 2$. Moreover, we provide additional Feynman diagrams that arise specifically within lattice calculations.

There are numerous possible variants of GIRS, depending on which Green's functions and which renormalization four-vectors are selected for imposing renormalization conditions. A variant of choice, which is expected to result in reduced statistical noise in lattice simulations, includes integration (summation on the lattice) over time slices of the operator-insertion points in all Green's functions. For instance, we integrate the Eq. (5.13) over three out of the four components of the position vector $(x-y)$, with the fourth component set to a reference scale t. To clarify, for scalar and pseudoscalar operators, the direction of the unintegrated component does not matter. However, for other operators, there are two possible options depending on whether this direction aligns with one of the indices carried by the operators or not. Given the anisotropic nature of the lattice used in simulations, the temporal direction holds special significance. Therefore, a natural choice for the component t is to be temporal. The Green's functions for this variant of GIRS can be expressed as follows:

$$\tilde{G}^{\text{2pt}}_{\mathcal{O}_{\Gamma\tilde{\Gamma}};\mathcal{O}_{\Gamma'\tilde{\Gamma}'}}(z_4) \equiv \int d^3\vec{z}\, G^{\text{2pt}}_{\mathcal{O}_{\Gamma\tilde{\Gamma}};\mathcal{O}_{\Gamma'\tilde{\Gamma}'}}(\vec{z}, z_4), \qquad z_4 > 0, \quad (5.17)$$

$$\tilde{G}^{\text{3pt}}_{\mathcal{O}_{\Gamma'};\mathcal{O}_{\Gamma\tilde{\Gamma}};\mathcal{O}_{\Gamma''}}(z_4, z_4') \equiv \int d^3\vec{z} \int d^3\vec{z'}\, G^{\text{3pt}}_{\mathcal{O}_{\Gamma'};\mathcal{O}_{\Gamma\tilde{\Gamma}};\mathcal{O}_{\Gamma''}}((\vec{z}, z_4), (\vec{z'}, z_4')), \qquad z_4 > 0,\ z_4' > 0. \quad (5.18)$$

This method offers the advantage of reducing the four reference scales to just one. The aforementioned variant of GIRS have been employed in a number of previous studies, regarding the renormalization of fermion bilinear operators [9], the study of mixing between the gluon and quark energy-momentum tensor operators [9], as well as the renormalization of supersymmetric operators, such as gluino-glue [70] and supercurrent [71, 117] in Super-Yang-Mills theory.

5.2.3 Renormalization Conditions and Conversion Matrices

In the case of the Parity Conserving operators (Q_i), the mixing matrix is 5×5 for both $S = +1$ and $S = -1$. Therefore, for each case we need 25 conditions to obtain these mixing coefficients. Computing the relevant two-point Green's functions, we extract 15 conditions and we need another 10 conditions that will be extracted from the relevant three-point Green's functions. The 15 conditions in GIRS which include two-point

Green's functions are the following:

$$[\tilde{G}^{\rm 2pt}_{Q_i^{S=\pm1};Q_j^{S=\pm1}}(t)]^{\rm GIRS} \equiv \sum_{k,l=1}^{5} (Z_{ik}^{S\pm1})^{\rm GIRS} (Z_{jl}^{S\pm1})^{\rm GIRS}\, \tilde{G}^{\rm 2pt}_{Q_k^{S=\pm1};Q_l^{S=\pm1}}(t) = [\tilde{G}^{\rm 2pt}_{Q_i^{S=\pm1};Q_j^{S=\pm1}}(t)]^{\rm tree}, \tag{5.19}$$

where the indices i and j run from 1 to 5 and $i \leq j$; $z_4 := t$ is the GIRS renormalization scale. We have a variety of options for selecting the remaining conditions involving three-point Green's functions:

$$[\tilde{G}^{\rm 3pt}_{\mathcal{O}_\Gamma;Q_i^{S=\pm1};\mathcal{O}_\Gamma}(t,t')]^{\rm GIRS} \equiv (Z^{\rm GIRS}_{\mathcal{O}_\Gamma})^2 \sum_{k=1}^{5} (Z_{ik}^{S\pm1})^{\rm GIRS}\, \tilde{G}^{\rm 3pt}_{\mathcal{O}_\Gamma;Q_k^{S=\pm1};\mathcal{O}_\Gamma}(t,t') = [\tilde{G}^{\rm 3pt}_{\mathcal{O}_\Gamma;Q_i^{S=\pm1};\mathcal{O}_\Gamma}(t,t')]^{\rm tree}, \tag{5.20}$$

where the index i runs from 1 to 5, $\Gamma \in \{\mathbb{1},\, \gamma_5,\, \gamma_\mu,\, \gamma_\mu\gamma_5,\, \sigma_{\mu\nu}\}$, and $z_4 := t$, $z_4' := t'$ are GIRS renormalization scales. In this case, the two bilinears must be the same in order to obtain a nonzero Green's function. $Z^{\rm GIRS}_{\mathcal{O}_\Gamma}$ is the renormalization factor of the bilinear operator $\mathcal{O}_\Gamma$ calculated in Ref. [9]. To avoid having more than one renormalization scales, a natural choice is to set $t' = t$; in this way, the original set of two four-vector renormalization scales (given by specific values of z and z', cf. Eqs. (5.15)-(5.16)), following integration over time slices and setting $t' = t$, is reduced to just one real variable. Changing the values of t and/or t' would obviously affect the results for the nonperturbative Green's functions in Eqs. (5.19)-(5.20); nevertheless, after multiplication by the appropriate conversion factors, one should arrive at the *same* $\overline{\rm MS}$-renormalized Green's functions, independently of t and t' (assuming that various standard sources of systematic error are under control). This then provides a powerful consistency check for the renormalization of four-quark operators.

As we conclude, by doing the perturbative calculation, not all sets of conditions given in Eqs. (5.19)-(5.20) can lead to viable solutions. We will provide some feasible choices in Section 5.3. In practice, one can choose the specific conditions that provide a more stable signal in numerical simulations.

In the case of the Parity Violating operators ($\mathcal{Q}_i$), the 5×5 mixing matrix is block diagonal for both $S = +1$ and $S = -1$, as dictated by symmetries. In particular, there are three mixing subsets: $\{\mathcal{Q}_1\}$, $\{\mathcal{Q}_2, \mathcal{Q}_3\}$ and $\{\mathcal{Q}_4, \mathcal{Q}_5\}$, for each S. The first subset includes only 1 operator, which is multiplicatively renormalizable; thus, only one condition is needed and can be obtained from the two-point Green's functions. The second and third subsets include two operators and thus, 4 conditions are needed for

each subset to obtain the mixing coefficients. Three of them will be extracted from the two-point Green's functions, while the remaining 1 condition requires the calculation of three-point Green's functions. In total, we need 9 conditions for each S: 7 will be extracted from two-point Green's functions, and 2 will be extracted from three-point Green's functions. The seven conditions that include two-point Green's functions are the following:

$$[\tilde{G}^{\rm 2pt}_{\mathcal{Q}_1^{S=\pm1};\mathcal{Q}_1^{S=\pm1}}(t)]^{\rm GIRS} \equiv [(\mathcal{Z}_{11}^{S\pm1})^{\rm GIRS}]^2\ \tilde{G}^{\rm 2pt}_{\mathcal{Q}_1^{S=\pm1};\mathcal{Q}_1^{S=\pm1}}(t) = [\tilde{G}^{\rm 2pt}_{\mathcal{Q}_1^{S=\pm1};\mathcal{Q}_1^{S=\pm1}}(t)]^{\rm tree}, \tag{5.21}$$

$$\begin{aligned}[\tilde{G}^{\rm 2pt}_{\mathcal{Q}_i^{S=\pm1};\mathcal{Q}_j^{S=\pm1}}(t)]^{\rm GIRS} &\equiv \sum_{k,l=2}^{3} (\mathcal{Z}_{ik}^{S\pm1})^{\rm GIRS}(\mathcal{Z}_{jl}^{S\pm1})^{\rm GIRS}\ \tilde{G}^{\rm 2pt}_{\mathcal{Q}_k^{S=\pm1};\mathcal{Q}_l^{S=\pm1}}(t) \\ &= [\tilde{G}^{\rm 2pt}_{\mathcal{Q}_i^{S=\pm1};\mathcal{Q}_j^{S=\pm1}}(t)]^{\rm tree},\ (i,j=2,3),\end{aligned} \tag{5.22}$$

$$\begin{aligned}[\tilde{G}^{\rm 2pt}_{\mathcal{Q}_i^{S=\pm1};\mathcal{Q}_j^{S=\pm1}}(t)]^{\rm GIRS} &\equiv \sum_{k,l=4}^{5} (\mathcal{Z}_{ik}^{S\pm1})^{\rm GIRS}(\mathcal{Z}_{jl}^{S\pm1})^{\rm GIRS}\ \tilde{G}^{\rm 2pt}_{\mathcal{Q}_k^{S=\pm1};\mathcal{Q}_l^{S=\pm1}}(t) \\ &= [\tilde{G}^{\rm 2pt}_{\mathcal{Q}_i^{S=\pm1};\mathcal{Q}_j^{S=\pm1}}(t)]^{\rm tree},\ (i,j=4,5).\end{aligned} \tag{5.23}$$

Note that in the above equations $i \leq j$. The two conditions that include three-point Green's functions can be:

$$\begin{aligned}[\tilde{G}^{\rm 3pt}_{\mathcal{O}_\Gamma;\mathcal{Q}_i^{S=\pm1};\mathcal{O}_{\Gamma\gamma_5}}(t,t')]^{\rm GIRS} &\equiv Z^{\rm GIRS}_{\mathcal{O}_\Gamma}\ Z^{\rm GIRS}_{\mathcal{O}_{\Gamma\gamma_5}} \sum_{k=2}^{3} (\mathcal{Z}_{ik}^{S\pm1})^{\rm GIRS}\ \tilde{G}^{\rm 3pt}_{\mathcal{O}_\Gamma;\mathcal{Q}_k^{S=\pm1};\mathcal{O}_{\Gamma\gamma_5}}(t,t') \\ &= [\tilde{G}^{\rm 3pt}_{\mathcal{O}_\Gamma;\mathcal{Q}_i^{S=\pm1};\mathcal{O}_{\Gamma\gamma_5}}(t,t')]^{\rm tree},\ (i=2 \text{ or } 3),\end{aligned} \tag{5.24}$$

$$\begin{aligned}[\tilde{G}^{\rm 3pt}_{\mathcal{O}_\Gamma;\mathcal{Q}_i^{S=\pm1};\mathcal{O}_{\Gamma\gamma_5}}(t,t')]^{\rm GIRS} &\equiv Z^{\rm GIRS}_{\mathcal{O}_\Gamma}\ Z^{\rm GIRS}_{\mathcal{O}_{\Gamma\gamma_5}} \sum_{k=4}^{5} (\mathcal{Z}_{ik}^{S\pm1})^{\rm GIRS}\ \tilde{G}^{\rm 3pt}_{\mathcal{O}_\Gamma;\mathcal{Q}_k^{S=\pm1};\mathcal{O}_{\Gamma\gamma_5}}(t,t') \\ &= [\tilde{G}^{\rm 3pt}_{\mathcal{O}_\Gamma;\mathcal{Q}_i^{S=\pm1};\mathcal{O}_{\Gamma\gamma_5}}(t,t')]^{\rm tree},\ (i=4 \text{ or } 5),\end{aligned} \tag{5.25}$$

where $\Gamma \in \{\mathbb{1},\ \gamma_\mu,\ \sigma_{\mu\nu}\}$. In this case, the two bilinears must differ by γ_5 in order to obtain a nonzero Green's function. As in the Parity Conserving operators, we simplify the conditions by setting $t' = t$. It is not guaranteed that all possible choices can give a solution to the system of conditions. We test all options and we provide the choices that can work in Section 5.3.

To connect with phenomenological studies effectively, which mainly rely on operators renormalized within the $\overline{\rm MS}$ scheme of dimensional regularization, the conversion matrices $(C^{S=\pm1})^{\overline{\rm MS},\rm GIRS}$ and $(\tilde{C}^{S=\pm1})^{\overline{\rm MS},\rm GIRS}$ between GIRS and $\overline{\rm MS}$ schemes are

necessary:

$$(Z^{S=\pm1})^{\overline{\rm MS}} = (C^{S=\pm1})^{\overline{\rm MS},{\rm GIRS}}(Z^{S=\pm1})^{\rm GIRS}, \qquad (\mathcal{Z}^{S=\pm1})^{\overline{\rm MS}} = (\tilde{C}^{S=\pm1})^{\overline{\rm MS},{\rm GIRS}}(\mathcal{Z}^{S=\pm1})^{\rm GIRS}. \tag{5.26}$$

These can be computed only perturbatively due to the very nature of $\overline{\rm MS}$. Being regularization independent, they are evaluated more easily in DR. The one-loop expressions of the conversion matrices for different variants of GIRS are extracted from our calculations and are given in Section 5.3 for a selected version of GIRS. The conversion matrices along with the lattice mixing matrices in GIRS, calculated nonperturbatively, allow the extraction of the lattice mixing matrices in the $\overline{\rm MS}$ scheme.

From the Green's functions, which are computed by using coordinate space in DR, we can extract directly the $\overline{\rm MS}$-renormalized Green's functions; this can be done by isolating the pole terms (negative powers of ϵ in the Laurent series expansion) in the bare two-point and three-point Green's functions. We obtain the mixing coefficients for the Parity Conserving operators in $\overline{\rm MS}$ by solving the following system of conditions:

$$\sum_{k,l=1}^{5} (Z^{S=\pm1})^{\overline{\rm MS}}_{ik} (Z^{S=\pm1})^{\overline{\rm MS}}_{jl} G^{\rm 2pt}_{Q_k^{S=\pm1};Q_l^{S=\pm1}}(z)\Big|_{\epsilon^{-n}} = 0, \quad n \in \mathbb{Z}^+, \tag{5.27}$$

$$(Z^{\overline{\rm MS}}_{\mathcal{O}_\Gamma})^2 \sum_{k=1}^{5} (Z^{S=\pm1})^{\overline{\rm MS}}_{ik} G^{\rm 3pt}_{\mathcal{O}_\Gamma;Q_k^{S=\pm1};\mathcal{O}_\Gamma}(z,z')\Big|_{\epsilon^{-n}} = 0, \quad n \in \mathbb{Z}^+, \tag{5.28}$$

where the indices i and j run from 1 to 5, $i \le j$ and $\Gamma \in \{\mathbb{1}, \gamma_5, \gamma_\mu, \gamma_\mu\gamma_5, \sigma_{\mu\nu}\}$. $Z^{\overline{\rm MS}}_{\mathcal{O}_\Gamma}$ is the renormalization factor of the bilinear operator $\mathcal{O}_\Gamma$ in $\overline{\rm MS}$ calculated in Ref. [9]. For the Parity Violating operators the following conditions are valid:

$$[(\mathcal{Z}^{S\pm1}_{11})^{\overline{\rm MS}}]^2 \; G^{\rm 2pt}_{\mathcal{Q}_1^{S=\pm1};\mathcal{Q}_1^{S=\pm1}}(z)\Big|_{\epsilon^{-n}} = 0, \quad n \in \mathbb{Z}^+, \tag{5.29}$$

$$\sum_{k,l=2}^{3} (\mathcal{Z}^{S\pm1}_{ik})^{\overline{\rm MS}} (\mathcal{Z}^{S\pm1}_{jl})^{\overline{\rm MS}} \; G^{\rm 2pt}_{\mathcal{Q}_k^{S=\pm1};\mathcal{Q}_l^{S=\pm1}}(z)\Big|_{\epsilon^{-n}} = 0, \quad n \in \mathbb{Z}^+, (i,j=2,3), \tag{5.30}$$

$$\sum_{k,l=4}^{5} (\mathcal{Z}^{S\pm1}_{ik})^{\overline{\rm MS}} (\mathcal{Z}^{S\pm1}_{jl})^{\overline{\rm MS}} \; G^{\rm 2pt}_{\mathcal{Q}_k^{S=\pm1};\mathcal{Q}_l^{S=\pm1}}(z)\Big|_{\epsilon^{-n}} = 0, \quad n \in \mathbb{Z}^+, (i,j=4,5). \tag{5.31}$$

Note that in the above equations $i \leq j$. For these operators the renormalization conditions including three-point Green's functions in $\overline{\text{MS}}$ are shown below:

$$Z_{\mathcal{O}_\Gamma}^{\overline{\text{MS}}}\, Z_{\mathcal{O}_{\Gamma\gamma_5}}^{\overline{\text{MS}}} \sum_{k=2}^{3} (\mathcal{Z}_{ik}^{S\pm1})^{\overline{\text{MS}}}\, G^{\text{3pt}}_{\mathcal{O}_\Gamma;\mathcal{Q}_k^{S=\pm1};\mathcal{O}_{\Gamma\gamma_5}}(z,z')\Big|_{\epsilon^{-n}} = 0, \quad n \in \mathbb{Z}^+, \, (i = 2 \text{ or } 3), \tag{5.32}$$

$$Z_{\mathcal{O}_\Gamma}^{\overline{\text{MS}}}\, Z_{\mathcal{O}_{\Gamma\gamma_5}}^{\overline{\text{MS}}} \sum_{k=4}^{5} (\mathcal{Z}_{ik}^{S\pm1})^{\overline{\text{MS}}}\, G^{\text{3pt}}_{\mathcal{O}_\Gamma;\mathcal{Q}_k^{S=\pm1};\mathcal{O}_{\Gamma\gamma_5}}(z,z')\Big|_{\epsilon^{-n}} = 0, \quad n \in \mathbb{Z}^+, \, (i = 4 \text{ or } 5), \tag{5.33}$$

where $\Gamma \in \{\mathbb{1},\, \gamma_\mu,\, \sigma_{\mu\nu}\}$. As we previously mentioned, the bilinear operators must be chosen in such a way as to give nonzero Green's functions.

5.2.4 Loop Integrals in Coordinate Space

At this point, we briefly describe the methodology that we follow for calculating the two-point and three-point GIRS Green's functions defined in the previous section using dimensional regularization.

There are two types of prototype scalar Feynman integrals that enter the calculation of the two-point Green's functions $G^{\text{2pt}}_{\mathcal{O}_{\Gamma\tilde{\Gamma}};\mathcal{O}_{\Gamma'\tilde{\Gamma}'}}(z)$ to the tree-level and one-loop, respectively:

$$I_1^D(\xi_1;\alpha_1) \equiv \int \frac{d^D p_1}{(2\pi)^D} \frac{e^{ip_1\cdot\xi_1}}{(p_1^2)^{\alpha_1}}, \tag{5.34}$$

$$I_2^D(\xi_1;\alpha_1,\alpha_2,\alpha_3,\alpha_4,\alpha_5) \equiv \int \frac{d^D p_1\, d^D p_2\, d^D p_3}{(2\pi)^{3D}} \times \frac{e^{ip_3\cdot\xi_1}}{(p_1^2)^{\alpha_1}\, ((-p_1+p_3)^2)^{\alpha_2}\, \left((-p_1+p_2)^2\right)^{\alpha_3}\, (p_2^2)^{\alpha_4}\, \left((-p_2+p_3)^2\right)^{\alpha_5}}, \tag{5.35}$$

where $D \equiv 4 - 2\varepsilon$ is the number of spacetime dimensions and the vector ξ_1 satisfies: $\xi_1 \neq 0$. Tensor integrals with an arbitrary number of momentum-loop components p_{1_μ}, p_{2_ν}, p_{3_ρ} in the numerator can be reduced to scalars through derivatives w.r.t. ξ_1 of the above scalar integrals or integration by parts (see Eq. (45) in Ref. [118]).

Integral I_1^D is computed by introducing a Schwinger parameter: $1/(p_1^2)^{\alpha_1} = 1/\Gamma(\alpha_1)\int_0^\infty D\lambda\ \lambda^{\alpha_1-1}e^{-\lambda p_1^2}$, leading to the following resulting expression:

$$I_1^D(\xi_1;\alpha_1) = \frac{\Gamma(-\alpha_1+D/2)\ (\xi_1^2)^{\alpha_1-D/2}}{4_1^\alpha\ \pi^{D/2}\ \Gamma(\alpha_1)}. \tag{5.36}$$

Integral I_2^D is calculated in two steps: first, the integration over p_1 and p_2 is performed, which is independent of the phase factor of the numerator. This inner two-loop integral is evaluated through the standard "diamond"-type recursive formula of Ref. [119]. The resulting expression depends on the scalar quantity p_3^2. Then, the remaining integral over p_3 takes the form of I_1^D.

The calculation of the three-point Green's functions $G^{\rm 3pt}_{\mathcal{O}_{\Gamma'};\mathcal{O}_{\Gamma\tilde{\Gamma}};\mathcal{O}_{\Gamma''}}(z,z')$ involve the following prototype scalar Feynman integrals, in addition to I_1^D:

$$I_3^D(\xi_1,\xi_2;\alpha_1,\alpha_2,\alpha_3) \equiv \int \frac{d^Dp_1\ d^Dp_2}{(2\pi)^{2D}} \frac{e^{ip_1\cdot\xi_1}\ e^{ip_2\cdot\xi_2}}{(p_1^2)^{\alpha_1}\ (p_2^2)^{\alpha_2}\ \left((-p_1+p_2)^2\right)^{\alpha_3}}, \tag{5.37}$$

$$I_4^D(\xi_1,\xi_2;\alpha_1,\alpha_2,\alpha_3,\alpha_4,\alpha_5) \equiv \int \frac{d^Dp_1\ d^Dp_2\ d^Dp_3}{(2\pi)^{3D}} \times \frac{e^{ip_2\cdot\xi_1}\ e^{ip_3\cdot\xi_2}}{(p_1^2)^{\alpha_1}\ (p_2^2)^{\alpha_2}\ \left((-p_1+p_2)^2\right)^{\alpha_3}\ (p_3^2)^{\alpha_4}\ \left((-p_1+p_3)^2\right)^{\alpha_5}}, \tag{5.38}$$

where $\xi_1 \neq 0$, $\xi_2 \neq 0$, and $(\xi_1+\xi_2) \neq 0$. As in the case of the two-point Green's functions, tensor integrals can be reduced to scalars through derivatives w.r.t. ξ_1, ξ_2 of the scalar integrals or integration by parts.

The two-loop integral I_3^D can be reduced to one-loop integral J^D by using Schwinger parametrization:

$$I_3^D(\xi_1,\xi_2;\alpha_1,\alpha_2,\alpha_3) = \frac{\Gamma(D/2-s)}{4^s\pi^{D/2}\Gamma(s)}\ (\xi_1^2)^{s-\alpha_3}\ (\xi_2^2)^{s-\alpha_1}\ ((\xi_1+\xi_2)^2)^{s-\alpha_2}\ J^D(\xi_1,\xi_2;\alpha_1,\alpha_2,\alpha_3), \tag{5.39}$$

where $s \equiv \alpha_1+\alpha_2+\alpha_3-D/2$, and

$$J^D(\xi_1,\xi_2;\alpha_1,\alpha_2,\alpha_3) \equiv \int \frac{d^Dx}{(2\pi)^D} \frac{1}{((-x+\xi_1)^2)^{\alpha_1}\ (x^2)^{\alpha_2}((x+\xi_2)^2)^{\alpha_3}}. \tag{5.40}$$

The "triangle" integral J^D is well-studied in Refs. [120, 121]. By using the recursive relations of Ref. [120], the integrals of type J^D appearing in our calculation can be

expressed in terms of the following master integrals, calculated in Ref. [121] up to $\mathcal{O}(\epsilon)$:

$$J^{4-2\epsilon}(\xi_1,\xi_2;1,1,1) = \frac{\pi^{2-\epsilon}\,\Gamma(1+\epsilon)}{(\xi_3^2)^{1+\epsilon}}\left\{\Phi^{(1)}\left(\frac{\xi_1^2}{\xi_3^2},\frac{\xi_2^2}{\xi_3^2}\right)+\epsilon\;\Psi^{(1)}\left(\frac{\xi_1^2}{\xi_3^2},\frac{\xi_2^2}{\xi_3^2}\right)+\mathcal{O}(\epsilon^2)\right\}, \tag{5.41}$$

$$J^{4-2\epsilon}(\xi_1,\xi_2;1,1+\epsilon,1) = \frac{\pi^{2-\epsilon}\,\Gamma(1+\epsilon)}{(\xi_3^2)^{1+2\epsilon}}\left\{\Phi^{(1)}\left(\frac{\xi_1^2}{\xi_3^2},\frac{\xi_2^2}{\xi_3^2}\right)\left(1-\frac{\epsilon}{2}\ln\left(\frac{\xi_1^2\xi_2^2}{\xi_3^2}\right)\right)\right.$$
$$\left.+\epsilon\;\Psi^{(1)}\left(\frac{\xi_1^2}{\xi_3^2},\frac{\xi_2^2}{\xi_3^2}\right)+\mathcal{O}(\epsilon^2)\right\}, \tag{5.42}$$

$$J^{4-2\epsilon}(\xi_1,\xi_2;1,\epsilon,1) = \frac{\pi^{2-\epsilon}\,\Gamma(1+\epsilon)}{(\xi_3^2)^{2\epsilon}\;2\;(1-3\epsilon)}\left\{\frac{1}{\epsilon}-\epsilon\left[\frac{\pi^2}{6}+\ln\left(\frac{\xi_1^2}{\xi_3^2}\right)\ln\left(\frac{\xi_2^2}{\xi_3^2}\right)\right.\right.$$
$$\left.\left.-\frac{2\;\xi_1\cdot\xi_2}{\xi_3^2}\;\Phi^{(1)}\left(\frac{\xi_1^2}{\xi_3^2},\frac{\xi_2^2}{\xi_3^2}\right)\right]+\mathcal{O}(\epsilon^2)\right\}, \tag{5.43}$$

where $\xi_3^2 \equiv (\xi_1+\xi_2)^2$ and $\Phi^{(1)}(\xi_1^2/\xi_3^2,\xi_2^2/\xi_3^2)$, $\Psi^{(1)}(\xi_1^2/\xi_3^2),\xi_2^2/\xi_3^2)$ are polylogarithmic functions given in [121]. Note that by summing all Feynman diagrams, $\Phi^{(1)}$ and $\Psi^{(1)}$ functions are cancelled from the final expressions of the three-point Green's functions.

Integral I_4^D is simplified by applying integration by parts w.r.t. p_1, thus, leading to the following recursive relation, which can eliminate inverse powers of p_1^2, or p_2^2, or p_3^2 [9]:

$$I_4^D(\xi_1,\xi_2;\alpha_1,\alpha_2,\alpha_3,\alpha_4,\alpha_5) = \frac{1}{-2\alpha_1-\alpha_3-\alpha_5+D}\cdot$$
$$\Big[\alpha_3\Big(I_4^D(\xi_1,\xi_2;\alpha_1-1,\alpha_2,\alpha_3+1,\alpha_4,\alpha_5)$$
$$-I_4^D(\xi_1,\xi_2;\alpha_1,\alpha_2-1,\alpha_3+1,\alpha_4,\alpha_5)\Big)+$$
$$\alpha_5\Big(I_4^D(\xi_1,\xi_2;\alpha_1-1,\alpha_2,\alpha_3,\alpha_4,\alpha_5+1)$$
$$-I_4^D(\xi_1,\xi_2;\alpha_1,\alpha_2,\alpha_3,\alpha_4-1,\alpha_5+1)\Big)\Big]. \tag{5.44}$$

In the case where α_1, α_2, α_4 are positive integers, which is true in the computation at hand, an iterative implementation of Eq. (5.44) leads to terms with one propagator less. One momentum can then be integrated using a well-known one-loop formula (see Eqs. (A.1) - (A.2) in Ref. [119]); the remaining integrals are of type I_1^D or I_3^D.

5.3 Results

In this section, we present perturbative results for the two-point and three-point Green's functions, along with the mixing matrices and conversion matrices between GIRS and $\overline{\rm MS}$, utilizing DR in $D \equiv 4-2\epsilon$ dimensions. Since there are various conditions that lead to different solutions (within one-loop perturbation theory), we have chosen to present one set.

5.3.1 Bare Green's Functions

We present our results for the bare tree-level two-point Green's function of two four-quark operators with arbitrary Dirac matrices (X_i, $i=1,2,3,4$) and arbitrary flavors (f_i, f_i', $i=1,2,3,4$) carried by the quark fields. The result is given to all orders in ϵ, and it depends, explicitly, on the d-vector $z \equiv y-x$, which connects the positions of the two operators:

$$\begin{aligned}\langle\big(\bar\psi_{f_1}(x)X_1\psi_{f_3}(x)\bar\psi_{f_2}(x)X_2\psi_{f_4}(x)\big)\ \big(\bar\psi_{f_1'}(y)X_1'\psi_{f_3'}(y)\bar\psi_{f_2'}(y)X_2'\psi_{f_4'}(y)\big)\rangle^{\rm tree} = \frac{N_c\ \Gamma(2-\epsilon)^4}{16\ \pi^{8-4\epsilon}\ (z^2)^{8-4\epsilon}}\times\\ \Big\{\delta_{f_1f_3'}\delta_{f_2f_4'}\ [N_c\ \delta_{f_3f_1'}\delta_{f_4f_2'}\ {\rm tr}(X_1\not{z}X_1'\not{z})\ {\rm tr}(X_2\not{z}X_2'\not{z}) - \delta_{f_3f_2'}\delta_{f_4f_1'}\ {\rm tr}(X_1\not{z}X_2'\not{z}X_2\not{z}X_1'\not{z})]\\ +\delta_{f_1f_4'}\delta_{f_2f_3'}\ [N_c\ \delta_{f_3f_2'}\delta_{f_4f_1'}\ {\rm tr}(X_1\not{z}X_2'\not{z})\ {\rm tr}(X_2\not{z}X_1'\not{z}) - \delta_{f_3f_1'}\delta_{f_4f_2'}\ {\rm tr}(X_1\not{z}X_1'\not{z}X_2\not{z}X_2'\not{z})]\Big\},\end{aligned} \tag{5.45}$$

where N_c is the number of colors.

The tree-level three-point Green's function of one four-quark and two quark bilinear operators for arbitrary Dirac matrices and flavors is given below to all orders in ϵ and in terms of the D-vectors $z \equiv x-y$ and $z' \equiv y-w$, which connect the four-quark operator with the left and right bilinear operators, respectively:

$$\begin{aligned}\langle\big(\bar\psi_{f_1'}(x)X'\psi_{f_2'}(x)\big)\ \big(\bar\psi_{f_1}(y)X_1\psi_{f_3}(y)\bar\psi_{f_2}(y)X_2\psi_{f_4}(y)\big)\ \big(\bar\psi_{f_1''}(w)X''\psi_{f_2''}(w)\big)\rangle^{\rm tree} =\\ \frac{N_c\ \Gamma(2-\epsilon)^4}{16\ \pi^{8-4\epsilon}\ (z^2)^{4-2\epsilon}\ (z'^2)^{4-2\epsilon}}\times\\ \Big\{\delta_{f_3f_1'}\delta_{f_4f_1''}[N_c\ \delta_{f_1f_2'}\delta_{f_2f_2''}\ {\rm tr}(X'\not{z}X_1\not{z})\ {\rm tr}(X_2\not{z}'X''\not{z}') - \delta_{f_2f_2'}\delta_{f_1f_2''}\ {\rm tr}(X'\not{z}X_2\not{z}'X''\not{z}'X_1\not{z})]\\ +\delta_{f_4f_1'}\delta_{f_3f_1''}[N_c\ \delta_{f_2f_2'}\delta_{f_1f_2''}\ {\rm tr}(X'\not{z}X_2\not{z})\ {\rm tr}(X_1\not{z}'X''\not{z}') - \delta_{f_1f_2'}\delta_{f_2f_2''}\ {\rm tr}(X'\not{z}X_1\not{z}'X''\not{z}'X_2\not{z})]\Big\}.\end{aligned} \tag{5.46}$$

In order to extract the renormalization matrices to one-loop order, we require only the above tree-level expressions up to $\mathcal{O}(\epsilon^1)$.

The corresponding one-loop expressions are more involved and more lengthy, and thus, we do not provide the explicit expressions in the manuscript. In particular, the one-loop three-point Green's functions are difficult to be expressed in a closed form without expanding over ϵ. For the determination of the one-loop renormalization matrices, we need only the $\mathcal{O}(\epsilon^0)$ contributions of the bare one-loop Green's functions.

5.3.2 Mixing matrices in the $\overline{\text{MS}}$ scheme

An outcome of our calculation is the one-loop coefficients of the mixing matrices $(Z^{S=\pm1})^{\overline{\text{MS}}}$ and $(\mathcal{Z}^{S=\pm1})^{\overline{\text{MS}}}$ in the $\overline{\text{MS}}$ scheme. By isolating the pole terms (negative powers of ϵ in the Laurent series expansion) in the bare two-point and three-point Green's functions, we extract the mixing coefficients for the four-quark operators. It is worth mentioning that even though we can construct multiple systems of conditions for different Γ matrices, all must give the same unique solution. We have confirmed that indeed all Green's functions calculated in this work give a consistent solution, provided below:

$$Z_{ij}^{S=\pm1,\overline{\text{MS}}} = \delta_{ij} + \frac{g^2_{\overline{\text{MS}}}}{16\pi^2\epsilon} z_{ij}^{\pm} + \mathcal{O}(g^4_{\overline{\text{MS}}}), \qquad \mathcal{Z}_{ij}^{S=\pm1,\overline{\text{MS}}} = \delta_{ij} + \frac{g^2_{\overline{\text{MS}}}}{16\pi^2\epsilon} \tilde{z}_{ij}^{\pm} + \mathcal{O}(g^4_{\overline{\text{MS}}}), \quad (5.47)$$

for Parity Conserving and for Parity Violating operators, respectively. The nonzero coefficients $z_{ij}^{\pm}, \tilde{z}_{ij}^{\pm}$ of the Eq. (5.47) are shown in Table 5.2 ($C_F = (N_c^2 - 1)/(2N_c)$). We observe that the $\overline{\text{MS}}$ mixing matrices of Parity Conserving and Parity Violating operators coincide for both $S = +1$ and $S = -1$, and they take the block diagonal form of $\mathcal{Z}^{S=\pm1}$ in Eq. (5.11). Our results agree with previous calculations in Refs [122, 123].

We note that in our calculation in this project, we have employed the t'Hooft-Veltman prescription for defining γ_5 in D dimensions, which does not violate Ward identities involving pseudoscalar and axial-vector operators. We also note that Lorentz indices appearing in the definition of the four-quark operators and quark bilinear operators are taken to lie in 4 instead of D dimensions in order to handle potential mixing with evanescent operators in dimensional regularization.

i	j	$z_{ij}^{\pm} = \tilde{z}_{ij}^{\pm}$
1	1	$-3(1 \mp N_c)/N_c$
2	2	$3/N_c$
2	3	± 6
3	2	0
3	3	$-6C_F$
4	4	$-3(2C_F \mp 1)$
4	5	$-(2 \mp N_c)/(2N_c)$
5	4	$-6(2 \pm N_c)/N_c$
5	5	$2C_F \pm 3$

TABLE 5.2: Numerical values of the coefficients $z_{ij}^{\pm}$, $\tilde{z}_{ij}^{\pm}$ appearing in the nonvanishing blocks of Eq. (5.47).

5.3.3 $\overline{\text{MS}}$-renormalized Green's functions

By removing the pole parts $(1/\epsilon)$ in the bare Green's function one defines the $\overline{\text{MS}}$-renormalized Green's functions. As an example, we provide one two-point and one three-point Green's function renormalized in $\overline{\text{MS}}$; they depend on the scales z and/or z' corresponding to the separations between the operators that present in each Green's function, as well as on the $\overline{\text{MS}}$ renormalization scale $\bar{\mu}$ appearing in the renormalization of the coupling constant in D dimensions: $g_R = \mu^{-\epsilon} Z_g^{-1} g_B$ (g_B (g_R) is the bare (renormalized) coupling constant, $\mu = \bar{\mu}\sqrt{e^{\gamma_E}/4\pi}$).

$$[G^{\rm 2pt}_{Q_1^{S=\pm1};Q_1^{S=\pm1}}(z)]^{\overline{\rm MS}} = \frac{4N_c}{\pi^8 (z^2)^6} \left(\delta_{f_1 f_4'}\,\delta_{f_2 f_3'} \pm \delta_{f_1 f_3'}\,\delta_{f_2 f_4'}\right)\left(\delta_{f_3 f_2'}\,\delta_{f_4 f_1'} \pm \delta_{f_3 f_1'}\,\delta_{f_4 f_2'}\right) \times \left\{ \pm 1 + N_c + 2\,\frac{g^2_{\overline{\rm MS}}\,C_F}{16\pi^2}\,\Big[\pm 6 + 7N_c \mp 6\left(\ln(\bar{\mu}^2 z^2) + 2\gamma_E - 2\ln(2)\right)\Big] + \mathcal{O}(g^4_{\overline{\rm MS}}) \right\}, \tag{5.48}$$

$$\begin{aligned}[G^{\rm 3pt}_{V_\mu;Q_1^{S=\pm1};V_\mu}(z,z')]^{\overline{\rm MS}} = {} & \frac{N_c}{\pi^8 (z^2)^3 (z'^2)^3} \left(\delta_{f_1' f_4}\,\delta_{f_1'' f_3} \pm \delta_{f_1' f_3}\,\delta_{f_1'' f_4}\right)\left(\delta_{f_2' f_2}\,\delta_{f_2'' f_1} \pm \delta_{f_2' f_1}\,\delta_{f_2'' f_2}\right) \times \\ & \left\{ \frac{N_c \pm 1}{2}\left[1 - 2\frac{z_\mu}{z^2} - 2\frac{z'_\mu}{z'^2} + 4\frac{(z\cdot z')z_\mu z'_\mu}{z^2 z'^2}\right] \pm \frac{g^2_{\overline{\rm MS}}\,C_F}{16\pi^2}\left[1 - 2\frac{(z_\mu + z'_\mu)^2}{(z+z')^2}\right] \right. \\ & \pm \frac{g^2_{\overline{\rm MS}}\,C_F}{16\pi^2}\left[1 - 2\frac{z_\mu}{z^2} - 2\frac{z'_\mu}{z'^2} + 4\frac{(z\cdot z')z_\mu z'_\mu}{z^2 z'^2}\right] \times \\ & \left. \left[2 - 3\left(\ln\left(\frac{\bar{\mu}^2 z^2 z'^2}{(z+z')^2}\right) + 2\gamma_E - 2\ln(2) \mp N_c\right)\right] + \mathcal{O}(g^4_{\overline{\rm MS}}) \right\}, \end{aligned} \tag{5.49}$$

where the flavor indices follow the conventions of Eqs. (5.45), (5.46).

We also provide the $\overline{\rm MS}$-renormalized two-point and three-point Green's functions after integration over timeslices (see Eqs. (5.17) - (5.18)), which are relevant for the extraction of the conversion matrices. These are written in a compact form for all four-quark and quark bilinear operators, as follows:

$$[\tilde{G}^{\rm 2pt}_{Q_i^{S=\pm1};Q_j^{S=\pm1}}(t)]^{\overline{\rm MS}} = \frac{N_c}{\pi^6|t|^9}\left(\delta_{f_1f_4'}\,\delta_{f_2f_3'} \pm \delta_{f_1f_3'}\,\delta_{f_2f_4'}\right)\left(\delta_{f_3f_2'}\,\delta_{f_4f_1'} \pm \delta_{f_3f_1'}\,\delta_{f_4f_2'}\right)\times$$
$$\left\{\left(a^{\pm}_{ij;0} + a^{\pm}_{ij;1}N_c\right) + \frac{g^2_{\overline{\rm MS}}\,C_F}{16\pi^2}\,\left[\left(b^{\pm}_{ij;0} + b^{\pm}_{ij;1}N_c\right) + \left(\ln(\bar{\mu}^2t^2) + 2\gamma_E\right)\left(c^{\pm}_{ij;0} + c^{\pm}_{ij;1}N_c\right)\right] + \mathcal{O}(g^4_{\overline{\rm MS}})\right\}, \tag{5.50}$$

$$[\tilde{G}^{\rm 2pt}_{\mathcal{Q}_i^{S=\pm1};\mathcal{Q}_j^{S=\pm1}}(t)]^{\overline{\rm MS}} = \frac{N_c}{\pi^6|t|^9}\left(\delta_{f_1f_4'}\,\delta_{f_2f_3'} \pm \delta_{f_1f_3'}\,\delta_{f_2f_4'}\right)\left(\delta_{f_3f_2'}\,\delta_{f_4f_1'} \pm (-1)^{\delta_{i2}+\delta_{i3}}\delta_{f_3f_1'}\,\delta_{f_4f_2'}\right)\times$$
$$\left\{\left(\tilde{a}^{\pm}_{ij;0} + \tilde{a}^{\pm}_{ij;1}N_c\right) + \frac{g^2_{\overline{\rm MS}}\,C_F}{16\pi^2}\,\left[\left(\tilde{b}^{\pm}_{ij;0} + \tilde{b}^{\pm}_{ij;1}N_c\right) + \left(\ln(\bar{\mu}^2t^2) + 2\gamma_E\right)\left(\tilde{c}^{\pm}_{ij;0} + \tilde{c}^{\pm}_{ij;1}N_c\right)\right] + \mathcal{O}(g^4_{\overline{\rm MS}})\right\}, \tag{5.51}$$

$$[\tilde{G}^{\rm 3pt}_{\mathcal{O}_\Gamma;Q_i^{S=\pm1};\mathcal{O}_{\Gamma\gamma_5}}(t,t)]^{\overline{\rm MS}} = \frac{N_c}{\pi^4t^6}\left(\delta_{f_1'f_4}\,\delta_{f_1''f_3} \pm \delta_{f_1'f_3}\,\delta_{f_1''f_4}\right)\left(\delta_{f_2'f_2}\,\delta_{f_2''f_1} \pm \delta_{f_2'f_1}\,\delta_{f_2''f_2}\right)\times$$
$$\left\{\left(d^{\pm}_{i\Gamma;0} + d^{\pm}_{i\Gamma;1}N_c\right) + \frac{g^2_{\overline{\rm MS}}\,C_F}{16\pi^2}\,\left[\left(e^{\pm}_{i\Gamma;0} + e^{\pm}_{i\Gamma;1}N_c\right) + \left(\ln(\bar{\mu}^2t^2) + 2\gamma_E\right)\left(f^{\pm}_{i\Gamma;0} + f^{\pm}_{i\Gamma;1}N_c\right)\right] + \mathcal{O}(g^4_{\overline{\rm MS}})\right\}, \tag{5.52}$$

$$[\tilde{G}^{\rm 3pt}_{\mathcal{O}_\Gamma;\mathcal{Q}_i^{S=\pm1};\mathcal{O}_{\Gamma\gamma_5}}(t,t)]^{\overline{\rm MS}} = \frac{N_c}{\pi^4t^6}\left(\delta_{f_1'f_4}\,\delta_{f_1''f_3} \pm \delta_{f_1'f_3}\,\delta_{f_1''f_4}\right)\left(\delta_{f_2'f_2}\,\delta_{f_2''f_1} \pm (-1)^{\delta_{i2}+\delta_{i3}}\delta_{f_2'f_1}\,\delta_{f_2''f_2}\right)\times$$
$$\left\{\left(\tilde{d}^{\pm}_{i\Gamma;0} + \tilde{d}^{\pm}_{i\Gamma;1}N_c\right) + \frac{g^2_{\overline{\rm MS}}\,C_F}{16\pi^2}\,\left[\left(\tilde{e}^{\pm}_{i\Gamma;0} + \tilde{e}^{\pm}_{i\Gamma;1}N_c\right) + \left(\ln(\bar{\mu}^2t^2) + 2\gamma_E\right)\left(\tilde{f}^{\pm}_{i\Gamma;0} + \tilde{f}^{\pm}_{i\Gamma;1}N_c\right)\right] + \mathcal{O}(g^4_{\overline{\rm MS}})\right\}, \tag{5.53}$$

where the coefficients $a^{\pm}_{ij;k}$, $b^{\pm}_{ij;k}$, $c^{\pm}_{ij;k}$, $\tilde{a}^{\pm}_{ij;k}$, $\tilde{b}^{\pm}_{ij;k}$, $\tilde{c}^{\pm}_{ij;k}$, $d^{\pm}_{i\Gamma;k}$, $e^{\pm}_{i\Gamma;k}$, $f^{\pm}_{i\Gamma;k}$, $\tilde{d}^{\pm}_{i\Gamma;k}$, $\tilde{e}^{\pm}_{i\Gamma;k}$, $\tilde{f}^{\pm}_{i\Gamma;k}$ are given in Tables 5.3 – 5.6.

For simplicity, we have presented algebraic results for the three-point Green's functions at $t = t'$. In Fig. 5.3, we examine the dependence of the three-point Green's functions on more general relative values of t and t'. As an example, we provide plots for the $\overline{\rm MS}$-renormalized three-point Green's functions of the Parity Conserving operators for $S = +1$ as a function of $t/(t+t')$, keeping $t+t'$ constant. All other three-point Green's functions (of Parity Conserving operators with $S = -1$, or Parity Violating operators with $S = \pm1$) have similar behavior. We have employed certain values of the free parameters used in lattice simulations: $N_c = 3$, $g^2_{\overline{\rm MS}} = 6/\beta$, $\beta = 1.788$, $\bar{\mu} = 2$ GeV, $(t + t') = T/2$ (T is the temporal lattice size), $T = 64a$ (a is the lattice spacing), $a = 0.07957$ fm.

We observe in Fig. 5.3 that the three-point Green's functions are symmetric over $t/(t + t') = 0.5$ (or equivallenty, $t = t'$), as expected. Green's functions with $Q_{i\neq1}$ take

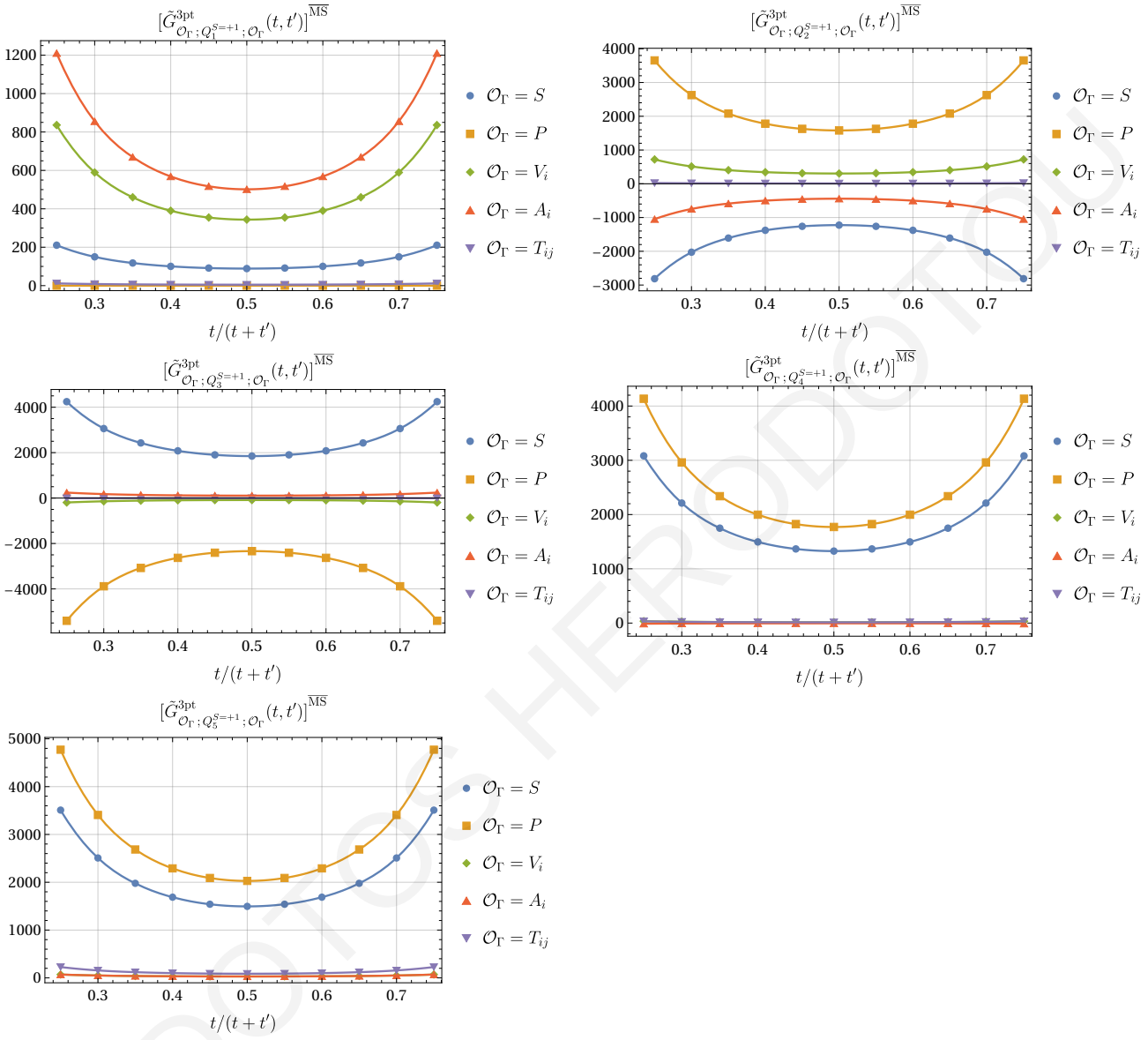

FIGURE 5.3: Plots of three-point Green's functions $[\tilde{G}^{3\text{pt}}_{\mathcal{O}_\Gamma;Q_i^{S=+1};\mathcal{O}_\Gamma}(t,t')]^{\overline{\text{MS}}}$, $i \in [1,5]$, as a function of $t/(t+t')$. A common factor of $N_c/(\pi^8\ (t+t')^6) \times \left(\delta_{f_1' f_4}\,\delta_{f_1'' f_3} + \delta_{f_1' f_3}\,\delta_{f_1'' f_4}\right)\left(\delta_{f_2' f_2}\,\delta_{f_2'' f_1} + \delta_{f_2' f_1}\,\delta_{f_2'' f_2}\right)$ is excluded from all graphs. Here, we set $N_c = 3$, $g^2_{\overline{\text{MS}}} = 6/\beta$, $\beta = 1.788$, $\bar{\mu} = 2$ GeV, $(t+t') = T/2$, $T = 64a$, $a = 0.07957$ fm.

larger absolute values when scalar (S) or pseudoscalar (P) operators are considered, while for Q_1, the three-point Green's functions with vector (V_i) or axial-vector (A_i) operators (where i is a spatial direction) give the highest values. Green's functions with tensor (T_{ij}) operators have much smaller values compared to all other three-point functions.

i	j	$a^{\pm}_{ij;0}$	$a^{\pm}_{ij;1}$	$b^{\pm}_{ij;0}$	$b^{\pm}_{ij;1}$	$c^{\pm}_{ij;0}$	$c^{\pm}_{ij;1}$
1	1	$\pm 7/32$	$7/32$	$\pm 869/160$	$49/16$	$\mp 21/8$	0
1	2	0	0	$\mp 7/4$	$-7/4$	0	0
1	3	0	0	$\pm 7/8$	0	0	0
1	4	0	0	$\pm 7/8$	0	0	0
1	5	0	0	$\pm 21/4$	0	0	0
2	2	0	$7/32$	$\pm 7/4$	$49/16$	0	0
2	3	$\mp 7/64$	0	$\mp 391/320$	0	$\mp 21/16$	0
2	4	0	0	$\pm 7/4$	0	0	0
2	5	0	0	0	0	0	0
3	3	0	$7/128$	$\pm 7/16$	$251/640$	0	$21/32$
3	4	0	0	$\pm 7/16$	$-7/8$	0	0
3	5	0	0	$\mp 21/8$	0	0	0
4	4	$\mp 7/256$	$7/128$	$\pm 87/1280$	$251/640$	$\mp 63/64$	$21/32$
4	5	$\pm 21/128$	0	$\pm 1651/640$	0	$\pm 21/32$	0
5	5	$\pm 21/64$	$21/32$	$\pm 3563/320$	$1709/160$	$\mp 147/16$	$-21/8$

TABLE 5.3: Numerical values of the coefficients $a^{\pm}_{ij;0}$, $a^{\pm}_{ij;1}$, $b^{\pm}_{ij;0}$, $b^{\pm}_{ij;1}$, $c^{\pm}_{ij;0}$, $c^{\pm}_{ij;1}$ appearing in $\overline{\text{MS}}$-renormalized two-point Green's functions with Parity Conserving operators (Eq. (5.50)).

i	j	$\tilde{a}^{\pm}_{ij;0}$	$\tilde{a}^{\pm}_{ij;1}$	$\tilde{b}^{\pm}_{ij;0}$	$\tilde{b}^{\pm}_{ij;1}$	$\tilde{c}^{\pm}_{ij;0}$	$\tilde{c}^{\pm}_{ij;1}$
1	1	$\pm 7/32$	$7/32$	$\pm 869/160$	$49/16$	$\mp 21/8$	0
1	2	0	0	0	0	0	0
1	3	0	0	0	0	0	0
1	4	0	0	0	0	0	0
1	5	0	0	0	0	0	0
2	2	0	$-7/32$	0	$-49/16$	0	0
2	3	$\pm 7/64$	0	$\pm 391/320$	0	$\pm 21/16$	0
2	4	0	0	0	0	0	0
2	5	0	0	0	0	0	0
3	3	0	$-7/128$	0	$-251/640$	0	$-21/32$
3	4	0	0	0	0	0	0
3	5	0	0	0	0	0	0
4	4	$\mp 7/256$	$7/128$	$\pm 87/1280$	$251/640$	$\mp 63/64$	$21/32$
4	5	$\pm 21/128$	0	$\pm 1651/640$	0	$\pm 21/32$	0
5	5	$\pm 21/64$	$21/32$	$\pm 3563/320$	$1709/160$	$\mp 147/16$	$-21/8$

TABLE 5.4: Numerical values of the coefficients $\tilde{a}^{\pm}_{ij;0}$, $\tilde{a}^{\pm}_{ij;1}$, $\tilde{b}^{\pm}_{ij;0}$, $\tilde{b}^{\pm}_{ij;1}$, $\tilde{c}^{\pm}_{ij;0}$, $\tilde{c}^{\pm}_{ij;1}$ appearing in $\overline{\text{MS}}$-renormalized two-point Green's functions with Parity Violating operators (Eq. (5.51)).

i	Γ	$d^{\pm}_{i\Gamma;0}$	$d^{\pm}_{i\Gamma;1}$	$e^{\pm}_{i\Gamma;0}$	$e^{\pm}_{i\Gamma;1}$	$f^{\pm}_{i\Gamma;0}$	$f^{\pm}_{i\Gamma;1}$
1	S	0	0	$\pm 1/2$	0	0	0
2	S	$\mp 1/16$	0	0	0	$\mp 3/4$	0
3	S	0	$1/32$	$\pm 1/4$	$-1/16$	0	$3/8$
4	S	$\mp 1/64$	$1/32$	$\mp 3/8\ (1/8 - \ln(2))$	$-1/16$	$\mp 3/8$	$3/8$
5	S	$\pm 3/32$	0	$\mp 3/4\ (1/8 - \ln(2))$	0	$\pm 3/4$	0
1	P	0	0	0	0	0	0
2	P	$\pm 1/16$	0	± 2	0	$\pm 3/4$	0
3	P	0	$-1/32$	0	$-15/16$	0	$-3/8$
4	P	$\mp 1/64$	$1/32$	$\mp 3/8\ (35/24 - \ln(2))$	$15/16$	$\mp 3/8$	$3/8$
5	P	$\pm 3/32$	0	$\pm 3/4\ (93/24 + \ln(2))$	0	$\pm 3/4$	0
1	V_j	$\pm 1/72$	$1/72$	$\pm 1/6\ (41/48 + \ln(2))$	$1/12$	$\mp 1/12$	0
2	V_j	0	$1/72$	0	$1/12$	0	0
3	V_j	$\mp 1/144$	0	$\mp 1/12\ (23/48 - \ln(2))$	0	$\mp 1/24$	0
4	V_j	0	0	$\pm 1/12$	0	0	0
5	V_j	0	0	$\pm 1/6$	0	0	0
1	A_j	$\pm 1/72$	$1/72$	$\pm 1/6\ (35/16 + \ln(2))$	$11/36$	$\mp 1/12$	0
2	A_j	0	$-1/72$	$\mp 1/9$	$-11/36$	0	0
3	A_j	$\pm 1/144$	0	$\pm 1/12\ (29/16 - \ln(2))$	0	$\pm 1/24$	0
4	A_j	0	0	$\mp 1/36$	0	0	0
5	A_j	0	0	$\pm 1/6$	0	0	0
1	T_{jk}	0	0	$\pm 1/36$	0	0	0
2	T_{jk}	0	0	$\pm 11/192$	0	0	0
3	T_{jk}	0	0	$\mp 1/72$	0	0	0
4	T_{jk}	$\pm 1/576$	0	$\pm 1/72\ (15/8 - \ln(2))$	0	0	0
5	T_{jk}	$\pm 1/288$	$1/144$	$\pm 1/12\ (89/72 + \ln(2))$	$25/216$	$\mp 1/18$	$-1/36$
1	T_{j4}	0	0	$\pm 1/36$	0	0	0
2	T_{j4}	0	0	$\mp 11/192$	0	0	0
3	T_{j4}	0	0	$\mp 1/72$	0	0	0
4	T_{j4}	$\pm 1/576$	0	$\pm 1/72\ (15/8 - \ln(2))$	0	0	0
5	T_{j4}	$\pm 1/288$	$1/144$	$\pm 1/12\ (89/72 + \ln(2))$	$25/216$	$\mp 1/18$	$-1/36$

TABLE 5.5: Numerical values of the coefficients $d^{\pm}_{i\Gamma;l}$, $e^{\pm}_{i\Gamma;l}$, $f^{\pm}_{i\Gamma;l}$ appearing in $\overline{\text{MS}}$-renormalized three-point Green's functions with Parity Conserving operators (Eq. (5.52)).

i	Γ	$\tilde{d}^{\pm}_{i\Gamma;0}$	$\tilde{d}^{\pm}_{i\Gamma;1}$	$\tilde{e}^{\pm}_{i\Gamma;0}$	$\tilde{e}^{\pm}_{i\Gamma;1}$	$\tilde{f}^{\pm}_{i\Gamma;0}$	$\tilde{f}^{\pm}_{i\Gamma;1}$
1	S	0	0	0	0	0	0
2	S	$\pm 1/16$	0	± 1	0	$\pm 3/4$	0
3	S	0	$-1/32$	0	$-7/16$	0	$-3/8$
4	S	$\pm 1/64$	$-1/32$	$\pm 3/8(19/24 - \ln(2))$	$-7/16$	$\pm 3/8$	$-3/8$
5	S	$\mp 3/32$	0	$\mp 3/4(15/8 + \ln(2))$	0	$\mp 3/4$	0
1	V_j	$\pm 1/72$	$1/72$	$\pm 1/6(73/48 + \ln(2))$	$7/36$	$\mp 1/12$	0
2	V_j	0	$-1/72$	0	$-7/36$	0	0
3	V_j	$\pm 1/144$	0	$\pm 1/12(55/48 - \ln(2))$	0	$\pm 1/24$	0
4	V_j	0	0	0	0	0	0
5	V_j	0	0	0	0	0	0
1	T_{jk}	0	0	0	0	0	0
2	T_{jk}	0	0	$\mp 11/192$	0	0	0
3	T_{jk}	0	0	0	0	0	0
4	T_{jk}	$\mp 1/576$	0	$\mp 1/72\ (15/8 - \ln(2))$	0	0	0
5	T_{jk}	$\mp 1/288$	$-1/144$	$\mp 1/12\ (89/72 + \ln(2))$	$-25/216$	$\pm 1/18$	$1/36$
1	T_{j4}	0	0	0	0	0	0
2	T_{j4}	0	0	$\pm 11/192$	0	0	0
3	T_{j4}	0	0	0	0	0	0
4	T_{j4}	$\mp 1/576$	0	$\mp 1/72\ (15/8 - \ln(2))$	0	0	0
5	T_{j4}	$\mp 1/288$	$-1/144$	$\mp 1/12\ (89/72 + \ln(2))$	$-25/216$	$\pm 1/18$	$1/36$

TABLE 5.6: Numerical values of the coefficients $\tilde{d}^{\pm}_{i\Gamma;l}$, $\tilde{e}^{\pm}_{i\Gamma;l}$, $\tilde{f}^{\pm}_{i\Gamma;l}$ appearing in $\overline{\text{MS}}$-renormalized three-point Green's functions with Parity Violating operators (Eq. (5.53)).

5.3.4 Conversion matrices

The one-loop conversion matrices between different variants of GIRS and the $\overline{\text{MS}}$ scheme are extracted from our results by rewriting the GIRS conditions (Eqs. (5.19)-(5.25)) in terms of the conversion matrices, as defined in Eq. (5.26):

$$[\tilde{G}^{\text{2pt}}_{Q_i^{S=\pm1};Q_j^{S=\pm1}}(t)]^{\overline{\text{MS}}} = \sum_{k,l=1}^{5} [(C_{ik}^{S\pm1})^{\overline{\text{MS}},\text{GIRS}}][(C_{jl}^{S\pm1})^{\overline{\text{MS}},\text{GIRS}}][\tilde{G}^{\text{2pt}}_{Q_k^{S=\pm1};Q_l^{S=\pm1}}(t)]^{\text{tree}}, \tag{5.54}$$

$$[\tilde{G}^{\text{3pt}}_{\mathcal{O}_\Gamma;Q_i^{S=\pm1};\mathcal{O}_\Gamma}(t,t)]^{\overline{\text{MS}}} = (C_{\mathcal{O}_\Gamma}^{\overline{\text{MS}},\text{GIRS}})^2 \sum_{k=1}^{5} [(C_{ik}^{S\pm1})^{\overline{\text{MS}},\text{GIRS}}][\tilde{G}^{\text{3pt}}_{\mathcal{O}_\Gamma;Q_k^{S=\pm1};\mathcal{O}_\Gamma}(t,t)]^{\text{tree}}, \tag{5.55}$$

$$[\tilde{G}^{\text{2pt}}_{\mathcal{Q}_i^{S=\pm1};\mathcal{Q}_j^{S=\pm1}}(t)]^{\overline{\text{MS}}} = \sum_{k,l=1}^{5} [(\tilde{C}_{ik}^{S\pm1})^{\overline{\text{MS}},\text{GIRS}}][(\tilde{C}_{jl}^{S\pm1})^{\overline{\text{MS}},\text{GIRS}}][\tilde{G}^{\text{2pt}}_{\mathcal{Q}_k^{S=\pm1};\mathcal{Q}_l^{S=\pm1}}(t)]^{\text{tree}}, \tag{5.56}$$

$$[\tilde{G}^{\text{3pt}}_{\mathcal{O}_\Gamma;\mathcal{Q}_i^{S=\pm1};\mathcal{O}_{\Gamma\gamma_5}}(t,t)]^{\overline{\text{MS}}} = (C_{\mathcal{O}_\Gamma}^{\overline{\text{MS}},\text{GIRS}})\ (C_{\mathcal{O}_{\Gamma\gamma_5}}^{\overline{\text{MS}},\text{GIRS}}) \sum_{k=1}^{5} [(\tilde{C}_{ik}^{S\pm1})^{\overline{\text{MS}},\text{GIRS}}][\tilde{G}^{\text{3pt}}_{\mathcal{O}_\Gamma;\mathcal{Q}_k^{S=\pm1};\mathcal{O}_{\Gamma\gamma_5}}(t,t)]^{\text{tree}}, \tag{5.57}$$

where $C_{\mathcal{O}_\Gamma}^{\overline{\text{MS}},\text{GIRS}}$ is the conversion factor of the quark bilinear operator $\mathcal{O}_\Gamma$ calculated to one loop in Ref. [9]:

$$C_S^{\overline{\text{MS}},\text{GIRS}} = 1 + \frac{g^2_{\overline{\text{MS}}}\ C_F}{16\pi^2}\ \left(-\frac{1}{2} + 3\ln(\bar{\mu}^2 t^2) + 6\gamma_E\right) + \mathcal{O}(g^4_{\overline{\text{MS}}}), \tag{5.58}$$

$$C_P^{\overline{\text{MS}},\text{GIRS}} = 1 + \frac{g^2_{\overline{\text{MS}}}\ C_F}{16\pi^2}\ \left(\frac{15}{2} + 3\ln(\bar{\mu}^2 t^2) + 6\gamma_E\right) + \mathcal{O}(g^4_{\overline{\text{MS}}}), \tag{5.59}$$

$$C_V^{\overline{\text{MS}},\text{GIRS}} = 1 + \frac{g^2_{\overline{\text{MS}}}\ C_F}{16\pi^2}\ \frac{3}{2} + \mathcal{O}(g^4_{\overline{\text{MS}}}), \tag{5.60}$$

$$C_A^{\overline{\text{MS}},\text{GIRS}} = 1 + \frac{g^2_{\overline{\text{MS}}}\ C_F}{16\pi^2}\ \frac{11}{2} + \mathcal{O}(g^4_{\overline{\text{MS}}}), \tag{5.61}$$

$$C_T^{\overline{\text{MS}},\text{GIRS}} = 1 + \frac{g^2_{\overline{\text{MS}}}\ C_F}{16\pi^2}\ \left(\frac{25}{6} - \ln(\bar{\mu}^2 t^2) - 2\gamma_E\right) + \mathcal{O}(g^4_{\overline{\text{MS}}}). \tag{5.62}$$

Note that the conversion matrix $(\tilde{C}^{S\pm1})^{\overline{\text{MS}},\text{GIRS}}$ has the block diagonal form of $\mathcal{Z}^{S=\pm1}$ in Eq. (5.11). As we discussed in the previous section, there are a lot of different choices of three-point Green's functions that can be included in the renormalization conditions, giving a different version of GIRS. In particular, for the Parity Conserving operators ($Q_i^{S=\pm1}$), where 15 conditions are obtained from the two-point Green's functions, there

are $30!\,/(10!\;20!\,) = 30,045,015$ choices for obtaining the remaining 10 conditions from the three-point Green's functions (see Table 5.5). However, some choices include linear dependent or incompatible conditions leading to infinite or no solutions, respectively. By examining all cases in one-loop perturbation theory, we conclude that there are 205,088 choices of conditions, which give a unique solution.

Even though, all solvable systems of conditions are acceptable, it is natural to set a criterion in order to select options which have better behavior compared to others. Such a criterion can be the size of the mixing contributions. To this end, we evaluate the sum of squares of the off-diagonal coefficients in the conversion matrices for all the accepted cases, and we choose the cases with the smallest values. We found that, in general, the sums of squares among different choices are comparable. We also observed that the mixing is less pronounced for the operators with $S = -1$, as compared to $S = +1$.

From the options that give the smallest sum of squares of the off-diagonal coefficients, we choose one to present below. We avoid to include tensor operators in the selected set of conditions, which are typically more noisy in simulations. Also, we prefer to have more scalar or pseudoscalar operators which are computationally cheaper compared to other bilinear operators. The selected set of conditions include the following 10 renormalized three-point Green's functions:

$$\tilde{G}^{\rm 3pt}_{S;Q_1^{S=\pm1};S}(t,t), \quad \tilde{G}^{\rm 3pt}_{P;Q_1^{S=\pm1};P}(t,t), \quad \tilde{G}^{\rm 3pt}_{V_i;Q_1^{S=\pm1};V_i}(t,t), \quad \tilde{G}^{\rm 3pt}_{S;Q_2^{S=\pm1};S}(t,t), \quad \tilde{G}^{\rm 3pt}_{P;Q_2^{S=\pm1};P}(t,t),$$
$$\tilde{G}^{\rm 3pt}_{S;Q_3^{S=\pm1};S}(t,t), \quad \tilde{G}^{\rm 3pt}_{S;Q_5^{S=\pm1};S}(t,t), \quad \tilde{G}^{\rm 3pt}_{P;Q_5^{S=\pm1};P}(t,t), \quad \tilde{G}^{\rm 3pt}_{V_i;Q_5^{S=\pm1};V_i}(t,t), \quad \tilde{G}^{\rm 3pt}_{A_i;Q_5^{S=\pm1};A_i}(t,t),$$

and the solution reads:

$$(C_{ij}^{S\pm1})^{\overline{\rm MS},\rm GIRS} = \delta_{ij} + \frac{g^2_{\overline{\rm MS}}}{16\pi^2}\sum_{k=-1}^{+1}\left[g^{\pm}_{ij;k} + \left(\ln(\bar{\mu}^2t^2) + 2\gamma_E\right)\;h^{\pm}_{ij;k}\right]N_c^k + \mathcal{O}(g^4_{\overline{\rm MS}}), \quad (5.63)$$

where the coefficients $g^{\pm}_{ij;k}$, $h^{\pm}_{ij;k}$, are given in Table 5.7.

In the case of Parity Violating operators, the number of possible sets of conditions is much smaller, since the 5×5 mixing matrices are decomposed into three blocks of 1×1, and two 2×2 sub-matrices, as explained in the previous section. For the 1×1 block, we consider the condition with the corresponding two-point Green's function and thus, there is no need to involve any three-point Green's functions. For the 2×2

i	j	$g^{\pm}_{ij;-1}$	$g^{\pm}_{ij;0}$	$g^{\pm}_{ij;+1}$	$h^{\pm}_{ij;-1}$	$h^{\pm}_{ij;0}$	$h^{\pm}_{ij;+1}$
1	1	$-869/140$	$\pm 379/140$	$7/2$	3	∓ 3	0
1	2	2	$\mp(723/280 - 6\ln(2))$	-2	0	0	0
1	3	$-723/140 + 12\ln(2)$	0	0	0	0	0
1	4	-4	± 4	0	0	0	0
1	5	-2	± 2	0	0	0	0
2	1	$397/280 + 6\ln(2)$	$\pm(163/280 - 6\ln(2))$	-2	0	0	0
2	2	$-9/2$	± 2	$7/2$	-3	0	0
2	3	4	∓ 2	0	0	∓ 6	0
2	4	4	± 8	0	0	0	0
2	5	-2	0	0	0	0	0
3	1	-1	± 1	0	0	0	0
3	2	1	$\pm 99/280$	0	0	0	0
3	3	$-38/35$	± 2	$251/140$	-3	0	3
3	4	4	$\pm 239/280$	$-321/140$	0	0	0
3	5	0	$\mp 239/560$	0	0	0	0
4	1	-1	± 1	0	0	0	0
4	2	1	$\mp 239/280$	0	0	0	0
4	3	4	± 2	$-799/140$	0	0	0
4	4	$-307/112 + 3\ln(2)$	$\pm 169/140$	$251/140$	-3	∓ 3	3
4	5	$-269/480 + 1/2\ \ln(2)$	$\pm(869/1680 - \ln(2))$	0	1	$\mp 1/2$	0
5	1	-6	± 6	0	0	0	0
5	2	-6	0	0	0	0	0
5	3	0	∓ 12	0	0	0	0
5	4	$-269/40 + 6\ln(2)$	$\mp(29/140 - 12\ln(2))$	0	12	± 6	0
5	5	$-1229/240 - 3\ln(2)$	$\pm 309/140$	$1709/420$	1	∓ 3	-1

TABLE 5.7: Numerical values of the coefficients $g^{\pm}_{ij;k}$, $h^{\pm}_{ij;k}$ appearing in Eq. (5.63).

blocks, there are 8 choices (for each block) for obtaining 1 condition from the three-point Green's functions (see Table 5.6), in addition to the 3 conditions obtained from the two-point Green's functions. However, only two (three) options for the block that involves $\{\mathcal{Q}_2, \mathcal{Q}_3\}$ ($\{\mathcal{Q}_4, \mathcal{Q}_5\}$) give a unique solution. By applying the same criterion, as in the Parity Conserving operators, for restricting the number of possible sets of conditions, we conclude that the block of $\{\mathcal{Q}_2, \mathcal{Q}_3\}$ has smaller mixing contributions compared to the block of $\{\mathcal{Q}_4, \mathcal{Q}_5\}$ for the Parity Violating operators with $S = +1$, and vice versa for the operators with $S = -1$.

The option that gives the smallest sum of squares of the off-diagonal coefficients include the following renormalized three-point Green's functions:

$$\tilde{G}^{\rm 3pt}_{S;\mathcal{Q}_2^{S=\pm1};P}(t,t), \qquad \tilde{G}^{\rm 3pt}_{S;\mathcal{Q}_5^{S=\pm1};P}(t,t),$$

and the solution reads:

$$(\tilde{C}_{ij}^{S\pm1})^{\overline{\rm MS},\rm GIRS} = \delta_{ij} + \frac{g^2_{\overline{\rm MS}}}{16\pi^2}\sum_{k=-1}^{+1}\left[\tilde{g}^{\pm}_{ij;k} + \left(\ln(\bar{\mu}^2t^2) + 2\gamma_E\right)\ \tilde{h}^{\pm}_{ij;k}\right] N_c^k + \mathcal{O}(g^4_{\overline{\rm MS}}), \quad (5.64)$$

where the coefficients $\tilde{g}^{\pm}_{ij;k}$, $\tilde{h}^{\pm}_{ij;k}$, are given in Table 5.8.

i	j	$\tilde{g}^{\pm}_{ij;-1}$	$\tilde{g}^{\pm}_{ij;0}$	$\tilde{g}^{\pm}_{ij;+1}$	$\tilde{h}^{\pm}_{ij;-1}$	$\tilde{h}^{\pm}_{ij;0}$	$\tilde{h}^{\pm}_{ij;+1}$
1	1	$-869/140$	$\pm379/140$	$7/2$	3	∓3	0
1	2	0	0	0	0	0	0
1	3	0	0	0	0	0	0
1	4	0	0	0	0	0	0
1	5	0	0	0	0	0	0
2	1	0	0	0	0	0	0
2	2	$-9/2$	0	$7/2$	-3	0	0
2	3	0	∓2	0	0	∓6	0
2	4	0	0	0	0	0	0
2	5	0	0	0	0	0	0
3	1	0	0	0	0	0	0
3	2	0	$\pm99/280$	0	0	0	0
3	3	$-38/35$	0	$251/140$	-3	0	3
3	4	0	0	0	0	0	0
3	5	0	0	0	0	0	0
4	1	0	0	0	0	0	0
4	2	0	0	0	0	0	0
4	3	0	0	0	0	0	0
4	4	$-307/112 + 3\ln(2)$	$\pm169/140$	$251/140$	-3	∓3	3
4	5	$-269/480 + 1/2\ \ln(2)$	$\pm(869/1680 - \ln(2))$	0	1	$\mp1/2$	0
5	1	0	0	0	0	0	0
5	2	0	0	0	0	0	0
5	3	0	0	0	0	0	0
5	4	$-269/40 + 6\ln(2)$	$\mp(29/140 - 12\ln(2))$	0	12	±6	0
5	5	$-1229/240 - 3\ln(2)$	$\pm309/140$	$1709/420$	1	∓3	-1

TABLE 5.8: Numerical values of the coefficients $\tilde{g}^{\pm}_{ij;k}$, $\tilde{h}^{\pm}_{ij;k}$ appearing in Eq. (5.64).

Other accepted options include the renormalized three-point Green's functions of:

$$\tilde{G}^{\rm 3pt}_{V_i;\mathcal{Q}_3^{S=\pm1};A_i}(t,t) \quad \text{and} \quad \tilde{G}^{\rm 3pt}_{T_{ij};\mathcal{Q}_4^{S=\pm1};T'_{ij}}(t,t) \quad \left(\text{or} \quad \tilde{G}^{\rm 3pt}_{T_{i4};\mathcal{Q}_4^{S=\pm1};T'_{i4}}(t,t)\right).$$

5.4 Possible Extensions

In this Chapter, we compute two-point and three-point Green's functions within the GIRS scheme. This computation allows us to establish the conversion matrices between GIRS and $\overline{\text{MS}}$. In this work, we concentrate only in renormalizing the four-quark operators which involved in flavor-changing $\Delta F = 2$ processes. In this case, these operators mix only among themselves and the mixing with lower dimensional operators is forbidden.

However, a natural extension of this project would be the study of the renormalization of the four-quark operators related to processes that alter flavors with $\Delta F = 1$ and $\Delta F = 0$ changes. The main obstacle in these investigations lies in the mixing between the four-quark operators and lower-dimensional operators, such as the Chromomagnetic operator.

Chapter 6

Summary and Conclusions

In this dissertation, we examine the perturbative renormalization within the framework of lattice strong interaction physics. Specifically, we study the following two projects: Fine-Tuning of the Yukawa and Quartic Couplings in Supersymmetric QCD and Gauge-invariant Renormalization of Four-quark Operators in Lattice QCD. The main purpose of these projects is to produce ingredients which will be utilized in numerical simulations and in non-perturbative calculations on the lattice. In the second project, our results can also be combined with nonperturbative data to facilitate the conversion of the lattice results into renormalized quantities in continuum renormalization schemes.

For the fine-tuning of the Yukawa couplings, we calculate three-point Green's functions with external elementary fields of the SQCD action in the Wess-Zumino gauge. In particular, we perform one-loop calculations for a complete set of three-point Green's functions with external gluino, quark and squark fields, employing Wilson fermions and gluons. For the fine-tuning of the quartic couplings, we compute one-loop four-point Green's functions with external squark fields again of the SQCD action in the Wess-Zumino gauge. To extract the fine-tunings of Yukawa and quartic couplings in the $\overline{\text{MS}}$ scheme, we compute the relevant Green's functions in two regularizations: dimensional and lattice. The lattice calculations are the crux of this work; and the continuum calculations serve as a necessary ingredient, allowing us to relate our lattice results to the $\overline{\text{MS}}$ scheme.

Our findings indicate that the multiplicative renormalization of the Yukawa coupling and the coefficient of the mirror Yukawa counterterm on the lattice are finite and gauge independent, aligning with the principles of renormalization and gauge

invariance. Additionally, we observe that, at the quantum level, the multiplicative renormalization of the quartic coupling in dimensional regularization remains unaffected by one-loop corrections. Consequently, we anticipate that the corresponding renormalization on the lattice will be finite and a finite mixture of terms with four squarks that obey the symmetries of the SQCD, potentially emerging in the $\overline{\text{MS}}$ scheme on the lattice. Furthermore, we expect these renormalization constants to be gauge independent. The computation regarding the renormalization of the quartic couplings on the lattice is currently in progress.

With the perturbative renormalization of the Yukawa and the quartic couplings in Supersymmetric QCD, all renormalizations (fields, masses, couplings) in the Wilson formulation are completed [48, 66]. The outcomes of this study will hold significant relevance for the setup and the calibration of lattice numerical simulations of SQCD. In the coming years, it is expected that simulations of supersymmetric theories will become ever more feasible and precise.

As previously mentioned, a follow up study of this work would be the perturbative calulations of all fine-tunings in SQCD on the lattice using chirally invariant actions. Specifically, we can utilize the overlap action for gluino and quark fields. Although this approach may be computationally intensive, it minimizes the number of parameters requiring fine-tuning, which is an important advantage for these types of calculations.

In the second project, we calculate two-point and three-point Green's functions in the GIRS scheme. This calculation enables us to derive the elements of the conversion matrices connecting GIRS and $\overline{\text{MS}}$. Operator mixing was addressed through a set of conditions involving these Green's functions, ensuring that renormalized values revert to tree-level standards at specific reference scales. Proposed variants of GIRS, including time-slice integration, successfully reduced statistical noise in lattice simulations. This effect was particularly evident in the renormalization of fermion bilinear operators and the examination of mixing between gluon and quark energy-momentum tensor operators [9], as well as the supercurrent in supersymmetric QCD [71, 117].

A natural extension of this project will involve the study of four-quark operators with $\Delta F = 1$ and $\Delta F = 0$. The primary challenge of these investigations is the mixing between the four-quark operators and lower-dimensional operators, including the Chromomagnetic operator.

Appendix A

The Path Integral over the Gluino Field

To elucidate the Majorana nature of the gluino field within the functional integral, and the way to properly address it in the calculation of Feynman diagrams, we first reformulate the action from Eq. (2.97) to express it in exclusively in terms of λ, rather than $\bar{\lambda}$. We proceed in a way analogous to Ref. [124], but we now take into account the additional complication brought about by the Yukawa terms. By applying the Majorana condition ($(\bar{\lambda}^\alpha)^T = C\lambda^\alpha$), the part of the action which contains gluino fields has the general form:

$$S_{\text{gluino}} = \bar{\lambda} D \lambda + \bar{A}\lambda + \bar{\lambda} B = \lambda^T M \lambda + (\bar{A} + B')\lambda, \tag{A.1}$$

where $M \equiv CD$. The first term represents both the kinetic energy of the gluino and the interaction with the gluon field. The subsequent terms correspond to the Yukawa interactions:

$$\bar{A} = i\sqrt{2}\, g\, (-\bar{\psi} P_- T^\alpha A_+ - \bar{\psi} P_+ T^\alpha A_-^\dagger), \quad B = i\sqrt{2}\, g\, (A_+^\dagger T^\alpha P_+ \psi + A_- T^\alpha P_- \psi)\,, \tag{A.2}$$

where $B' = -B^T C$ and $B'^T = CB$. Therefore, the path integral reads:

$$Z[J] = \int \mathcal{D}U_{\text{other}}\, e^{-S_{\text{other}}} \int \mathcal{D}\lambda\, e^{-\lambda^T M \lambda - (\bar{A} + B')\lambda - J\lambda}\,, \tag{A.3}$$

where J is an external source, U_{other} stands for all of the fields in the theory except gluino fields, and S_{other} denotes the action part devoid of gluinos. In order to integrate

out the gluino field, we implement the following standard change of variables:

$$\lambda^{'T} \equiv \lambda^T + \frac{1}{2}(J + \bar{A} + B')\, M. \tag{A.4}$$

This leads to:

$$\begin{aligned} Z[J] &= \int \mathcal{D}U_{\text{other}}\, e^{-S_{\text{other}}} \int \mathcal{D}\lambda'\, e^{-\lambda^{'T} M \lambda' - \frac{1}{4}(\bar{A}+B'+J)M^{-1}(\bar{A}+B'+J)^T} \\ &= \int \mathcal{D}U_{\text{other}}\, e^{-S_{\text{other}}}\, Pf[M]\, e^{-\frac{1}{4}(\bar{A}+B'+J)M^{-1}(\bar{A}+B'+J)^T}, \end{aligned} \tag{A.5}$$

where $Pf[M]$ is the Pfaffian of the antisymmetric matrix M. In the absence of Yukawa terms, and in case one is interested only in Green's functions without external gluinos (so that one can set $J = 0$ from the start), the exponential in Eq. (A.5) becomes trivial and the only remnant of gluinos is the Pfaffian; in those cases, the only effect of the gluinos' Majorana nature is the well-known factor of $1/2$ for every closed gluino loop, due to the fact that $Pf[M] = \det[\mathrm{M}]^{1/2}$. Note that we do not assume that J, $\bar{A}$ and B are Majorana spinors.

Let us examine the exponent appearing in Eq. (A.5):

$$-S' \equiv -\frac{1}{4}(\bar{A} + B' + J)M^{-1}(\bar{A} + B' + J)^T. \tag{A.6}$$

When we compute Green's functions without external gluinos, we can set $J = 0$ and thus, S' can be written as:

$$\begin{aligned} -S'|_{J=0} &= -\frac{1}{4}(\bar{A} + B')M^{-1}(\bar{A} + B')^T \\ &= -\frac{1}{4}(\bar{A}M^{-1}\bar{A}^T + B'M^{-1}B^{'T} + \bar{A}M^{-1}CB - B^TCM^{-1}\bar{A}^T) \\ &= -\frac{1}{4}(\bar{A}M^{-1}\bar{A}^T + B'M^{-1}B^{'T} + 2\,\bar{A}D^{-1}B). \end{aligned} \tag{A.7}$$

Green's functions with one external gluino field can be generated via functional differentiation with respect to the gluino source J (cf. Eqs. (A.3), (A.6)):

$$\lambda(x): \qquad e^{-S'} \to -\frac{d}{dJ_x}\, e^{-S'}|_{J=0} = \frac{1}{2}\, D^{-1}_{x,y}\, C^{-1}\, (\bar{A} + B')^T_y\, e^{-S'}|_{J=0}. \tag{A.8}$$

The above expression gives rise to all 3 diagrams of Fig. 4.1; the diagrams are redrawn in Fig. A.1 with a shaded area indicating the contribution of the "effective vertex"

$1/2\, D^{-1}C^{-1}\,(\bar{A}+B')^T$ appearing in Eq. (A.8) (note that D contains contributions with zero or more gluons). We note also the factor of $1/2$ present in Eq. (A.8); it is similar to the factor accompanying closed gluino loops, even though it does not stem from the Pfaffian.

In order to compute Green's functions with two external gluinos, for example $\lambda(x)\lambda(y)$, we have to consider the following second derivative with respect to the external source J:

$$\lambda(x)\lambda(y): \qquad e^{-S'} \to \left(-\frac{d}{dJ_x}\right)\left(-\frac{d}{dJ_y}\right) e^{-S'}|_{J=0}. \tag{A.9}$$

Gluon fields contained in the matrices M^{-1} and D^{-1} of Eqs. (A7), (A8), can be extracted via a series expansion in g; thus, one gluon field emerges by calculating the quantity $g\frac{\partial}{\partial g}(M^{-1})\Big|_{g=0}$:

$$g\frac{\partial}{\partial g}(M^{-1})\Big|_{g=0} = -M^{-1}\left(g\frac{\partial M}{\partial g}\right)M^{-1}\Big|_{g=0}, \tag{A.10}$$

where $g\frac{\partial M}{\partial g}$ is the normal vertex with two gluino fields and one gluon field. Similarly, extraction of two gluon fields follows from:

$$\begin{aligned}\frac{1}{2}g^2\frac{\partial^2}{\partial g^2}(M^{-1})\Big|_{g=0} &= -\frac{1}{2}\,g^2\,\frac{\partial}{\partial g}\left(M^{-1}\frac{\partial M}{\partial g}M^{-1}\right)\Big|_{g=0} \\ &= g^2 M^{-1}\left(\frac{\partial M}{\partial g}\right)M^{-1}\left(\frac{\partial M}{\partial g}\right)M^{-1}\Big|_{g=0} - \frac{1}{2}\,g^2 M^{-1}\,\frac{\partial^2 M}{\partial g^2}\,M^{-1}.\end{aligned} \tag{A.11}$$

The term with $\frac{\partial^2 M}{\partial g^2}$ appears only on the lattice.

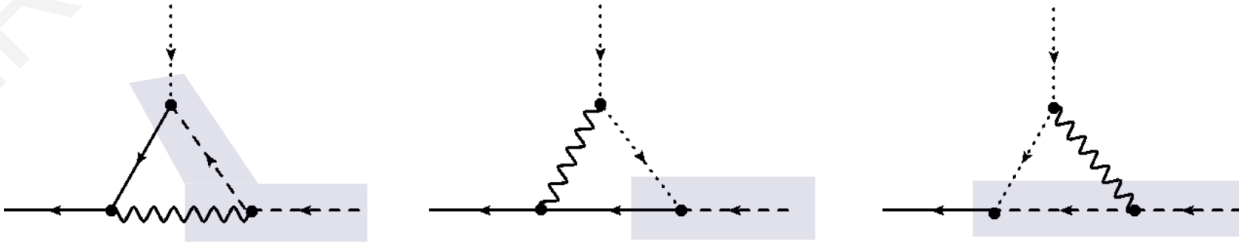

FIGURE A.1: Redrawn one-loop Feynman diagrams with a shaded area indicating the contribution of the "effective vertex" appearing in Eq. (A.8).

Appendix B

Additional Feynman Diagrams for $\Delta F < 2$ Four-quark Operators

In this appendix we illustrate diagrams that are absent for $\Delta F = 2$ four-quark operators and they contribute to the Green's functions with products of four-quark operators with $\Delta F < 2$. Furthermore, we present additional Feynman diagrams that arise on the lattice.

For the Green's functions with two $\Delta F < 2$ four-quark operators, these diagrams are illustrated in Fig. B.1.

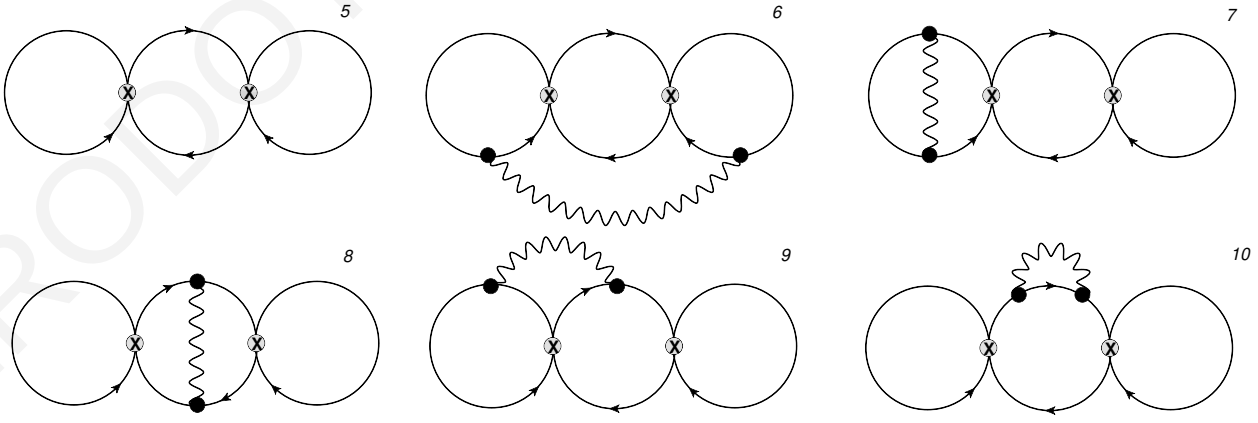

FIGURE B.1: Feynman diagrams contributing to $\langle \mathcal{O}_{\Gamma\tilde{\Gamma}}(x)\, \mathcal{O}^{\dagger}_{\Gamma'\tilde{\Gamma}'}(y) \rangle$ with two four-quark operators with $\Delta F < 2$, to order $\mathcal{O}(g^0)$ (diagram 5) and $\mathcal{O}(g^2)$ (the remaining diagrams). Notation is identical to that of Figure 5.1. Diagrams 6-10 can have mirror variants.

In Fig. B.2 and Fig. B.3, we show the disconnected Feynman diagrams and the additional Feynman diagrams on the lattice contributing to the two-point Green's functions with two four-quark operators, respectively. Note that for Green's functions with $\Delta F = 2$ four-quark operators there cannot be any disconnected diagrams.

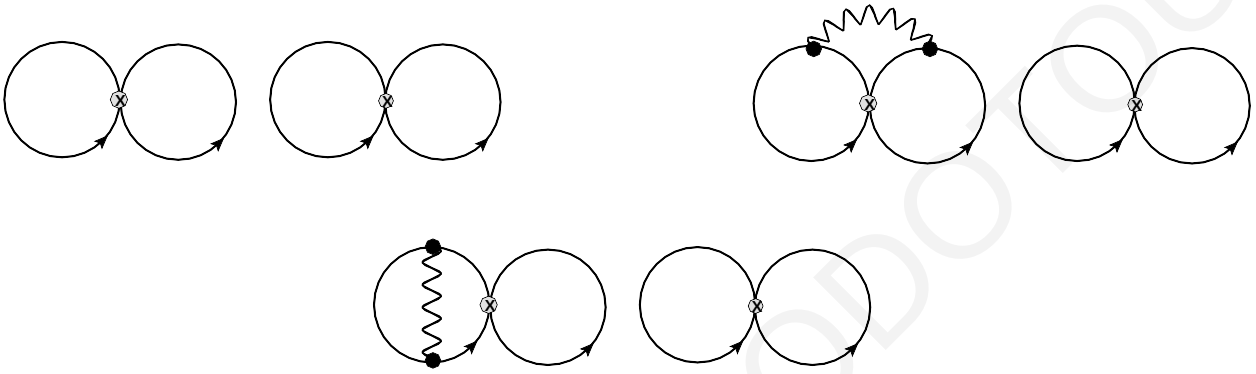

FIGURE B.2: Disconnected Feynman diagrams contributing to $\langle \mathcal{O}_{\Gamma\tilde{\Gamma}}(x)\, \mathcal{O}^{\dagger}_{\Gamma'\tilde{\Gamma}'}(y)\rangle$, to order $\mathcal{O}(g^0)$ (first diagram) and $\mathcal{O}(g^2)$ (the remaining diagrams). Notation is identical to that of Figure 5.1. These diagrams contribute to $\langle \mathcal{O}_{\Gamma\tilde{\Gamma}}(x)\, \mathcal{O}_{\Gamma'\tilde{\Gamma}'}(y)\rangle$ beyond one loop.

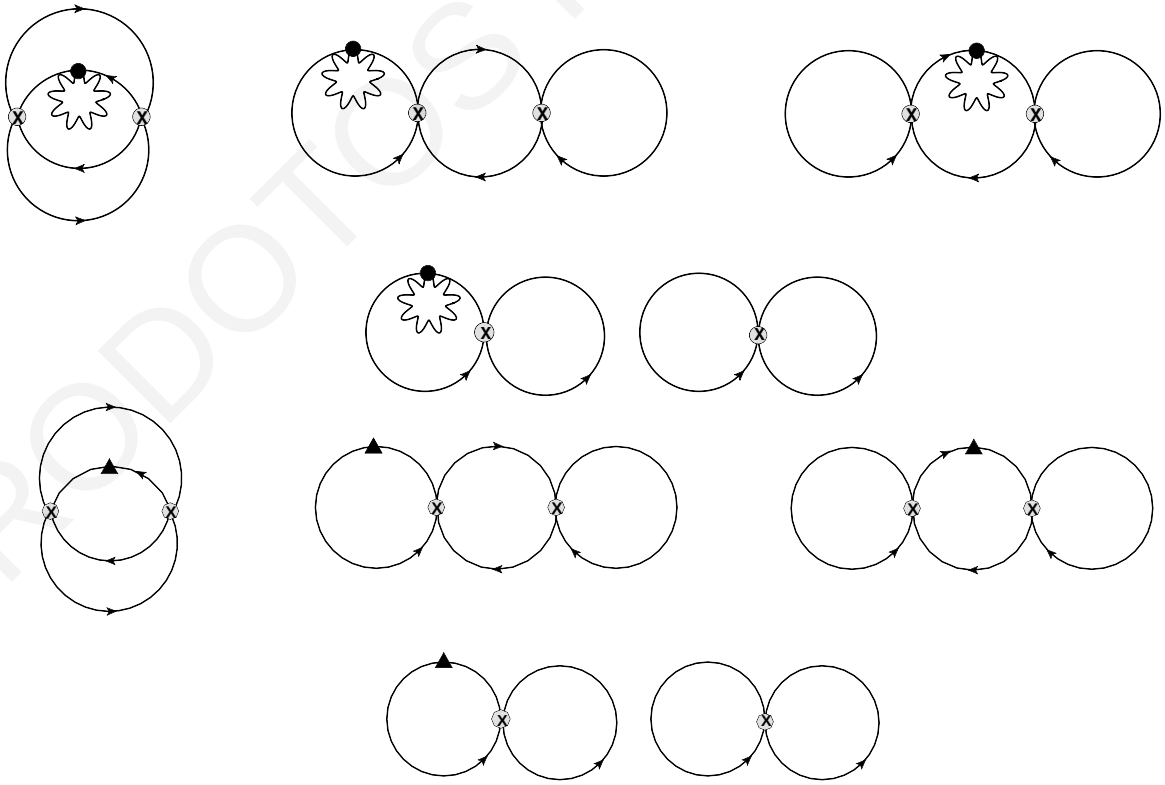

FIGURE B.3: Additional Feynman diagrams contributing to $\langle \mathcal{O}_{\Gamma\tilde{\Gamma}}(x)\, \mathcal{O}^{\dagger}_{\Gamma'\tilde{\Gamma}'}(y)\rangle$ on the lattice. Notation is identical to that of Figure 5.1. The triangle denotes insertion of the critical mass counterterm.

In the case that we study the renormalization of $\Delta F < 2$ four-quark operators, we have to consider additional two-point Green's functions of the product of one four-quark operator and one bilinear $\langle \mathcal{O}_{\Gamma\tilde{\Gamma}}(x)\, \mathcal{O}_{\Gamma'}(y) \rangle$. Take into consideration that these Green's functions are zero when we investigate $\Delta F = 2$ four-quark operators.

The Feynman diagrams contributing to the two-point Green's functions of the product of one four-quark operator and one bilinear, to order $\mathcal{O}(g^0)$ (diagram 1) and $\mathcal{O}(g^2)$ (the remaining diagrams), are shown in Fig. B.4. In Fig. B.5 and Fig. B.6, we illustrate the disconnected Feynman diagrams and the lattice Feynman diagrams contributing to the aforementioned two-point Green's functions, respectively.

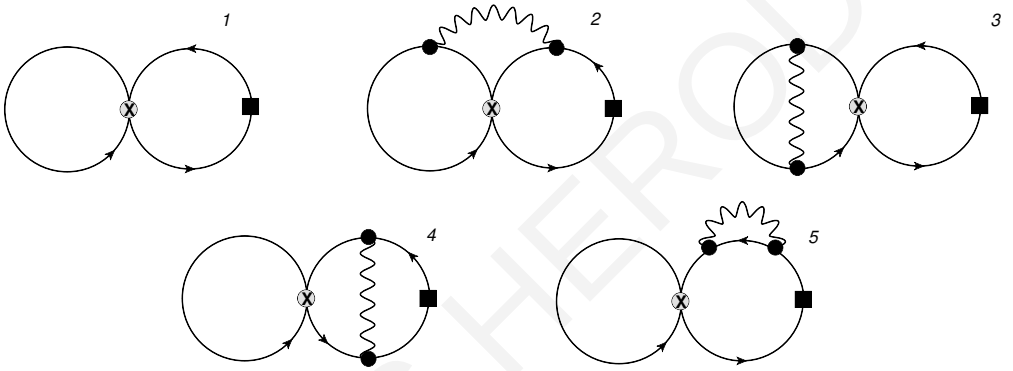

FIGURE B.4: Feynman diagrams contributing to $\langle \mathcal{O}_{\Gamma\tilde{\Gamma}}(x)\, \mathcal{O}_{\Gamma'}(y) \rangle$, to order $\mathcal{O}(g^0)$ (diagram 1) and $\mathcal{O}(g^2)$ (the remaining diagrams). Notation is identical to that of Figure 5.2. All of these are absent for $\Delta F = 2$ operators and they contribute to operators with $\Delta F < 2$. Diagrams 2-5 can have mirror variants.

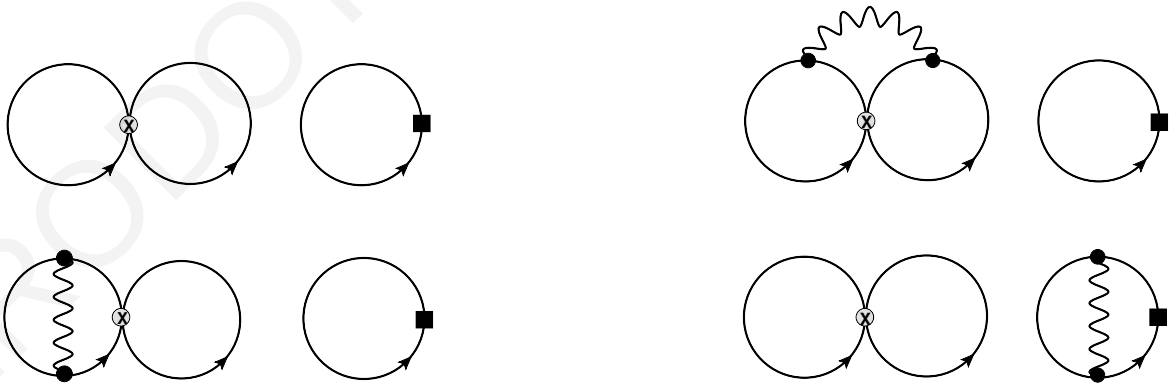

FIGURE B.5: Disconnected Feynman diagrams contributing to $\langle \mathcal{O}_{\Gamma\tilde{\Gamma}}(x)\, \mathcal{O}_{\Gamma'}(y) \rangle$, to order $\mathcal{O}(g^0)$ (first diagram) and $\mathcal{O}(g^2)$ (the remaining diagrams). Notation is identical to that of Figure 5.2. These diagrams contribute to $\langle \mathcal{O}_{\Gamma\tilde{\Gamma}}(x)\, \mathcal{O}_{\Gamma'}(y) \rangle$ beyond one loop.

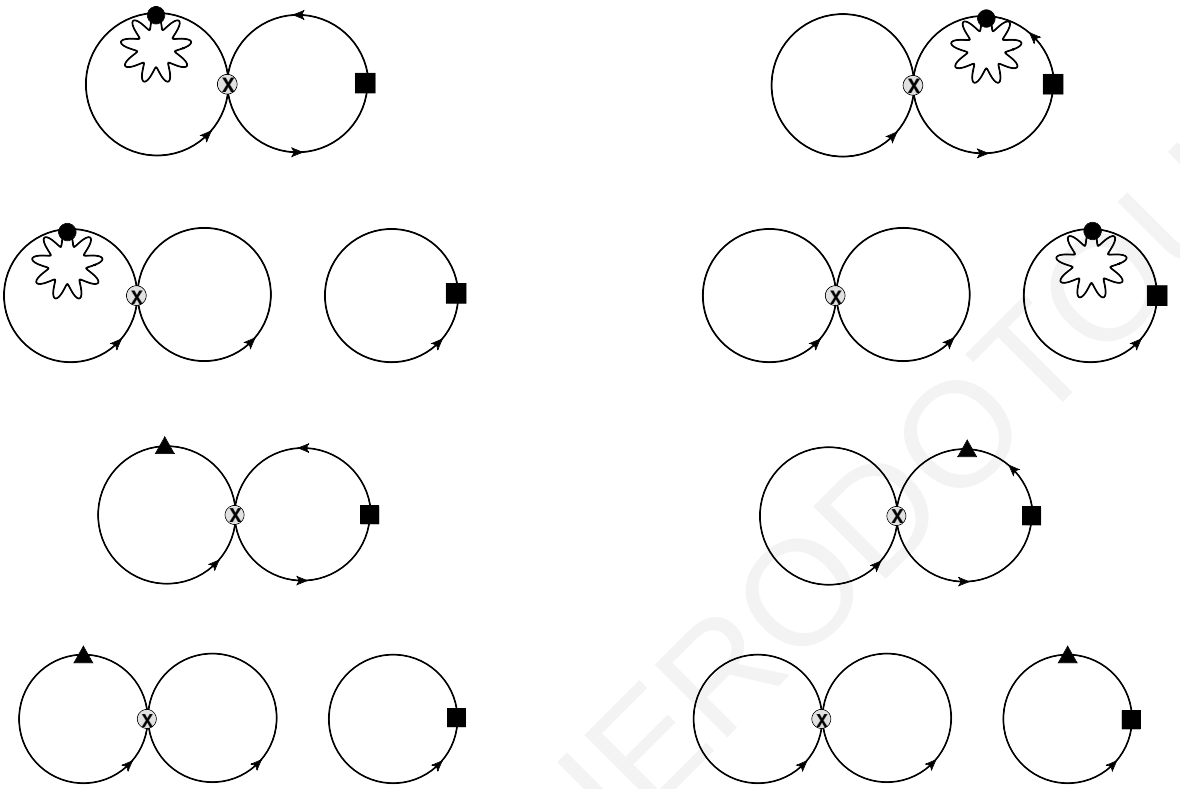

FIGURE B.6: Additional Feynman diagrams contributing to $\langle \mathcal{O}_{\Gamma\tilde{\Gamma}}(x)\, \mathcal{O}_{\Gamma'}(y) \rangle$ on the lattice. Notation is identical to that of Figure 5.2. The triangle denotes insertion of the critical mass counterterm.

The Feynman diagrams contributing to the three-point Green's functions of the product of one four-quark operator and two quark bilinear operators that are absent for $\Delta F = 2$ operators and contribute to operators with $\Delta F < 2$ are shown in Fig. B.7.

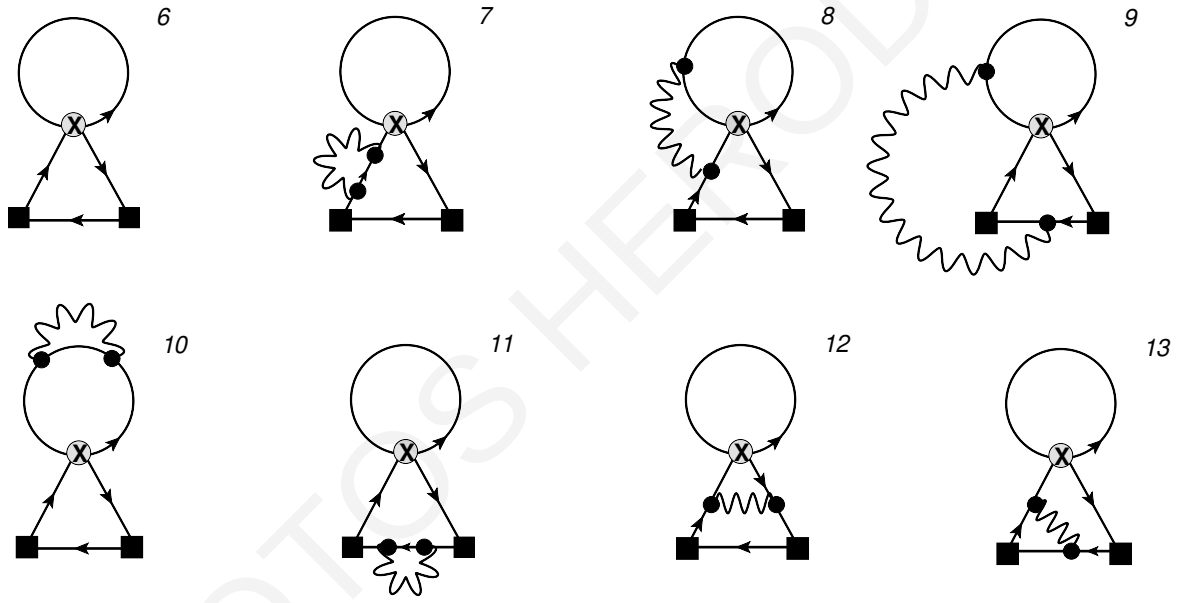

FIGURE B.7: Feynman diagrams contributing to $\langle \mathcal{O}_{\Gamma'}(x)\, \mathcal{O}_{\Gamma\tilde{\Gamma}}(0) \mathcal{O}_{\Gamma''}(y) \rangle$ with a $\Delta F < 2$ four-quark operator, to order $\mathcal{O}(g^0)$ (diagram 6) and $\mathcal{O}(g^2)$ (the remaining diagrams). Notation is identical to that of Figure 5.2. Diagrams 7-13 can have mirror variants.

References

[1] K. G. Wilson, "Confinement of Quarks", Phys. Rev. **D10** (1974), 2445-2459

[2] M. Creutz, "Monte Carlo Study of Quantum Chromodynamics", Phys. Lett. **45** (1980), 313-316

[3] G. Martinelli, C. Pittori, C. T. Sachraj, M. Testa and A. Vladikas, "A General method for nonperturbative renormalization of lattice operators", Nucl. Phys. B **445** (1995), 81-108 [arXiv:hep-lat/9411010].

[4] M. Constantinou et al., "Non-perturbative renormalization of quark bilinear operators with $N_f = 2$ (tmQCD) Wilson fermions and the tree-level improved gauge action", JHEP **08** (2010), 068 [arXiv:hep-lat/1004.1115].

[5] M. Gockeler et al., "Perturbative and Nonperturbative Renormalization in Lattice QCD", Phys. Rev. D **82** (2010), 114511 [arXiv:hep-lat/1003.5756].

[6] M. Luscher, R. Narayanan, P. Weisz and U. Wolff, "The Schrödinger functional: A Renormalizable probe for nonAbelian gauge theories", Nucl. Phys. B **384** (1992), 168-228 [arXiv:hep-lat/9207009].

[7] R. Sommer, "Nonperturbative renormalization of QCD", Lect. Notes Phys. **512** (1998), 65-113 [arXiv:hep-lat/9711243].

[8] R. Sommer, "Non-perturbative QCD: Renormalization, O(a)-improvement and matching to Heavy Quark Effective Theory", DESY-06-206, SFB-CPP-06-51 (2006) [arXiv:hep-lat/0611020].

[9] M. Costa, I. Karpasitis, T. Pafitis, G. Panagopoulos, H. Panagopoulos, A. Skouroupathis and G. Spanoudes, "Gauge-invariant renormalization scheme in QCD: Application to fermion bilinears and the energy-momentum tensor", Phys. Rev. D **103** (2021), 094509 [arXiv:hep-lat/2102.00858].

[10] V. Gimenez, L. Giusti, S. Guerriero, V. Lubicz, G. Martinelli, S. Petrarca, J. Reyes, B. Taglienti and E. Trevigne, "Non-perturbative renormalization of lattice operators in coordinate space", Phys. Lett. B **598** (2004), 227-236 [arXiv:hep-lat/0406019].

[11] P. H. Dondi and H. Nicolai, "Lattice Supersymmetry", Nuovo Cim. A41 (1977) 1.

[12] G. Curci and G. Veneziano, "SUPERSYMMETRY AND THE LATTICE: A RECONCILIATION?", Nucl. Phys. **B292** (1987) 555.

[13] D. Schaich, "Lattice studies of supersymmetric gauge theories", Eur. Phys. J. ST **232** (2023) no.3, 305-320 doi:10.1140/epjs/s11734-022-00708-1 [arXiv:hep-lat/2208.03580].

[14] J. Giedt, "Progress in four-dimensional lattice supersymmetry" Int. J. Mod. Phys. **A24** (2009) 4045-4095 [arXiv:0903.2443].

[15] D. Schaich, "Progress and prospects of lattice supersymmetry" PoS (**LATTICE2018**) 005 [arXiv:1810.09282].

[16] G. Bergner and S. Catterall, "Supersymmetry on the lattice", Int. J. Mod. Phys. A **31** (2016) no.22, 1643005 doi:10.1142/S0217751X16430053 [arXiv:hep-lat/1603.04478].

[17] G. Bergner, P. Giudice, G. Münster, I. Montvay and S. Piemonte, "The light bound states of supersymmetric SU(2) Yang-Mills theory", JHEP **03** (2016), 080 [arXiv:hep-lat/1512.07014].

[18] S. Ali, G. Bergner, H. Gerber, P. Giudice, I. Montvay, G. Münster et al., "The light bound states of $\mathcal{N}$=1 supersymmetric SU(3) Yang-Mills theory on the lattice", JHEP **03** (2018), 113 [arXiv:hep-lat/1801.08062].

[19] B. Wellegehausen, A. Wipf, M. Steinhauser and A. Sternbeck, "$\mathcal{N}$=1 Supersymmetric SU(3) Gauge Theory – Pure Gauge sector with a twist", PoS (**LATTICE2018**) 211.

[20] D. August, B. H. Wellegehausen and A. Wipf, "Mass spectrum of 2-dimensional $\mathcal{N} = (2,2)$ super Yang-Mills theory on the lattice", JHEP **01** (2019), 099 [arXiv:hep-lat/1802.07797].

[21] H. Suzuki and Y. Taniguchi, "Two-dimensional $\mathcal{N} = (2,2)$ super Yang-Mills theory on the lattice via dimensional reduction", JHEP **10** (2005), 082 [arXiv:hep-lat/0507019].

[22] M. Constantinou, P. Dimopoulos, R. Frezzotti, V. Lubicz, H. Panagopoulos, A. Skouroupathis, F. Stylianou, "Perturbative renormalization factors and $\mathcal{O}(a^2)$ corrections for lattice 4-fermion operators with improved fermion/gluon actions", Phys. Rev. **D83** (2011) 074503 [arXiv:1011.6059].

[23] M. Constantinou, M. Costa, M. Gockeler, R. Horsley, H. Panagopoulos, H. Perlt, P. E. L. Rakow, G. Schierholz, A. Schiller, "Perturbatively improving regularization-invariant momentum scheme renormalization constants", Rev. **D87** (9) (2013) 096019 [arXiv:1303.6776].

[24] C. Alexandrou, M. Constantinou, H. Panagopoulos, "Renormalization functions for $N_f = 2$ and $N_f = 4$ twisted mass fermions", Phys. Rev. **D95** (3) (2017) 034505 [arXiv:1509.00213].

[25] G. Xiang, "Overview of hadron structure form lattice QCD", PoS (**LATTICE2023**) 128.

[26] K. Gurtej, "Flow-based sampling for lattice field theories", PoS (**LATTICE2023**) 114 [arXiv:hep-lat/2401.01297].

[27] A. Pasztor, "The QCD phase diagram at finite temperature and density - a lattice perspective", PoS (**LATTICE2023**) 108.

[28] M. Yu, "Lattice QCD calculation of the invisible decay $J/\psi \to \gamma\nu\bar{\nu}$", PoS (**LATTICE2023**) 129 [arXiv:hep-lat/2309.15436].

[29] D. Grabowska, "Quantum simulations of lattice field thoeries", PoS (**LATTICE2023**) 110.

[30] R. Gupta, "Isovector Axial Charge and Form Factors of Nucleons from Lattice QCD", PoS (**LATTICE2023**) 124 [arXiv:hep-lat/2401.166146].

[31] A. Hanlon, "Hadron spectroscopy and few-body dynamics from Lattice QCD", PoS (**LATTICE2023**) 106 [arXiv:hep-lat/2402.05185].

[32] H.T. Shu, "Transport and Connection to Heavy-ion Collisions via Heavy Flavor Probes", PoS (**LATTICE2023**) 115 [arXiv:hep-lat/2401.08040].

[33] J. Zhang, "Renormalons in Large-Momentum Effective Theory", PoS (**LATTICE2023**) 117.

[34] S. Meinel, "Quark flavor physics with lattice QCD", PoS (**LATTICE2023**) 126 [arXiv:hep-lat/2401.08006].

[35] L. Leskovec, "Electroweak transitions involving resonances", PoS (**LATTICE2023**) 119 [arXiv:hep-lat/2401.02495].

[36] J.W. Lee, "Strongly coupled gauge theories towards physics beyond the Standard Model", PoS (**LATTICE2023**) 118 [arXiv:hep-lat/2402.01087].

[37] S. Kuberski, "Muon $g-2$: Lattice calculations of the hadronic vacuum polarization", PoS (**LATTICE2023**) 125 [arXiv:hep-lat/2312.13753].

[38] J. Wess, "From symmetry to supersymmetry", Eur. Phys. J. C, **59 2** (2009), 177-193 [arXiv:0707.2906].

[39] G. Bertone, D. Hooper and J. Silk, "Particle dark matter: Evidence, candidates and constraints", Phys. Rept. **405** (2005), 279-390 doi:10.1016/j.physrep.2004.08.031 [arXiv:hep-ph/0404175].

[40] K. A. Olive et al., "Review of Particle Physics", Chin. Phys. C**38** (2015), 090001.

[41] L. Susskind, "The Gauge Hierarchy problem, Technicolor, Supersymmetry, and all that", Phys. Rept. **104** (1984), 181-193 doi:10.1016/0370-1573(84)90208-4

[42] J. R. Ellis, J. S. Hagelin, D. V. Nanopoulos, K. A. Olive and M. Srednicki, "Supersymmetric Relics from the Big Bang", Nucl. Phys. B **238** (1984), 453-476 doi:10.1016/0550-3213(84)90461-9

[43] M. Dine, "Supersymmetry and String Theory : Beyond the Standard Model," Oxford University Press, 2016, ISBN 978-1-107-04838-6, 978-1-316-40530-7, 978-1-00-929088-3, 978-1-00-929092-0, 978-1-00-929089-0 doi:10.1017/9781009290883

[44] J. Wess and J. Bagger, "Supersymmetry and Supergravity", Princeton University Press (1992).

[45] S.J. Gates, M.T. Grisaru, M. Rocek, W. Siegel, "Superspace, or One thousand and one lessons in supersymmetry", *Superspace or One Thousand and One Lessons in Supersymmetry*, Front. Phys. **58** (1983) 1, [arXiv:hep-th/0108200].

[46] S. Weinberg, *The Quantum Theory of Fields, Volume III Supersymmetry*, Cambridge University Press (2000).

[47] S. P. Martin, *A Supersymmetry Primer*, Adv. Ser. Dir. High Energy Phys. **18** (1998) 1, [arXiv:hep-ph/9709356].

[48] M. Costa and H. Panagopoulos, "Supersymmetric QCD on the Lattice: An Exploratory Study", Phys. Lett. D **76** (2017), 094514 [arXiv:1706.05222].

[49] H. Suzuki, "Supersymmetry, chiral symmetry and the generalized BRS transformation in lattice formulations of 4D $\mathcal{N} = 1$ SYM", Nucl. Phys. **B861** (2012) 290, [arXiv:1202.2598].

[50] R.D.C. Miller, "Supersymmetric gauge fixing and the effective potential" Phys. Lett. **129B** (1983) 72.

[51] R. L. Workman *et al.* [Particle Data Group], "Review of Particle Physics", PTEP **2022** (2022), 083C01 doi:10.1093/ptep/ptac097.

[52] J. Terning, "Modern supersymmetry: Dynamics and duality," doi:10.1093/acprof:oso/9780198567639.001.0001.

[53] A. Casher and Y. Shamir, "Feynman rules for non-perturbative sectors and anomalous supersymmetry ward identities" (1999) [arXiv:hep-th/9908074].

[54] N. Seiberg and E. Witten, "Monopoles, duality and chiral symmetry breaking in $\mathcal{N}$=2 supersymmetric qcd" Nucl. Phys. B431 (1994) 484 [arXiv:hep-th/9408099].

[55] P. Athron and D. J. Miller, "A New Measure of Fine Tuning", Phys. Rev. D **76** (2007), 075010 doi:10.1103/PhysRevD.76.075010 [arXiv:hep-ph/0705.2241].

[56] F. Farchioni, C. Gebert, R. Kirchner, I. Montvay, A. Feo, G. Munster, T. Galla and A. Vladikas, "The supersymmetric Ward identities on the lattice", Eur. Phys. J. D **76** (2002), 719 [arXiv:hep-lat/0111008].

[57] S. Ali, H. Gerber, I. Montvay, G. Munster, S. Piemonte, P. Scior and G. Bergner, "Analysis of Ward identities in supersymmetric Yang-Mills theory", Eur. Phys. J. C **78** (2019), 404 [arXiv:1802.07067].

[58] Y. Taniguchi, "One loop calculation of SUSY Ward-Takahashi identity on lattice with Wilson fermion", Phys. Rev. D **63** (2000), 014502 doi:10.1103/PhysRevD.63.014502 [arXiv:hep-lat/9906026].

[59] F. Sugino, "Lattice Formulation of Two-Dimensional $\mathcal{N}$=(2,2) SQCD with Exact Supersymmetry", Nucl. Phys. B **808** (2009), 292-325 doi:10.1016/j.nuclphysb.2008.09.035 [arXiv:hep-lat/0807.2683].

[60] S. Catterall, D. B. Kaplan and M. Unsal, "Exact lattice supersymmetry", Phys. Rept. **484** (2009), 71-130 doi:10.1016/j.physrep.2009.09.001 [arXiv:hep-lat/0903.4881].

[61] S. Catterall, D. Schaich, P.H. Damgaard, T. DeGrand and J. Giedt, "$\mathcal{N}$ = 4 supersymmetry on a space-time lattice", Phys. Rev. D **90** (2014), 065013 [arXiv:1405.0644].

[62] M. Kato, M. Sakamoto and H. So, "Non-renormalization theorem in a lattice supersymmetric theory and the cyclic Leibniz rule", PTEP 2017 (2017) 043B09 [arXiv:1609.08793].

[63] M. Kato, M. Sakamoto and H. So, "A criterion for lattice supersymmetry: cyclic Leibniz rule", Jour. High En. Phys. 1305 (2013) 089 [arXiv:1303.4472].

[64] A. D'Adda, N. Kawamoto and J. Saito, "An Alternative Lattice Field Theory Formulation Inspired by Lattice Supersymmetry", Jour. High En. Phys. 1712 (2017) 089 [arXiv:1706.02615].

[65] P. H. Ginsparg and K. G. Wilson, "A remnant of chiral symmetry on the lattice" Phys. Rev. **D25** (1982) 2649.

[66] M. Costa and H. Panagopoulos, "Supersymmetric QCD: Renormalization and Mixing of Composite Operators", Phys. Lett. D **99** (2019), 074512 [arXiv:1812.06770].

[67] H. Herodotou, M. Costa and H. Panagopoulos, "Fine-Tuning of the Yukawa and Quartic Couplings in Supersymmetric QCD", PoS **LATTICE2022** (2022), 276 doi:10.22323/1.430.0276 [arXiv:hep-lat/2210.03695].

[68] M. Costa, H. Herodotou and H. Panagopoulos, "Renormalization of the Yukawa and Quartic Couplings in $\mathcal{N}$ = 1 Supersymmetric QCD", PoS **LATTICE2023** (2023), 088 [arXiv:hep-lat/2311.16710].

[69] M. Costa, H. Herodotou, P. Philippides and H. Panagopoulos, "Renormalization and mixing of the Gluino-Glue operator on the lattice", Eur. Phys. J. C **81**, no.5, 401 (2021) doi:10.1140/epjc/s10052-021-09173-x [arXiv:hep-lat/2010.02683].

[70] M. Costa, G. Panagopoulos, H. Panagopoulos and G. Spanoudes, "Gauge-invariant Renormalization of the Gluino-Glue operator", Phys. Lett. B **816**, 136225 (2021) doi:10.1016/j.physletb.2021.136225 [arXiv:hep-lat/2102.02036].

[71] G. Bergner, M. Costa, H. Panagopoulos, I. Soler and G. Spanoudes, "Perturbative renormalization of the supercurrent operator in lattice $\mathcal{N}$=1

supersymmetric Yang-Mills theory", Phys. Rev. D **106**, no.3, 034502 (2022) doi:10.1103/PhysRevD.106.034502 [arXiv:hep-lat/2205.02012].

[72] I. Affleck, M. Dine and N. Seiberg, "Dynamical Supersymmetry Breaking in Supersymmetric QCD," Nucl. Phys. B **241** (1984), 493-534 doi:10.1016/0550-3213(84)90058-0

[73] D. R. T. Jones, "More on the Axial Anomaly in Supersymmetric Yang-Mills Theory", Phys. Lett. B **123** (1983), 45-46 doi:10.1016/0370-2693(83)90955-3

[74] S. A. Larin, "The Renormalization of the axial anomaly in dimensional regularization", Phys. Lett. B **303** (1993), 113-118 doi:10.1016/0370-2693(93)90053-K [arXiv:hep-ph/9302240 containing an extra section].

[75] M. S. Chanowitz, M. Furman and I. Hinchliffe, "The Axial Current in Dimensional Regularization", Nucl. Phys. B **159** (1979), 225-243 doi:10.1016/0550-3213(79)90333-X

[76] G. 't Hooft and M. J. G. Veltman, "Regularization and Renormalization of Gauge Fields", Nucl. Phys. B **44** (1972), 189-213 doi:10.1016/0550-3213(72)90279-9

[77] W. Siegel, "Supersymmetric Dimensional Regularization via Dimensional Reduction", Phys. Lett. B **84** (1979), 193-196 doi:10.1016/0370-2693(79)90282-X

[78] A. Patel and S. R. Sharpe, "Perturbative corrections for staggered fermion bilinears", Nucl. Phys. B **395** (1993), 701-732 doi:10.1016/0550-3213(93)90054-S [arXiv:hep-lat/9210039].

[79] A. J. Buras, P. H. Weisz, "QCD nonleading corrections to weak decays in dimensional regularization and 't Hooft-Veltman schemes", Nucl. Phys. **B333** (1990) 66.

[80] M. Costa, H. Herodotou and H. Panagopoulos, "Supersymmetric QCD on the Lattice: Fine-Tuning of the Yukawa Couplings", Phys. Rev. D **109** (2024) no.3, 035015 doi:10.1103/PhysRevD.109.035015 [arXiv:hep-lat: 2310.20207].

[81] M. Costa, H. Herodotou and H. Panagopoulos, "Supersymmetric QCD on the Lattice: Fine-Tuning and Counterterms for the Quartic Couplings", in preparation.

[82] K. G. Chetyrkin and A. Retey, "Renormalization and running of quark mass and field in the regularization invariant and MS-bar schemes at three loops and four loops", Nucl. Phys. B **583** (2000), 3-34 doi:10.1016/S0550-3213(00)00331-X [arXiv:hep-ph/9910332].

[83] B. Ruijl, T. Ueda, J. A. M. Vermaseren and A. Vogt, "Four-loop QCD propagators and vertices with one vanishing external momentum", JHEP **06** (2017), 040 doi:10.1007/JHEP06(2017)040 [arXiv:hep-ph/1703.08532].

[84] T. Luthe, A. Maier, P. Marquard and Y. Schroder, "The five-loop Beta function for a general gauge group and anomalous dimensions beyond Feynman gauge", JHEP **10** (2017), 166 doi:10.1007/JHEP10(2017)166 [arXiv:hep-ph/1709.07718].

[85] K. G. Chetyrkin, G. Falcioni, F. Herzog and J. A. M. Vermaseren, "Five-loop renormalisation of QCD in covariant gauges", JHEP **10** (2017), 179 doi:10.1007/JHEP10(2017)179 [arXiv:hep-ph/1709.08541].

[86] J. A. Gracey and R. M. Simms, "Renormalization of QCD in the interpolating momentum subtraction scheme at three loops", Phys. Rev. D **97** (2018) no.8, 085016 doi:10.1103/PhysRevD.97.085016 [arXiv:hep-th/1801.10415].

[87] P. A. Baikov and K. G. Chetyrkin, "Transcendental structure of multiloop massless correlators and anomalous dimensions", JHEP **10** (2019), 190 doi:10.1007/JHEP10(2019)190 [arXiv:hep-ph/1908.03012].

[88] B. Wellegehausen and A. Wipf, "$\mathcal{N} = 1$ Supersymmetric $SU(3)$ Gauge Theory - Towards simulations of Super-QCD", PoS (**LATTICE2018**) 210 [arXiv:1811.01784].

[89] L. Bonora, P. Pasti and M. Tonin, "Abj Anomalies in Supersymmetric Yang-Mills Theories," Phys. Lett. B **156** (1985), 341-344 doi:10.1016/0370-2693(85)91621-1

[90] G. Girardi, R. Grimm and R. Stora, "Chiral Anomalies in $\mathcal{N}$=1 Supersymmetric Yang-Mills Theories," Phys. Lett. B **156** (1985), 203-208 doi:10.1016/0370-2693(85)91510-2

[91] S. Ali, G. Bergner, H. Gerber, I. Montvay, G. Munster, S. Piemonte and P. Scior, "Continuum extrapolation of Ward identities in $\mathcal{N} = 1$ supersymmetric SU(3) Yang-Mills theory", Eur. Phys. J. C **80** (2020), 548 [arXiv:hep-lat/2003.04110].

[92] R. Aaij, et al., "First Observation of a Doubly Charged Tetraquark and Its Neutral Partner", Phys. Rev. Lett. **131** (2023), 041902 [arXiv:hep-ex/2212.02716].

[93] R. Aaij, et al., "Amplitude analysis of B0→D¯0Ds+π- and B+→D-Ds+π+ decays", Phys. Rev. D **108** (2023), 012017 [arXiv:hep-ex/2212.02717].

[94] R. Aaij, et al., "Observation of a Resonant Structure near the Ds+Ds- Threshold in the B+→Ds+Ds-K+ Decay", Phys. Rev. Lett. **131** (2023), 071901 [arXiv:hep-ex/2210.15153].

[95] R. Aaij, et al., "First observation of the B+→Ds+Ds-K+ decay", Phys. Rev. D **108** (2023), 034012 [arXiv:hep-ex/2211.05034].

[96] N. Carrasco, P. Dimopoulos, R. Frezzotti, V. Lubicz, G. C. Rossi, S. Simula, C. Tarantino, "ΔS=2 and ΔC=2 bag parameters in the standard model and beyond from N_f=2+1+1 twisted-mass lattice QCD", Phys. Rev. D **92** (2015), 034516 [arXiv:hep-lat/1505.06639].

[97] D. Becirevic, P. Boucaud, V. Gimenez, V. Lubicz, G. Martinelli and M. Papinutto, "Matrix elements of $\Delta S = 2$ operators with Wilson fermions", Nucl. Phys. B Proc. Suppl. **106** (2002), 326-328 [arXiv:hep-lat/0110006].

[98] Y. Aoki et al., "Continuum Limit of B_K from 2+1 Flavor Domain Wall QCD", Phys. Rev. D **84** (2011), 014503 [arXiv:hep-lat/1012.4178].

[99] J. Aebischer, C. Bobeth, A. J. Buras and J. Kumar, "SMEFT ATLAS of $\Delta F = 2$ transitions", JHEP **12** (2020), 187 [arXiv:hep-ph/2009.07276].

[100] A. Suzuki, Y. Taniguchi, H. Suzuki, K. Kanaya, "Four quark operators for kaon bag parameter with gradient flow", Phys. Rev. D **102** (2020), 034508 [arXiv:hep-ph/2006.06999].

[101] R. Frezzotti and G. C. Rossi, "Chirally improving Wilson fermions. II. Four-quark operators", JHEP **10** (2004), 070 [arXiv:hep-lat/0407002].

[102] M. Constantinou et al., "B_K-parameter from $N_f = 2$ twisted mass lattice QCD", Phys. Rev. D **83** (2011), 014505 [arXiv:hep-lat/1009.5606].

[103] R. Gupta, D. Daniel, G. W. Kilcup, A. Patel, S. R. Sharpe, "The Kaon B parameter with Wilson fermions", Phys. Rev. D **47** (1993), 5113–5127 [arXiv:hep-lat/1009.5606].

[104] N. Ishizuka, K. I. Ishikawa, A. Ukawa, T. Yoshié, "Calculation of $K \to \pi\pi$ decay amplitudes with improved Wilson fermion action in non-zero momentum frame in lattice QCD", Phys. Rev. D **98** (2018), 114512 [arXiv:hep-lat/1809.03893].

[105] M. Ciuchini et al., "Delta M(K) and epsilon(K) in SUSY at the next-to-leading order", JHEP **10** (1998), 008 [arXiv:hep-lat/9808328].

[106] K. Jansen et al., "Nonperturbative renormalization of lattice QCD at all scales", Phys. Lett. B **372** (1996), 275-282 [arXiv:hep-lat/9512009].

[107] K. G. Chetyrkin and A. Maier, "Massless correlators of vector, scalar and tensor currents in position space at orders α_s^3 and α_s^4: Explicit analytical results", Nucl. Phys. B **844** (2011), 266-288 [arXiv:hep-lat/1010.1145].

[108] K. Cichy, K. Jansen and P. Korcyl, "Non-perturbative renormalization in coordinate space for $N_f = 2$ maximally twisted mass fermions with tree-level Symanzik improved gauge action", Nucl. Phys. B **865** (2012), 268-290 [arXiv:hep-lat/1207.0628].

[109] M. Tomii and N. H. Christ, "$O(4)$-symmetric position-space renormalization of lattice operators", Phys. Rev. D **99** (2019), 014515 [arXiv:hep-lat/1811.11238].

[110] P. Dimopoulos, G. Herdoíza, M. Papinutto, C. Pena, D. Preti, David and A. Vladikas, "Non-Perturbative Renormalisation and Running of BSM Four-Quark Operators in $N_f = 2$ QCD", Eur. Phys. J. C **78** (2018), 579 [arXiv:hep-lat/1801.09455].

[111] A. Maas, "Describing gauge bosons at zero and finite temperature", Phys. Rept. **524** (2013), 203-300 [arXiv:hep-lat/1106.3942].

[112] A. Cucchieri, D. Dudal, T. Mendes, O. Oliveira, M. Roelfs, P. J. Silva, "Faddeev-Popov Matrix in Linear Covariant Gauge: First Results", Phys. Rev. D **98** (2018), 091504 [arXiv:hep-lat/1809.08224].

[113] F. Herzog, S. Moch, B. Ruijl, T. Ueda, J. A. M. Vermaseren and A. Vogt, "Five-loop contributions to low-N non-singlet anomalous dimensions in QCD", Phys. Lett. B **790** (2019), 436–443 [arXiv:hep-lat/1812.11818].

[114] C. W. Bernard, T. Draper, G. Hockney and A.Soni, "Recent Developments in Weak Matrix Element Calculations", Nucl. Phys. B Proc. Suppl. **4** (1988), 483.

[115] A. Donini, V. Gimenez, G. Martinelli, M. Talevi and A. Vladikas, "Nonperturbative renormalization of lattice four fermion operators without power subtractions", Eur. Phys. J. C **10** (1999), 121–142 doi:10.1007/s100529900097 [arXiv:hep-lat/9902030].

[116] D. Becirevic, V. Gimenez, V. Lubicz, G. Martinelli, M. Papinutto and J. Reyes, "Renormalization constants of quark operators for the nonperturbatively improved Wilson action", JHEP **08** (2004), 022 [arXiv:hep-lat/0401033].

[117] G. Bergner, M. Costa, H. Panagopoulos, S. Piemonte, I. Soler and G. Spanoudes, "Nonperturbative renormalization of the supercurrent in N=1 supersymmetric Yang-Mills theory", Phys. Rev. D **107** (2023), 034502 [arXiv:hep-lat/2209.13934].

[118] G. Panagopoulos, H. Panagopoulos and G. Spanoudes, "Two-loop renormalization and mixing of gluon and quark energy-momentum tensor operators", Phys. Rev. D **103** (2021), 014515 [arXiv:hep-lat/2010.02062].

[119] K. G. Chetyrkin and F. V. Tkachov, "Integration by parts: The algorithm to calculate β-functions in 4 loops", Nucl. Phys. B **192** (1981), 159-204.

[120] A. I. Davydychev, "Recursive algorithm of evaluating vertex type Feynman integrals", J. Phys. A **25** (1992), 5587-5596.

[121] N. I. Usyukina and A. I. Davydychev, "New results for two loop off-shell three point diagrams", Phys. Lett. B **332** (1994), 159-167 [arXiv:hep-ph/9402223].

[122] M. Ciuchini et al., "Next-to-leading order QCD corrections to Δ F = 2 effective Hamiltonians", Nucl. Phys. B **523** (1998), 501-525 [arXiv:hep-ph/9711402].

[123] M. Papinutto, C. Pena and D. Preti, "On the perturbative renormalization of four-quark operators for new physics", Eur. Phys. J. C **77** (2017), 376 [arXiv:hep-lat/1612.06461].

[124] A. Donini, M. Guagnelli, P. Hernandez and A. Vladikas, "Towards $\mathcal{N}$=1 superYang-Mills on the lattice", Nucl. Phys. B **523** (1998), 529-552 doi:10.1016/S0550-3213(98)00166-7 [arXiv:hep-lat/9710065].